
A PHYLOGENETIC ANALYSIS OF ANT
MORPHOLOGY (HYMENOPTERA: FORMICIDAE)
WITH SPECIAL REFERENCE TO THE
PONEROMORPH SUBFAMILIES

ROBERTO A. KELLER



BULLETIN OF THE AMERICAN MUSEUM OF NATURAL HISTORY

A PHYLOGENETIC ANALYSIS OF ANT
MORPHOLOGY (HYMENOPTERA: FORMICIDAE)
WITH SPECIAL REFERENCE TO THE
PONEROMORPH SUBFAMILIES

ROBERTO A. KELLER

*Division of Invertebrate Zoology,
American Museum of Natural History,
and Department of Entomology, Comstock Hall
Cornell University, Ithaca, New York 14853
Current address: Instituto Gulbenkian de Ciência
Rua da Quinta Grande 6, Oeiras, P-2780-156,
Portugal*

BULLETIN OF THE AMERICAN MUSEUM OF NATURAL HISTORY

Number 355, 90 pp., 38 figures, 4 tables

Issued August 10, 2011

CONTENTS

Abstract	3
Introduction	3
The Importance of Studies of Ant Morphology	7
Digital Atlas of Ant Morphology	10
Goals of Present Study	11
Materials and Methods	12
Taxon Sampling	12
Character Sampling	13
Morphological Analysis	15
Digital Atlas	15
Cladistic Analysis	17
Character Descriptions and Discussion	17
Abbreviations and Conventions	17
Note on Anatomical Terminology	17
About Character Figures	19
Character Discussion	19
Characters Excluded from the Analysis	65
Results and Discussion	66
Morphological Analysis	66
Cladistic Analysis	67
Final Remarks	74
Acknowledgments	74
References	74
Appendix 1: List of Species Included in This Study	82
Appendix 2: Data Matrix	85

ABSTRACT

Efforts to reconstruct the phylogenetic history of ants (Hymenoptera: Formicidae) have been boosted in the last few years by accumulation of comprehensive molecular data sets exploring multiple loci on a wide range of taxa within the family. In contrast, the wealth of morphological information for the group remains scattered across the literature comprising more than a century's worth of taxonomic and anatomical research with little standardization. The present study addresses this problem by providing a synthesis of the external skeletal morphology of ants with special emphasis on the poneromorph subfamilies (Amblyoponinae, Ectatomminae, Heteroponerinae, Paraponerinae, Ponerinae, and Proceratiinae). Particular attention was devoted to documenting and standardizing morphological characters for phylogenetic inference. The morphological analysis was undertaken by constructing a digital atlas of 28 standard views containing 5250 scanning electron micrographs documenting worker ant morphology from which detailed anatomical comparison could be accurately performed. The final matrix describes 139 characters (60% of which are completely new or coded cladistically here for the first time) for 105 terminals representing ~90% of extant poneromorph genera plus all other extant formicid subfamilies, with the exception of the rare Martilinae, and nonformicid outgroups. This matrix was analyzed with parsimony under both equal weights and implied weights (i.e., where characters are downweighted as a function of their homoplasy). The poneromorph subfamilies form a paraphyletic assemblage with the dorylomorphs, leptanillo-morphs, and myrmicomorphs nested inside. All the above subfamilies are in turn reconstructed as nested within a paraphyletic group comprising the formicomorphs + myrmeciomorphs. These results are in concordance with traditional precladistic views of the subfamily relationships but are markedly different from current estimates based on molecular data.

INTRODUCTION

Poneromorph ants comprise an informal group of six subfamilies that were until recently classified as the single subfamily Ponerinae (herein *sensu lato*), but that currently includes the subfamilies Amblyoponinae, Ectatomminae, Heteroponerinae, Paraponerinae, Ponerinae *sensu stricto*, and Proceratiinae (Bolton, 2003). Taken together, poneromorphs total 1631 recognized species of worldwide distribution arranged in 54 genera (seven of them extinct) and 10 tribes (Agosti and Johnson, 2007).

Since first erected by Lepeletier de Saint-Fargeau (1835) as the family-group taxon *Ponérites*, the group has undergone many taxonomic changes in both its generic composition and its internal arrangement. Circumscription of Ponerinae s.l. became problematic as the number of included species expanded greatly from its original conception: it is now recognized that this assemblage was defined by symplesiomorphic characters while serving as an all-purpose taxon to host a diverse array of species that did not fit any of the other well established subfamilies (Keller, 2000). In addition, phylogenetic analyses have shown that different groups of genera

formally within Ponerinae s.l. are more closely related to other subfamilies than among themselves (Keller, 2000; Ward and Brady, 2003; Saux et al., 2004; Brady et al., 2006; Moreau et al., 2006; Ouellette et al., 2006). Such accumulation of evidence led Bolton (2003) to propose the elevation of the major tribes within the old assembly to subfamily status, hence splitting the group into six subfamilies and restricting the name Ponerinae to the subgroup of genera mostly corresponding to the previously recognized tribe Ponerini. In his 2003 *Synopsis and Classification of Formicidae* Bolton arranged the ant subfamilies into informal groups convenient for the "establishment of identity rather than the postulation of phylogenetic hypotheses" (Bolton, 2003: 3), and thus the name poneromorphs was introduced as a replacement term to refer to this traditional, long-standing, but now considered unnatural, taxon. Table 1 shows the classification of poneromorph genera followed in this study.

For most of the 20th century the subfamily, while considered a valid taxonomic entity, was explicitly treated as a paraphyletic group in discussions of ant phylogeny. W.M. Wheeler (1928) considered Ponerinae s.l. as the "prim-

TABLE 1
Generic Classification of Poneromorphs (Updated from Bolton, 2003, No. of Species and Updated Classification Following <http://antbase.org>, Accessed 10.V.2010). Extinct Taxa Denoted by †.

	spp
AMBLYOPONINAE Forel 1893	
Amblyoponini Forel 1893	
Adetomyrma Ward 1994	1
Amblyopone Erichson 1842	72
Bannapone Xu 2000	1
†Casaleia Pagliano & Scaramozzino 1981	1
Concoctio Brown 1974	1
Myopopone Roger 1861	2
Mystrium Roger 1862	11
Onychomyrmex Emery 1895	3
Prionopelta Mayr 1866	15
Incertae sedis:	
Paraprionopelta Kusnezov 1955	1
Ectatomminae Emery 1895	
Ectatommini Emery 1895	
Ectatomma Smith 1858	16
Gnamptogenys Roger 1863	169
Rhytidoponera Mayr 1862	114
Incertae sedis:	
†Electroponera Wheeler 1915	1
Typhlomyrmecini Emery 1911	
Typhlomyrmex Mayr 1862	7
Incertae sedis Ectatomminae:	
†Canapone Dlusky 1999	1
Heteroponerinae Bolton 2003	
Heteroponerini Bolton 2003	
Acanthoponera Mayr 1862	4
Heteroponera Mayr 1887	17
Incertae sedis:	
Aulacopone Arnol'di 1930	1
PARAPONERINAE Emery 1901	
Paraponerini Emery 1901	
Paraponera Smith 1858	2
PROCERATIINAE Emery 1895	
Proceratiini Emery 1895	
†Bradoponera Mayr 1868	3
Discothyrea Roger 1863	33
Proceratium Roger 1863	83
Probolomyrmecini Perrault 2000	
Probolomyrmex Mayr 1901	20
Ponerinae Lepeletier 1835	
Ponerini Lepeletier 1835	
Anochetus Mayr 1861	101
Asphinctopone Santschi 1914	2
Belonopelta Mayr 1870	2
Boloponera Fisher 2006	1
Centromyrmex Mayr 1866	15

TABLE 1
(Continued)

	spp
Cryptopone Emery 1893	22
Diacamma Mayr 1862	27
Dinoponera Roger 1861	6
Dolioponera Brown 1974	1
Emeryopone Forel 1912	5
Feroponera Bolton & Fisher 2008	7
Harpegnathos Jerdon 1851	7
Hypoponera Santschi 1938	138
Leptogenys Roger 1861	217
Loboponera Bolton & Brown 2002	9
Myopias Roger 1861	34
Odontomachus Latreille 1804	65
Odontoponera Mayr 1862	1
Pachycondyla Smith 1858	217
Phrynoponera Wheeler 1920	5
Plectroctena Smith 1858	16
Ponera Latreille 1804	54
Promyopias Santchi 1914	1
Psalidomyrmex André 1890	6
Simopelta Mann 1922	21
Streblognathus Mayr 1862	2
Incertae sedis:	
†Archiponera Carpenter 1930	1
†Poneropsis Heer 1867	19
†Protopone Dlussky 1988	1
Platythyreini Emery 1901	
Platythyrea Roger 1863	44
Thaumatomyrmecini Emery 1901	
Thaumatomyrmex Mayr 1887	8
Total:	1631

itive stock” from which all other ants radiated. On his first published diagram displaying a summary of hypothesized ant phylogenetic relationships, Brown (1954) arranged the subfamilies into two major “complexes” forming a basal dichotomy (fig. 1), one of which depicts Ponerinae (s.l.) as comprised of several independent lineages splitting early. He commented that the ponerine tribe Ectatommini “appear[s] to be the stock from which the Myrmicinae developed at an early stage,” noting in turn a similar fate for the subfamily Leptanillinae and the dorylomorph ants (army ants), then classified into the single subfamily Dorylinae. Brown’s (1954) original depiction of Ponerinae s.l. as a paraphyletic subfamily was followed by subsequent precladistic authors usually representing it in the form of a basal group of “primitive ponerines” followed

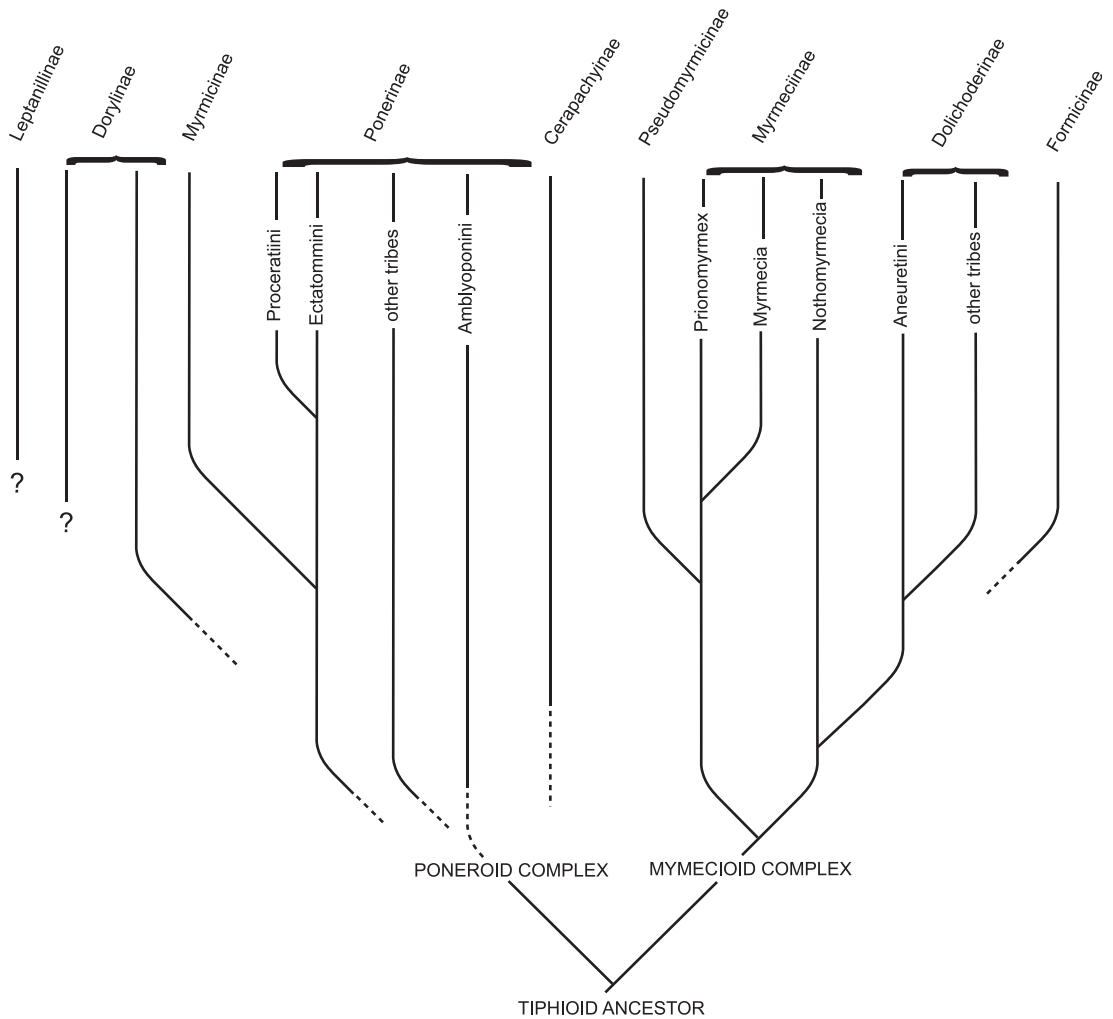


Fig. 1. Phylogenetic tree for the subfamilies of Formicidae after Brown (1954).

upward in the tree by a group of “advanced ponerines” from which other subfamilies arose (e.g., Wilson et al., 1967; Wilson, 1971; Taylor, 1978; figs. 2–3). This situation changed when quantitative cladistic analyses were first carried out in ants. In a couple of pioneer papers (Baroni Urbani, 1989; Baroni Urbani et al., 1992), the then recognized ant subfamilies were used, for convenience, as terminal taxa in the cladistic analyses with the implicit assumption of their monophyly. Since then *Ponerinae* s.l. was (implicitly or explicitly) conceptualized, for the first time, as a monophyletic taxon and was often treated as such by subsequent authors when discussing ant phylogeny (e.g., Bolton, 1990b).

It is worth noting the contribution to ant systematics made by William L. Brown, Jr. (1922–1997), when discussing the taxonomic history of this group. He is considered one of the greatest ant biologists of the 20th century (Gotwald, 1998; Wilson, 2000). His taxonomic work covered all ant taxa in all zoogeographical regions, but he was especially influential in shaping the taxonomy of ponerines through a methodical series of revisionary works on the group (Brown, 1952, 1958, 1960, 1965, 1975, 1976, 1978).

Regarding his philosophy on taxonomic methods, Brown can be considered a paradigm of the evolutionary taxonomy school of classification (i.e., Mayr, 1981; see also

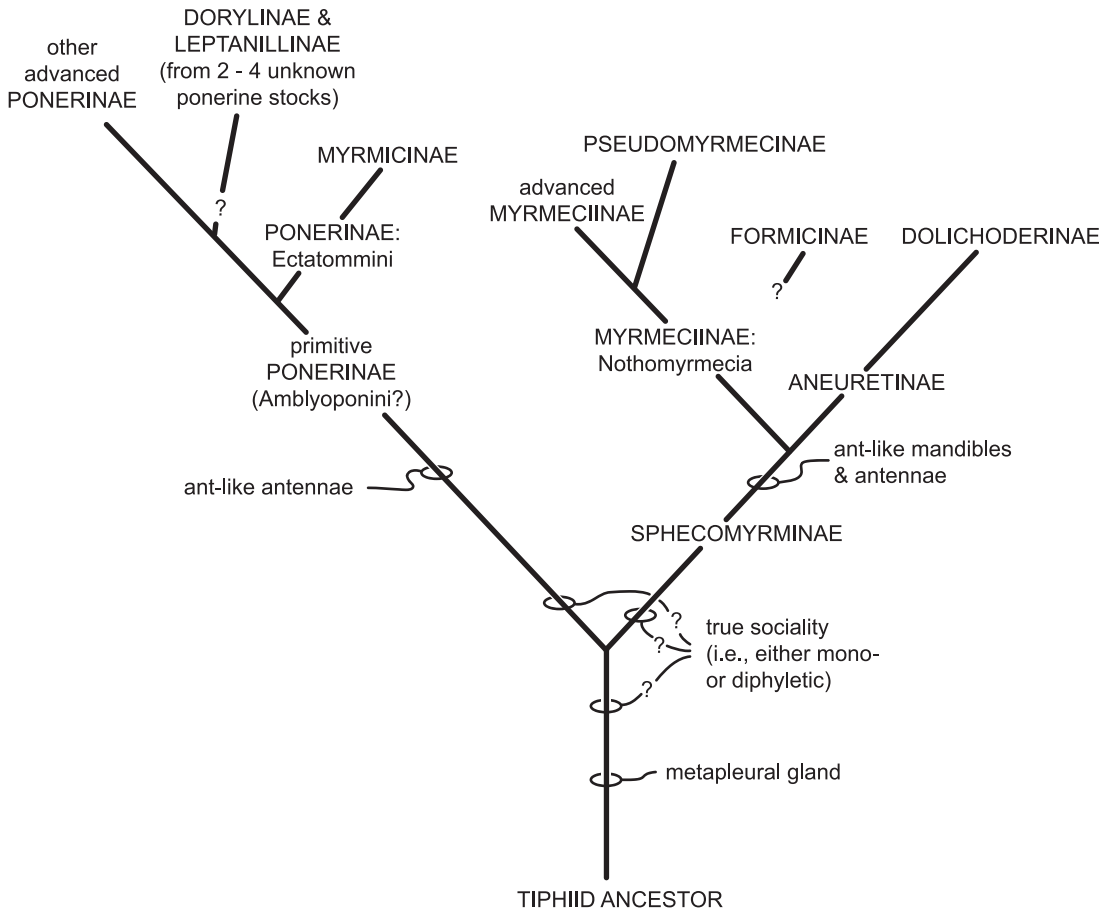


Fig. 2. Phylogenetic tree for the subfamilies of Formicidae after Wilson et al. (1967).

Wheeler, 1995), in which paraphyly played as important a role in translating phylogeny into classification as did monophyly, as well as considerations about grades and evolutionary tendencies, concepts that dropped out of favor with the advent of phylogenetic systematics (Hennig, 1966). In fact, until his very last publication Brown remained a staunch critic of cladistic methodology remarking that “cladistic techniques are not as robust for ants as have been hoped” (Brown, 2000: 74). It is therefore important to consider Brown’s intellectual position both when designing a phylogenetic study for poneromorphs (e.g., choosing exemplars for taxon sampling), as well as when comparing past classification with new phylogenetic results, since most of the hypothesized ant phylogenetic relationships should be read from

discussions he laid out through his revisionary work rather than by directly assuming that the current taxonomic hierarchy mirrors a nested system of monophyletic groups. A failure to consider the latter has generated the impression that ant taxonomy in itself has acted as an impediment for molecular phylogenetic studies of the group, and only the recent drastic taxonomic changes “freed molecular phylogeneticists trying to relate the subfamilies, making possible the studies than have appeared” (Crozier, 2006: 18030). This view results from the fact that taxon sampling in ant molecular studies has been predominantly guided (constrained) by the representation of available named taxa at a given taxonomic rank, rather than by the consideration of character variability and distribution among the group under study.

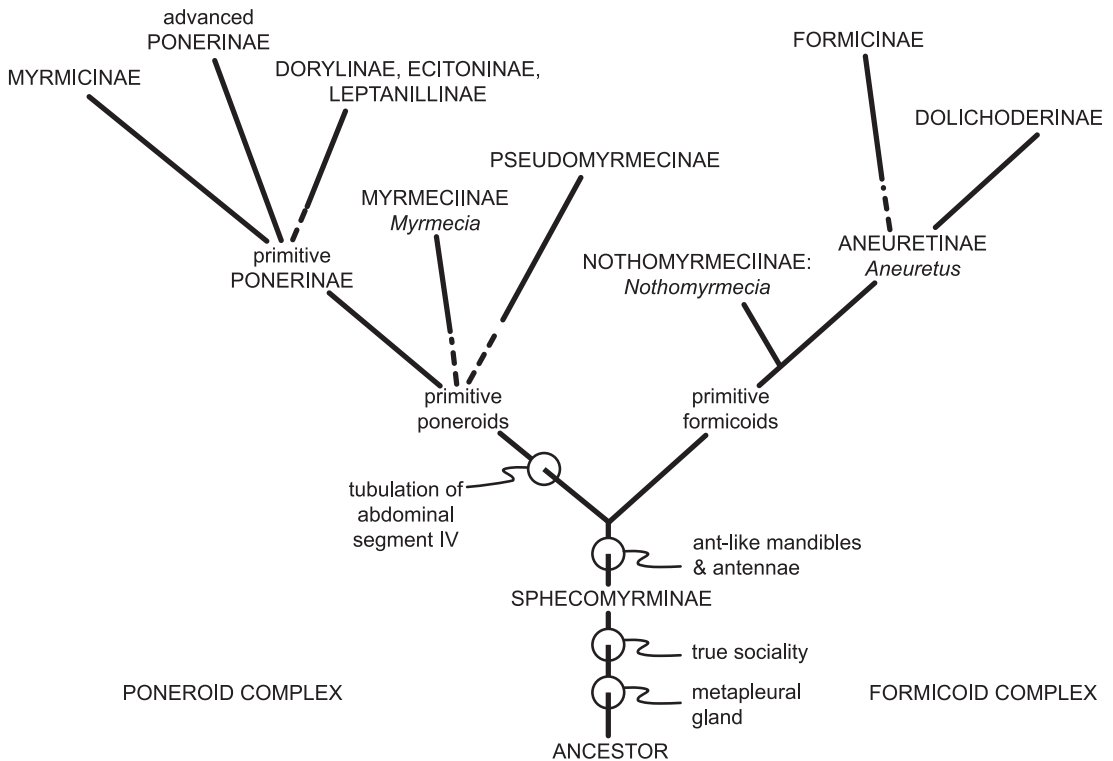


Fig. 3. Phylogenetic tree for the subfamilies of Formicidae after Taylor (1978).

However, given Brown's unmatched exhaustive and detailed knowledge of ant morphology it is not surprising that many of the "novel" discoveries brought by the recent large-scale molecular analyses (e.g., Brady et al., 2006; Moreau et al., 2006) have come to corroborate his long-standing views on ant phylogeny (fig. 4).

Despite its recognition as an artificial assemblage of subfamilies, poneromorphs are still the active focus of studies in phylogeny, morphology, and social organization, since these diverse subfamilies are considered key taxa for understanding ant biology as a whole given their status as the "socially primitive" taxa within the family (Wilson, 1971; Hölldobler and Wilson, 1990; Wilson and Hölldobler, 2005; Ward, 2006; Peeters and Molet, 2010). While great progress has been made in reconstructing the relationships among the ant subfamilies, the exact placement of the root for the ant clade remains elusive, although it is thought to lie somewhere within the poneromorphs (Brady et al., 2006; Crozier, 2006;

Rabeling et al., 2008). Consequently, the way in which poneromorph subfamilies relate to one another and to the rest of the ants is of major importance in understanding early ant diversification. From an anatomical perspective, the greatest variability in form and structural composition is found within the poneromorphs (Wilson and Hölldobler, 2005). Moreover, whereas the major nonponeromorph derived subfamilies each display an overall uniform skeletal type, despite containing the bulk of the known living ant species, it is among the poneromorphs that the key morphological transitional forms can be found. Hence, most major innovations of ant morphological evolution seem to have taken place in those early branches of the phylogeny.

THE IMPORTANCE OF STUDIES OF ANT MORPHOLOGY

The last few years have seen a surge in large-scale molecular phylogenetic studies on ants (e.g., Brady, 2003; Saux et al., 2004;

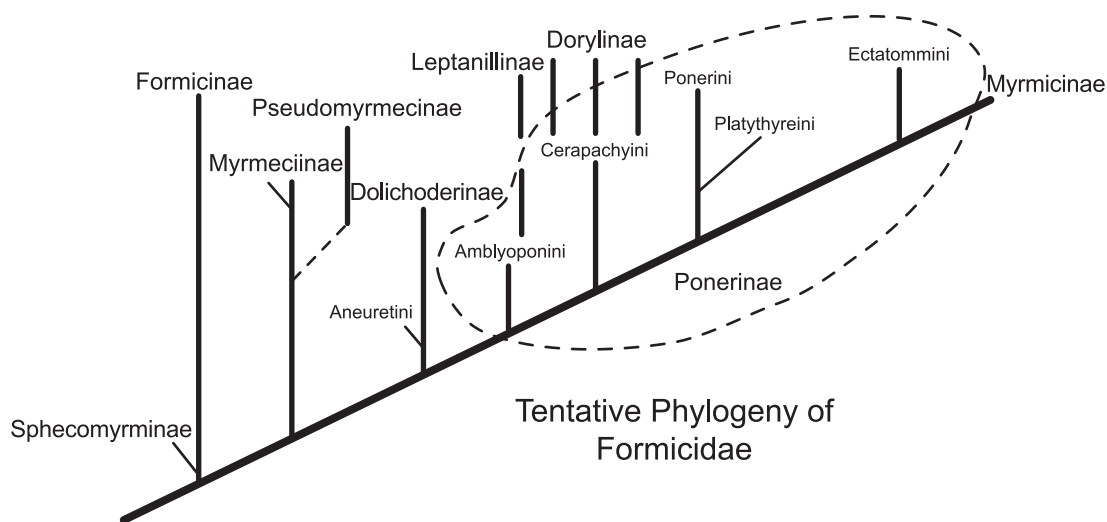


Fig. 4. Phylogenetic tree for the subfamilies of Formicidae after Brown (unpublished; circa 1986). Note the depiction of Ponerinae as comprising a paraphyletic subfamily, the sister-group relationship between Ectatommini and Myrmicinae, and the position of both Leptanillinae and Dorylinae (= dorylomorphs). This diagram was found by the author in a drawer of what used to be Brown's laboratory at Comstock Hall, Cornell University, in 1999. I thank Norman F. Johnson for helping date the plate.

Ward et al., 2005; Brady et al., 2006; Moreau et al., 2006; Ouellette et al., 2006), with analyses sampling several nuclear and mitochondrial gene regions for all recognized extant subfamilies or specific large portions of the ant phylogenetic tree. In contrast, comprehensive morphological data sets above the genus level have only been compiled for the dorylomorphs (Brady and Ward, 2005), Pseudomyrmecinae (Ward, 2001; Ward and Downie, 2005), and Myrmeciinae (Ward and Brady, 2003). No up-to-date morphological data sets exist covering any part of the poneromorph subfamilies let alone ants as a whole. Previously published data sets attempting to cover higher-level relationships or early ant diversification (e.g., Baroni Urbani et al., 1992; Shattuck, 1992b) are outdated mainly for relying on a ground-plan approach in character coding following a period of intense taxonomic rearrangement at the subfamily level. However, the increased activity in ant phylogenetic studies using molecular data have not superseded the need for acquiring and analyzing morphological data, but has rather increased the value of such data and made urgent the need to submit morphology to present-day analytical standards (see below).

The current morphological vacuum hampers our understanding of ant phylogeny and evolution at many levels. While our understanding of ant phylogeny has leapt forward greatly through the assemblage of large molecular-sequence data sets, a failure to incorporate morphology has caused a conceptual disassociation between the emerging phylogenetic pattern and the established taxonomy: current hypotheses about ant phylogeny are derived exclusively from molecular-sequence data (e.g., Brady et al., 2006; Moreau et al., 2006) while ant classification remains the summation of traditional nonphylogenetic considerations about ant morphology (e.g., Bolton, 2003). Given taxonomy's central role in linking all other areas of biology and in providing a common language to share and disseminate biological information, such a trend can have detrimental consequences in the field (Wheeler, 2004). Until the morphological information upholding traditional taxonomic decisions is properly codified into hypotheses of homology, such that they can be subjected to test by cladistic analysis in combination with molecular data, ant taxonomy will remain an uncorroborated, nonphylogenetic system existing in parallel with the emerging molecular-based phylogenies.

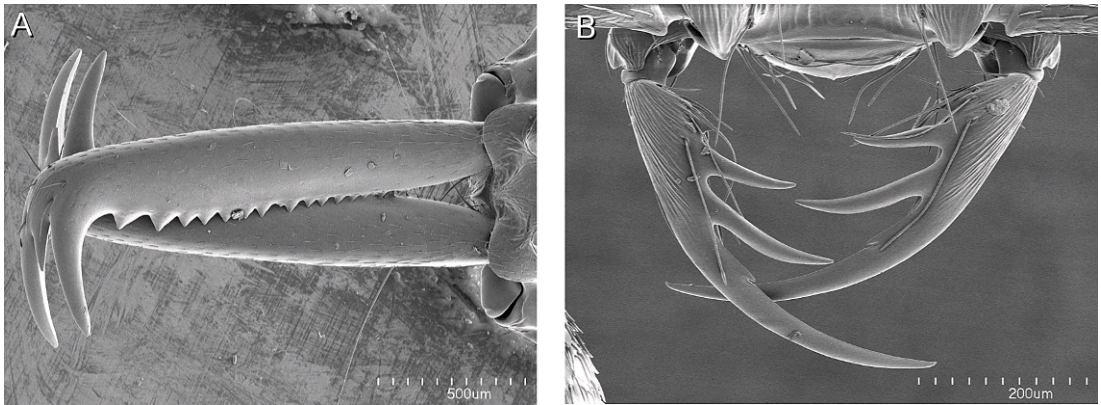


Fig. 5. Mandibles, dorsal view. **A.** *Anochetus emarginatus*. **B.** *Thaumatomyrmex atrox*.

Moreover, there is a rich and diverse fossil ant fauna extending into the early Cretaceous classified into exclusively extinct subfamilies (Engel and Grimaldi, 2005; Wilson and Hölldobler, 2005; Perrichot et al., 2007a). As additional taxa, fossils provide novel combinations of characters that can resolve problematic deep parts of phylogeny and can help in breaking up long branches (Donoghue et al., 1989; Cobbett et al., 2007). Also, importantly, fossils have the unique role of providing minimal ages of origin for taxa (Hennig, 1966) and thus calibration points for the estimation of lineage divergence times (Donoghue and Benton, 2007). However, incorporating this wealth of fossil information into phylogeny estimation is impossible without morphology. So far for ants, estimation of divergence times for molecular-based phylogenies have incorporated only that information on the fossil forms that can be assigned to extant taxa, mostly at the generic level (e.g., Brady, 2003; Ward et al., 2005; Brady et al., 2006; Moreau et al., 2006; Rabeling et al., 2008). Even then, the insertion of these fossils into a molecular-based phylogenetic tree has been achieved only indirectly by following the fossil's traditional taxonomic assignment rather than as a result of phylogenetic analysis combining both extinct and extant terminals. Clearly, the oldest known ant fossils, those currently classified into exclusively extinct taxa, have the potential to provide the best calibration points for deep nodes and thus increase the accuracy of divergence-time estimations for Formicidae

(Perrichot et al., 2007b). Building a comprehensive morphological data set is thus the first step necessary for the incorporation of these diverse and important fossil ant faunas into the reconstruction of ant phylogeny.

The study of ant morphology from a phylogenetic perspective is important in its own right and has the potential to have an impact on other areas outside systematics. Ants are one of the dominant groups of animals in terrestrial ecosystems (Hölldobler and Wilson, 1990), and the diversity of habitats they occupy is reflected in both their number of species (>12,000 spp. so far described, Agosti and Johnson, 2007) and morphological adaptations. To mention just one example, take foraging behavior: different ant species within a community can take specialized roles as scavengers, predators, granivores, and herbivores (Ward, 2006), and this wide range of roles is reflected in the extreme diversity of mandibular form and structure found across ant taxa. Even within a particular foraging specialization the multiplicity of structural specializations is impressive: compare the predatory mandibles of the trap-jaw ants (Gronenberg et al., 1993) of the genus *Anochetus* (fig. 5A) with those of the genus *Thaumatomyrmex* (fig. 5B), a group of species that feeds exclusively on polyxenid millipedes (Brandão et al., 1991), both members of Ponerinae s.s. The pattern of mandibular evolution in ants is best reconstructed by reducing its parts to statements of homology in the form of characters optimized in the best tree resulting from the

congruence of all the data at hand (Carpenter, 1992; Wenzel, 1997), while at the same time such a pattern serves as a proxy for understanding the evolution of foraging behavior in the light of phylogeny.

Another example of the interaction between basic studies of comparative morphology and other areas of ant biology can be found within the field of evolutionary developmental biology, aka *evodevo*. Here ants already feature prominently as a “natural” system for the study of the genetic developmental mechanism behind the skeletal-muscular morphogenesis of the winged thorax found in males and gynes, and its suppression during the development of the flightless thorax in workers (e.g., Abouheif and Wray, 2002; Robinson, 2002; Sameshima et al., 2004). These types of developmental studies are already being extended comparatively to the study of ant species in which the reproductive females display “aberrant” arrangements in the adult thoracic sclerites, but are nonetheless produced normally during the colony’s life cycle (e.g., Baratte et al., 2006). Such cases of unusual thoracic morphology can be found across a wide variety of ant taxa, but occur most commonly among poneroid ants (Peeters, 1987). Again, a comparative study of thoracic morphology among ant castes and across the family is necessary for establishing the hypotheses of homology that provide the basis for understanding thoracic evolution and development (Love, 2006). In sum, the phylogenetic study of ant morphology is a rich and interesting area per se and through the comparative perspective has the impact of aligning different fields of ant biology that by their nature deal with the study of form under the common language of phylogenetics and thus evolutionary theory.

DIGITAL ATLAS OF ANT MORPHOLOGY

The reason behind the scant availability of morphological data for phylogenetics is not the lack of published studies dealing with ant morphology, but the fact that such a body of work is scattered across many publications and varies greatly in its depth and scope. These legacy data include phylogenetic analyses, comparative anatomy studies, revisions,

monographs, identification keys, and even behavioral studies. Taxonomic scope ranges from studies covering several subfamilies to single species or a particular caste within a species. However, even with access to all the relevant publications, extracting the relevant information is a slow and laborious process, since there is little to no standardization in the way the morphological data have been recorded.

A tradition of studies in comparative ant morphology during the second half of the 20th century produced an extensive set of published work. Some of the systematic surveys covering particular structures or life stages across all ant taxa include: proventriculus (e.g., Eisner and Wilson, 1952; Eisner, 1957); mouthparts (e.g., Gotwald, 1969; Gotwald, 1970; Gotwald, 1973); sting apparatus (e.g., Kugler, 1978a, 1979a, 1979b, 1980, 1986, 1991, 1992); strigil (e.g., Francoeur and Loisel, 1988); and larvae (e.g., Wheeler and Wheeler, 1951, 1952a, 1952b, 1953, 1956, 1960). Although the wealth of illustrations accompanying these studies remain an invaluable source of morphological information, incorporating these legacy data, produced independently by many different authors over a period of half a century, into a phylogenetic analysis can become an insurmountable problem, not least because the descriptive part of the work requires thorough reinterpretation.

Of all the types of studies mentioned above, phylogenetic analyses provide the best way to summarize, document, and disseminate comparative data through the translation of anatomy into discrete character states (Ramírez et al., 2007). Ideally, morphological data should be no different from molecular-sequence data in terms of how easily it can be retrieved from previously published work and combined with newly generated data to perform phylogenetic analyses covering a wider range of taxa or previously unexplored groups. In practice, it is seldom the case that morphological data can be seamlessly integrated from one study to the next without the need to revisit the original specimens. Additionally, the complexity of morphology in comparison with molecular sequences means that the former often requires a reinterpretation of the anatomical observations in the light of a new or a different combination of

taxa (Rieppel and Kearney, 2002; Jenner, 2004a).

Issues of study design also have the potential to affect the future use of a given morphological data set. For example, Baroni Urbani et al.'s (1992) study of high-level Formicidae relationships was based on a ground-plan approach to character coding (*sensu* Prendini, 2001), utilizing the then-current system of subfamilies as terminal taxa in their analysis. The subsequent discovery of new important extant and extinct forms (e.g., Ward, 1994; Grimaldi et al., 1997) followed by a period of intense taxonomic rearrangements at the subfamily level (culminating in Bolton, 2003) has rendered the coded morphological data unusable since now there is little correspondence between the terminal taxa in that matrix and the currently recognized subfamilies.

Analysis, standardization, documentation, and dissemination of comparative morphological data can be improved greatly through the construction of digital atlases of morphology (Ramírez et al., 2007). Such atlases consist of a collection of images in the form of drawings, photographs, or electron micrographs depicting standardized views of all the anatomical structures of interest for all the taxa under study. Through a digital atlas, comparing a single anatomical feature across a wide range of taxa becomes straightforward, because the laborious process of gathering and preparing all the necessary specimens for a given observation has been dealt with beforehand. The ability to compare dozens of images quickly facilitates the evaluation of structural detail and variability found within a morphological feature, thus resulting in stronger hypotheses of homology and, hence, characters that reflect better the evidence at hand. This is especially true in the case of an atlas of high-resolution images derived from scanning electron microscopy. Since the information is in a digital format, management and curation of all the data are greatly facilitated.

A growing number of tools are being developed in taxonomy, tools that result from the interplay of digital imaging, cyber infrastructure, and information technology (Bisby et al., 2002; Wheeler, 2004); one result is that dissemination of morphological information is rapidly approaching the "same

data-sharing standards that our colleagues in molecular systematics already use to their great benefit" (Agosti, 2003). Myrmecology plays a leading role in this bioinformatics revolution (Clarke, 2002; Gewin, 2002) with the development of pioneer web-based tools like *antbase.org* and *antweb.org* (Agosti, 2005): the former offering a name server with the totality of information about ant nomenclature and a digital library containing all the systematic literature on ants from Linnaeus to the present, and the latter containing a database with images of type and general specimens in museum collections and their associated geographical data. At the same time, the Hymenoptera anatomy ontology (Yoder et al., *in press*) now provides access to an online controlled vocabulary of anatomical terms, and MorphoBank (O'Leary and Kaufman, 2007) and Morphbank (2007) are online databases created specifically for the archiving and dissemination of morphological data as single images or morphological atlases.

GOALS OF PRESENT STUDY

The present study is the first attempt to compile a comprehensive morphological data set for phylogenetic analysis of ants, with special emphasis on poneromorph subfamilies. The core of the project involves the construction of a digital atlas of skeletal morphology for adult workers, since this caste is that best represented in collections around the world.

The atlas contains exemplars of most extant poneromorph genera as well as representatives from all other living ant subfamilies with the exception of Martialinae, recently described from a single worker (Rabeling et al., 2008). In addition, morphological data were compiled from published work on Formicidae, ranging from traditional taxonomic treatments to cladistic analyses and comparative studies of particular character systems, with the goal of integrating much of the substantial, but fragmentary, body of literature dealing with ant morphology. However, each observation has been checked against actual specimens and the survey has been expanded to include many taxa never studied before. As a result, most characters are here

reinterpreted to account for the variability observed in this increased taxon sample. Emphasis was placed on defining each character in a standardized form across the whole Formicidae. The present survey yielded many new characters never used before in ant taxonomy or phylogenetics.

MATERIALS AND METHODS

Dry pinned specimens examined were obtained from the American Museum of Natural History, New York (AMNH; provided by James M. Carpenter); Museum of Comparative Zoology, Cambridge, Massachusetts (MCZ; provided by Stefan Cover); and the Natural History Museum, London (BMHN; provided by Barry Bolton). Additional specimens in ethanol were obtained by generous donations from Donat Agosti (Bern), Barry Bolton (BMHN), Christian Peeters (Université Pierre-et-Marie Curie, Paris), and Brian Fisher (California Academy of Sciences, San Francisco, CASC), as well as from the author's personal collection. All additional specimens used in this study have been deposited at the AMNH.

TAXON SAMPLING

The present study utilizes exemplar species as terminal taxa. There are a number of theoretical and practical reasons that have been put forward favoring the use of exemplar species over supraspecific ground plans as terminals in phylogenetic studies (reviewed in Prendini, 2001). The use of exemplar species as terminals is further justified given the superiority of this approach when it comes to the documentation, maintenance and continuity of morphological data. In the same way that compilation of DNA sequences rests on the use of exemplar specimens as units for molecular-based studies (Vrana and Wheeler, 1992), compilation and codification of morphology through the construction of an atlas of images leads naturally to the use of species as units for comparative anatomy. In the phylogenetic paradigm, species are the smallest aggregation of individual life cycles that can be diagnosed as sharing a unique combination of character states (Nixon and Wheeler, 1990; de Pinna, 1999). Under this

definition, species are not only the basic units of cladistic analysis (Wheeler and Platnick, 2000), but the emphasis on diagnosis and cluster homogeneity means that they are the basic units for documentation and dissemination of morphological information par excellence. Maintenance and continuity is facilitated because extrapolation of information can be kept to a minimum (Prendini, 2001) and data integrity is less prone to deteriorate because of changes in ideas on supraspecific relationships (as exemplified by Baroni-Urbani et al.'s 1992 study). Finally, the use of exemplar species renders the morphological data open-ended: by documenting the information at the level of species, expanding or assimilating a character matrix with data generated at a future stage becomes easier, because there is little further need to split and resolve terminals from one study to the next or when combining morphology with other types of data (e.g., DNA sequence data) in the construction of supermatrices (e.g., de Queiroz and Gatesy, 2006). Succinctly put, an exemplar approach confers on morphological data many of the benefits already existing for molecular data.

In order to avoid sampling bias due to preconceived notions of relationships, exemplars were chosen primarily to represent morphological diversity and only secondarily based on classification. An iterative procedure involving both taxon and character assessment was used as follows. A large collection of specimens belonging to as many species as possible from all poneromorph genera and from all geographical regions was first examined under a light stereomicroscope. One species was chosen to represent a genus when all the congeneric species examined proved to be homogeneous (invariable) for the characters initially under consideration. When different species within a genus showed different combinations of characters, the taxon was broken into smaller groups of species and one of them was chosen as exemplar for the new cluster. The process was repeated until all resulting groups were homogeneous. As the study advanced and new characters were deemed important, either suggested from the literature or newly discovered through dissections and scanning electron microscopy study, the exemplified

groups were reassessed and further broken into less inclusive homogeneous groups if necessary. This latter step was repeated also when taxa not originally examined were brought into consideration. In choosing exemplar species, an attempt was made to include the type species of each genus when available in order to ease nomenclatural stability.

In the case of the highly heterogeneous genus *Amblyopone* and the large and problematic genus *Pachycondyla* (sensu Bolton, 1995; Bolton et al., 2007), both suspected to comprise paraphyletic groups, only enough species were included potentially to refute their monophyly. However, further study will be needed to resolve satisfactorily their taxonomic circumscription.

A less-strict form of the iterative procedure outlined above was employed to choose exemplar species for the remaining extant formicid subfamilies. Exemplifying the non-poneromorph subfamilies proved to be straightforward because these either contain only one or two well defined extant genera (e.g., *Agroecomyrmecinae*, *Aneuretinae*, *Apomyrminae*, *Myrmeciinae*) or their members display low variability for the majority of the characters under consideration (e.g., *Pseudomyrmecinae*, *Formicinae*, *Dolichoderinae*, *Myrmicinae*).

The present survey includes 71 exemplar species representing 42 poneromorph genera. This includes all extant poneromorph genera with the exception of the following six for which no specimens were available for study: *Aulacopone*, a genus from southern Russia known from the holotype queen plus a second specimen, both in Russian collections (Arnol'di, 1930; Taylor, 1979); *Bannapone*, a genus from China known only from the holotype queen (Xu, 2000); *Paraprionopelta*, a genus from Tucumán, Argentina, known only from males (Kusnezov, 1955b); the recently described Afrotropical genus *Boloponera* (Fisher, 2006); and *Feraponera* and *Promyopias*, a pair of Afrotropical genera created and resurrected respectively to accommodate species resulting from a recent revision of the genus *Centromyrmex* (Bolton and Fisher, 2008). An additional 32 exemplar species are included to represent the remaining 14 extant formicid subfamilies, with the exclusion of the army ant subfamily

Aenictogitoninae, known only from males (see Brady and Ward, 2005) and *Martialinae*, known only from the holotype worker.

Choosing nonformicid outgroups for a phylogenetic analysis based solely on the morphology of the worker caste poses important practical problems. Presence of a wingless worker caste is an evolutionary novelty unique to ants, and so in principle there is no comparable semaphoront outside the family: eusociality in ants is an independent derivation from other cases of sociality within the Hymenoptera and workers in all of these other social taxa are fully winged (Wilson, 1971). Wingless females occur in some non-social vespoid families (e.g., *Mutillidae* and *Bradynobaenidae*), but these are not the result of a polyphenism (i.e., alternative, environmentally induced developmental morphs) as in the case of ants, and current phylogenetic hypotheses for the superfamily do not place such taxa as sister to Formicidae (J.M. Carpenter and L. Vilhelmsen, personal commun.). The independent evolution of winglessness in worker ants and in the nonsocial families with wingless females is further evident by the highly different configuration of the sclerites of the nonflying thorax (Reid, 1941; R.A. Keller, unpubl. data), which makes anatomical comparison difficult. However, with the exception of the thorax and visual organs (i.e., ocelli and compound eyes), most of the characters surveyed in this study seem common to all female ants and not exclusive to the worker caste. For this reason, exemplar species of winged solitary females of the nonformicid families Vespidae and Scoliidae were chosen as outgroups following Brothers and Carpenter (1993) and Brothers (1999) that consider those families as sister to Formicidae.

The total of 105 terminal taxa, their classification and geographical distribution, are listed in appendix 1.

CHARACTER SAMPLING

The character matrix was edited using WinClada, version 1.00.08 (Nixon, 2002). The characters compiled were derived from the skeleton of the adult worker in the case of the ants and from the females in the case of the outgroups, and include cranial features, mouthparts, thoracic sclerites, legs, abdominal

sclerites, and sting apparatus. Particular attention was devoted to the antennal sockets (including the basal articulation of the scape), the labrum and labiomaxillary complex, and the antenna cleaner (= strigil), since these systems have not been surveyed extensively before.

As described in the previous section, taxon and character sampling are treated as inter-related procedures in morphology-based analyses. Character selection was based on an assessment of the variability of each character among the exemplars under investigation. When a morphological feature was deemed important within an initial set of exemplars, its exact taxonomic distribution was determined by scanning further species related to those in the original set. Additional species were included as part of the exemplar set if this resulted in a better representation of the character's variability. For example, when an anatomical variant was found on an exemplar species typifying a genus, both congeneric species as well as species of putatively related genera (e.g., genera within the tribe) were examined to determine if the variant was present outside the realm of exemplars in the initial set. A character was deemed too variable for this analysis if complete representation of its variability would result in excessive introduction of exemplars into the matrix (e.g., having to include most of the species for most genera).

Some of the characters investigated require special manipulation of the specimen (e.g., protrusion of the maxillae and labium) or disarticulation of the skeleton (e.g., opening/closure of metacoxal acetabula) for proper assessment. In the few cases when this manipulation was deemed undesirable due to limited availability of material (i.e., genera only known from the type series), the taxa were coded as unknown "?" for those characters. Characters inapplicable for a given taxon are coded as "-."

A diverse source of published work on myrmecology and Hymenoptera in general was scanned for potential characters. The level to which morphological information has been documented in these studies varies greatly. Comparative anatomy studies of a particular character system, taxonomic monographs, and cladistic analyses provided the best sources,

because they excel in either morphological detail or taxonomic scope. However, some characters were obtained from nonsystematic publications in areas such as behavioral ecology, chemical ecology, and biomechanics.

All characters taken from the literature, independent of their level of documentation, were treated as a guide to conduct direct observation of specimens. Their usefulness was, therefore, reevaluated across the complete range of the exemplar taxa covering all Formicidae. As a result, some characters were ultimately excluded because their delimitation and definition became problematic in the increased sample. These include cases where a character was apparently discrete within a restricted collection of taxa, but became continuous once the sample was extended to include intermediate forms, or cases in which a character may have been well defined within a specific taxon, but its definition became ambiguous outside the group in question. The latter case was common in characters primarily used for taxonomic diagnosis—characters that make the identification of a particular taxon easy, but nevertheless fail as primary homologies (see below). Finally, characters from the literature that could not be evaluated by direct observation in specimens were excluded from the analysis. Most characters based on the occurrence of particular glands fell within this category, because the type of specimen preservation and histological preparation needed to evaluate their presence in the larger sample considered here was beyond the scope of this study (see also Characters Excluded from the Analysis, below). While the above criteria exclude many characters considered "traditional" in ant systematics, the decision was deemed justified for the gain in precision, consistency, and repeatability that can be achieved when morphology is submitted to such critical evaluation (Jenner, 2001, 2004b).

During the course of this study it became apparent that many characters currently used in ant systematics are based on broad generalizations, often derived from detailed morphological investigation that employed a very limited and selective taxon sample. The present work, instead, was done with a strong emphasis on character documentation, grounding each cell in the character

matrix explicitly to specimens in the hope that this will serve as a bedrock study for future work on phylogenetic morphology.

MORPHOLOGICAL ANALYSIS

Character coding was done following a comparative anatomical study of the exemplar specimens. This procedure involves the formation of primary conjectures of homology through the atomization of the skeletal structures under investigation, leaving aside considerations of a priori taxonomic schemes. Characters coded in this way represent the smallest particles of structural variation with putatively independent phylogenetic information. This procedure contrasts with the search for diagnostic characters to support intuitive a priori schemes of classification; with the reduction of different morphological variants within a set of serial homologs into the form of formulas (e.g., palp formula, Shattuck, 1995: char. 10); and with the concatenation of otherwise independent characters into structural wholes or Baupläne (e.g., Perrault, 1999, 2000, 2004). Such practices result in a potential loss of phylogenetic information and may obscure relations of homology, thus introducing unnecessary constraints in the process of translating anatomical observations into phylogenetic characters.

Following the criteria described above, character hypotheses suggested from the literature were evaluated based on how well they performed to identify and delimit primary homology. Characters that failed as conjectures of homology or provided a poor identification of homology were discarded or thoroughly reevaluated, the latter often resulting in merging or splitting of characters previously used in cladistic analysis.

One important aspect of taxonomic work is to provide tools for the identification of taxa, and hence the vocabulary used in the taxonomic literature is heavily diagnostic—morphology is often characterized in extrinsic terms (how it is viewed) rather than intrinsic ones (how it is). Although sufficient to allow identification (e.g., in taxonomic keys), such vocabulary may be ambiguous for communicating information about homology. In the present study, an attempt was made to describe characters in anatomical terms. For

example, characterizing the peculiarities of the labiomaxillary complex, as found in most dorylomorph ants, in terms of the shape of the stipites (see char. 35), was preferred over a characterization based on whether the prementum is visible or not when the mouthparts are fully closed (e.g., Brady and Ward, 2005: 6, char. 13). Referring to a structure by its proper anatomical term not only improves communication, but also effectively establishes the hypothesis of identity that is necessary in the inference of homology (Rieppel and Kearney, 2002).

To further improve communication and strengthen homology identification, each homolog (= character state) described has been typified by reference to a particular species (see Ramírez et al., 2007). The goal behind this practice is to ground explicitly the meaning of morphological terms with particular empirical examples, and so guide and facilitate the interpretation of the characters described here by subsequent workers. Such practice recognizes the ostensive element in the definition of homologies as “natural kind” terms (Rieppel, 2005, 2006).

DIGITAL ATLAS

Specimens were prepared for scanning electron microscopy (SEM) using the following procedure. Whole unpinched adult workers fixed in 70% ethanol were washed in distilled water and gently brushed to remove dirt particles, before placing them in 90% ethanol for at least 20 minutes. The left antenna was removed to expose the antennal socket and the mouthparts were protruded. Specimens were then transferred to filter paper where they were positioned with their antenna and legs spread away from the body in a “natural” position so as to allow an unobstructed view of all parts of the body without the need of further disarticulation. They were then point mounted to the right side of the mesosoma leaving a clear ventral view (i.e., with the coxae exposed), and left to air dry for at least 12 hours prior to scanning. The left antenna was also point mounted at the distal articulation of the scape with the pedicel, thus allowing a clear view of both the bulbus (= radicle) and the flagellar apex. Point-mounted dry specimens were remounted

by submerging them in warm distilled water to dissolve the mounting glue and relax the articulations, before placing them in 90% ethanol after which the same treatment was applied. Old dry specimens covered in body waxes were given an additional wash in 10% KOH for a few seconds and then rinsed thoroughly with distilled water prior to the ethanol step.

Additional specimens were completely disarticulated by digestion of the soft tissues in cold 10% KOH overnight. Then they were transferred to 10% acetic acid for a few seconds and finally rinsed in distilled water. All sclerites were kept in vials with 90% ethanol for inspection. This collection of disarticulated material was mainly used to double-check and further understand structures by examination under light microscopy (both compound and stereoscope), but was also used as a source of material for SEM work. In the latter case, the particular structures were mounted on SEM stubs using double-sided adhesive conducting tape, and returned to 90% ethanol afterward.

Point-mounted specimens and disarticulated structures mounted on stubs were coated with gold-palladium, except when the specimens were rare (i.e., poorly represented in collections). Images were taken using a Hitachi S4700 field emission scanning electron microscope at the AMNH, at a voltage of 5–10 kV for coated specimens and 1kV for uncoated ones.

The atlas of images was assembled from a set of 28 standard views of different parts of the body generated for all the exemplar species listed in appendix 1. These standard views were selected based on an assessment of character variability and to maximize the amount of information retrievable from the comparison of corresponding images across the different exemplar taxa. All lateral views are from the left side. Following is the list of 28 standard views and the details each shows.

Habitus, lateral view: full body from the anterior portion of the mandibles to the gastral apex.

Head, full face view: both the vertex and the apex of the mandibles.

Head, lateral view: the eyes and antennal scrobes if present.

Antennal socket, lateral view: the torulus with the antenna removed.

Antenna, dorsal view: the complete length of the scape and flagellum.

Bulbus, frontal view.

Bulbus, posterior view.

Antennal apex: magnification of the sensilla on the apical segment of the flagellum.

Mandible, lateral view: the malar area.

Mouthparts, ventral view: the labrum, maxillary stipes and palps, labial prementum and palps, and the hypostomal bridge; also the galea and glossa if possible.

Mesosoma, lateral view: from the anterior margin of the pronotum to the back of the propodeum.

Mesosoma, dorsal view: from the anterior margin of the pronotum to the propodeal foramen.

Mesosoma, ventral view: the pro-, meso-, and metacoxae.

Propleura, ventral view: the prosternal process.

Metapleural gland opening, lateral view: the posterior lower corner of the mesosoma, including the propodeal spiracle and the propodeal lobes if present.

Strigil, anterior view: the calcar, basitarsal notch, and distal articulation of the tibia.

Strigil, posterior view: the calcar, basitarsal notch, and distal articulation of the tibia.

Mesotibial spur, anterior view: part of the tibia and anterior face of the basitarsus.

Metatibial spur, anterior view: part of the tibia and anterior face of the basitarsus.

Metatibial spur, posterior view: the setal brush at the distal end of the metatibia if present.

Propretarsal claws: at least tarsi III–V.

Metapretarsal claws: at least tarsi III–V.

Metatrochanter, ventral view.

Petiole (= abdominal segment II), lateral view.

Petiole (= abdominal segment II), ventral view.

Metasoma (= abdominal segments III–VII), lateral view.

Metasoma (= abdominal segments III–VII), ventral view.

Metasomal apex, lateroposterior view: the pygidium, hypopygium, and sting if present.

Additional images were taken to document and compare features particular to a given

exemplar species or higher taxon (e.g., presence of stout setae on the mesotibial dorsum). The resulting set of images per exemplar species ranges from 28 to 68. All images are tied to voucher specimens deposited at the AMNH unless otherwise noted.

The digital atlas contains 5250 digital images from 105 different species in 72 genera (~25% of all extant ant genera). The atlas will be available for future reference as an online searchable database accessed through *antbase.org* (Agosti and Johnson, 2007), in partnership with Morphbank (2007) and Morphobank (O'Leary and Kaufman, 2007).

CLADISTIC ANALYSIS

The final matrix was analyzed under parsimony using the program NONA version 2.0 (Goloboff, 1997a) spawned via WinClada version 1.00.08 (Nixon, 2002), and TNT version 1.1 (Goloboff et al., 2003a). Parsimony was chosen over competing methods because it implements a model that seeks to maximize homology from the primary conjectures coded in the matrix to the optimal tree (Farris, 1983; de Laet, 2005). Searches were performed under equal weights using NONA and WinClada and under implied weights (Goloboff, 1993) as implemented by TNT.

Equal-weight searches were initially performed using the parsimony ratchet (Nixon, 1999) as implemented in WinClada executing 100 sequential ratchet runs, with 500 iterations per replication, holding four trees per iteration, and sampling 16 characters. In order to explore further potential islands of parsimonious trees (Maddison, 1991) and achieve total collapsibility of the most parsimonious trees (Nixon and Carpenter, 1996a), the final pool of trees resulting from the ratchet runs was resubmitted to NONA using the commands "hold 50000"; "amb ="; "poly -"; and "max*" (i.e., consider trees as dichotomous and keep trees with ambiguous support; perform a round of TBR swapping hold up to 50,000 trees in memory), followed by "amb-" "poly ="; and "best" (i.e., treat trees as polytomous and discard trees with ambiguous support, keep trees that are topologically different and of highest fit).

Implied-weight searches were performed using constants of concavity K from 1 to 10,

in order to compare the effect of down-weighting, strongly to weakly, against homoplasious characters. For all values of K , the searches consisted in 10,000 replicates with TBR swapping holding a maximum of 6 trees per replica and 100,000 trees in memory. The pool of resulting trees was submitted to an additional round of TBR swapping.

Clade support was assessed by calculating symmetric resampling values (Goloboff et al., 2003b) as implemented in TNT. For both equal-weight and implied-weight analyses, 1000 replicates were performed with a change probability of 0.33 (the default probability in TNT). Results from these analyses are expressed using the frequency differences (GC) option in TNT, where, in addition to the frequency of group occurrence, the final calculation of support values takes into account the frequency with which a given group is contradicted in the replicates.

Inspection of most parsimonious trees, generation of strict consensus, optimization, inspection of characters and generation of trees for figures was performed in WinClada.

CHARACTER DESCRIPTIONS AND DISCUSSION

ABBREVIATIONS AND CONVENTIONS

When an "absent" state occurs in a character it is arbitrarily coded as 0 (zero) for convenience. By default, all multistate characters are treated as nonadditive, unless specified as "additive" in the character description. Abbreviations of anatomical terms in figures follow Snodgrass (1956).

NOTE ON ANATOMICAL TERMINOLOGY

As discussed above (Morphological Analysis), some morphological terms commonly used in identification keys and taxonomic diagnoses were found to be too general or loosely defined to serve when translating results from comparative anatomy into defined characters. An effort was made to provide more exact definitions when necessary, while preserving common use and original intent as much as possible. Also, terms of broad use in Hymenoptera were preferred over synonyms used exclusively

within the myrmecological literature. New terms were introduced only when this resulted in better individuation of the structures and their parts (i.e., better statements of homology), and hence an increase in the precision of hypotheses regarding the putative identity of these structures across the taxa under consideration. New terms appearing in the text are indicated by “*” at their place of definition. The following are some terms used throughout this study.

Suture, *articulation*, *sulcus*, and *line* are used according to Daly (1964) and Gibson (1985) as follows: *suture* refers to a groove formed by the fusion of two formerly distinct sclerites, while *articulation* refers to a movable or flexible line of contact between sclerites; *sulcus* refers to an external groove or furrow corresponding to an internally invaginated ridge, while *line* refers to an external linear mark devoid of internal invagination.

Head orientation. All ants are prognathous insects, i.e., the head is tilted forward, so that the mandibles, rather than the antennae, are the frontalmost appendices (see char. 1). Because of this, structures in the head of ants are traditionally described following a different orientation from that of most other Hymenoptera. For example, in ants the clypeus is commonly described as extending *posterad* between the antennal sockets rather than *dorsad* (see char. 5). This system of head orientation, while specific to prognathous insects, has been followed here for consistency with all the literature dealing with the head anatomy in ants. The outgroups have been coded in turn for practical purposes only as if they were prognathous.

*Supraclypeal area** (= frontal triangle, Bolton, 1994) is a well-delineated, unpaired area, present almost universally within the Formicidae, lying immediately posterior to the median part of the clypeus between the frontal carinae (fig. 6). In taxa with separated antennal sockets this area is triangular in shape and has been referred to as the frontal triangle (e.g., Hölldobler and Wilson, 1990; Wilson, 2003). However, many deviations from a triangular shape occur in taxa where the antennal sockets are confluent (e.g., Ponerinae).

Following Prentice (1998), the medial section of the epistomal sulcus that runs between

the anterior tentorial pits is termed *frontoclypeal sulcus*. The lateral sections, running on each side from the anterior tentorial pit to the dorsal (= anterior) articulation of the mandible are termed *paroculoclypeal sulci*.

Mouthpart terminology follows Gotwald (1969).

Mesosoma refers to the tagma formed by the three thoracic segments plus the propodeum (= first true abdominal segment). This term has gained wide acceptance and use across apocritan Hymenoptera and should replace the terms “alitrunk” and “trunk” originally introduced by Brown (1975) and commonly used in Formicidae literature for the corresponding tagma.

Metasoma refers to all the remaining abdominal segments posterior to the mesosoma (e.g., external true abdominal segments II–VII in females) regardless of the number of abdominal constrictions found after the propodeum.

Petiole refers to the specialized second true abdominal segment found in all ants. Subsequent external abdominal segments are labeled by their corresponding homologous true segment roman numeral (i.e., III–VII), even when the third true abdominal segment is specialized to form a postpetiole. The term *gaster* (i.e., true abdominal segments II–VII, III–VII, or IV–VII) is not used in the present study.

Following Bolton (1990a), *presclerite* refers to the anterior articulatory region of each abdominal sclerite, either the tergum or sternum, which is overlapped by the preceding segment. The external surface of these areas is unambiguously delimited by microscopic, weakly reticulated sculpture devoid of pilosity, appearing smooth and usually shiny under light stereoscope. Thus, the remaining posterior part of the sclerite is termed *postsclerite*.

Helcium refers to the specialized presclerites of the third true abdominal segment (Bolton, 1990a), both pretergite and presternite. The helcium articulates within the narrow petiolar foramen (= true second abdominal segment) found in ants.

The tergite and sternite of the seventh true abdominal segment (in adult females) are labeled as *pygidium* and *hypopygium* respectively when referring to those sclerites individually. All other abdominal terminology follows Bolton (1990a).

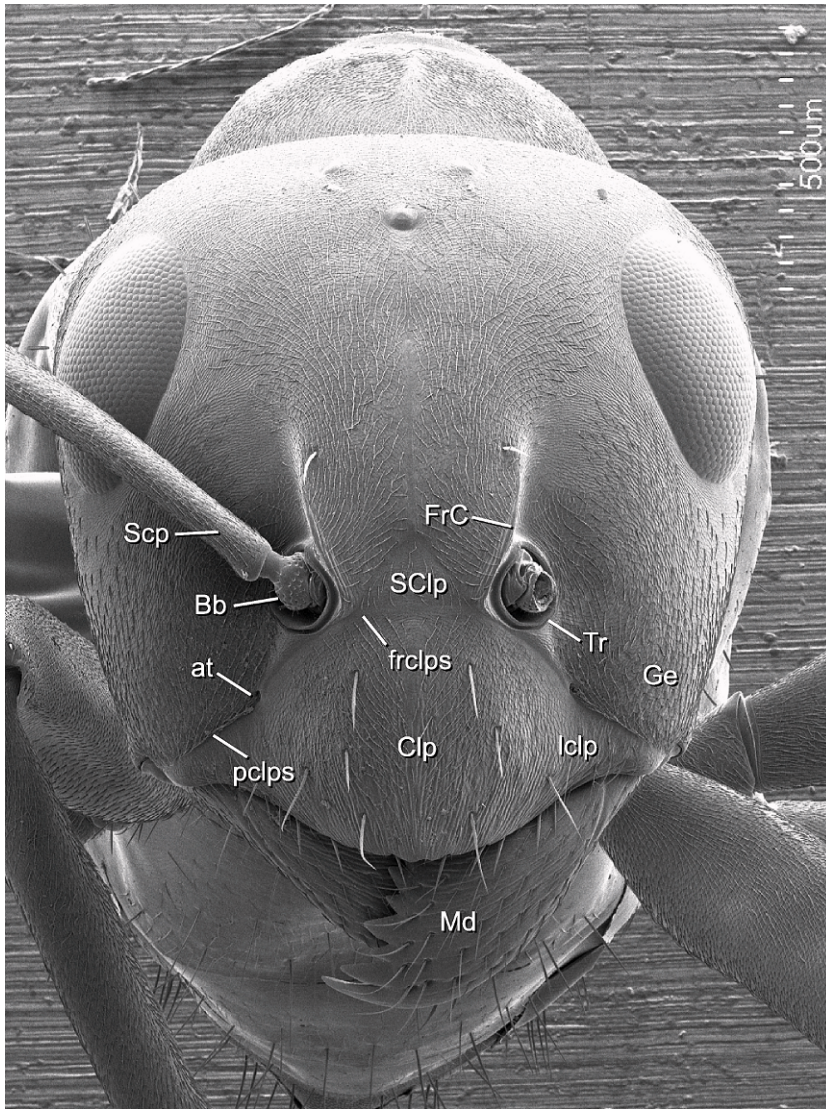


Fig. 6. Head of a *Formica fusca*-group worker, full-face view. Left antenna removed. Abbreviations: at, anterior tentorial pit; Bb, bulbus; Clp, clypeus; FrC, frontal carina; frcpls, frontoclypeal sulcus; Ge, gena; lclp, lateral clypeal area; Md, mandible; pclps, paroculoclypeal sulcus; Scp, scape; SClp, supraclypeal area; Tr, torulus.

ABOUT CHARACTER FIGURES

The digital atlas of morphology prepared during the course of this study provides extensive visual documentation for the majority of the characters listed below. Thus only a handful of figures is included here. Illustrations were chosen to aid the discussion of characters newly introduced here and characters from the literature that have been reinterpreted.

CHARACTER DISCUSSION

Head

1. *Head orientation*: (0) hypognathous; (1) prognathous.

The head of ants is turned upward, so that the mouthparts are directed forward and the foramen magnum is shifted to the ancestral posterior of the cranium (state 1). In most other Hymenoptera the mouthparts are

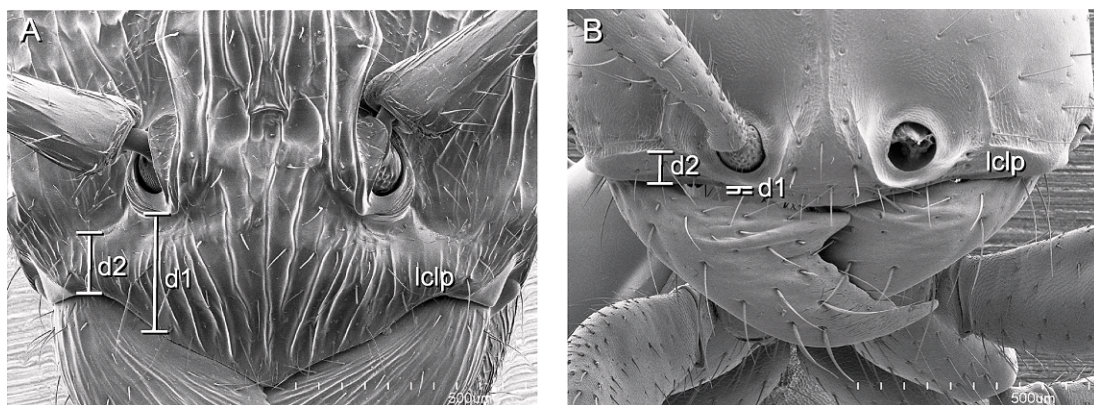


Fig. 7. Clypeus, full-face view. Note the relative longitudinal compression of the lateral clypeal areas between A and B by comparing the distance between the frontoclypeal sulcus and the anterior margin of the clypeus (d1), with the distance between the paroculoclypeal sulcus and the anterior margin of the clypeus (d2). **A.** *Rhytidoponera confusa*. **B.** *Cheliomyrmex morosus*, left antenna removed. Abbreviations: lclp, lateral clypeal area.

directed downward and the foramen magnum lies opposite the place of insertion of the antennae (state 0). Coded after Baroni-Urbani et al. (1992: char. 1) and Bolton (2003). See also Snodgrass (1935: 123) for a description of both conditions.

2. *Dentiform clypeal setae*: (0) absent; (1) present, single row; (2) present, double row. Additive.

These stout setae are usually arranged in a single row at the anterior clypeal margin overhanging the labro-clypeal articulation. Some taxa (e.g., *Myopopone castanea* and *Amblyopone mercovichii*) bear a second short, scattered row of stout setae in the medial area of the clypeus. The setal apex may be acute, blunt, truncated or slender and oblique (as in *Amblyopone mystriops*, see Brown, 1960: 185). Each seta can arise from a tuberclelike process or from the flat cuticle. While usually short, the setae may be hypertrophied in *Amblyopone pluto*. Although coded here as a three-state character, the variation outlined above holds great potential for a more detailed cladistic analysis within Amblyoponinae if more exemplars are included. Presence of dentiform setae in the clypeus and/or labrum has been cited as a synapomorphy for Amblyoponinae (Ward, 1994; Bolton, 2003; Saux et al., 2004). See also char. 28.

3. *Lateral clypeal tooth*: (0) absent; (1) present.

Each tooth consists of blunt outcurved projection of the lateral free margin of the clypeus just above the pleurostoma and overhanging the mandible. Listed as one putative synapomorphy for Leptanilloidinae, this clypeal tooth is usually described as an extension of the gena (e.g., Brandão et al., 1999; Brady and Ward, 2005), but is treated here as nonhomologous with genal tooth. True genal tooth occurs among some Amblyoponinae species (see also char. 23 for further discussion).

4. *Lateral area of clypeus*: (0) broad from the anterior to the posterior margin; (1) narrow in front of the antennal socket.

The lateral area of the clypeus (after Ettershank, 1966: 77) is considered broad from anterior to posterior margin when the section of the clypeus anterior to the antennal socket is equal or broader than the area of the clypeus between the free clypeal margin and the paroculoclypeal sulci (state 0, as in *Ectatomma tuberculatum*, *Amblyopone pallipes*, fig. 7A). The lateral area of the clypeus is considered narrow when the clypeal area in anterior to the antennal sockets is smaller than the distance of the lateral clypeal area between the free clypeal margin and the paroculoclypeal sulci (fig. 7B). In the latter case, in full-face view, the lateral area of the clypeus appears as a transverse strip interrupted by the forward-situated antennal insertion (state

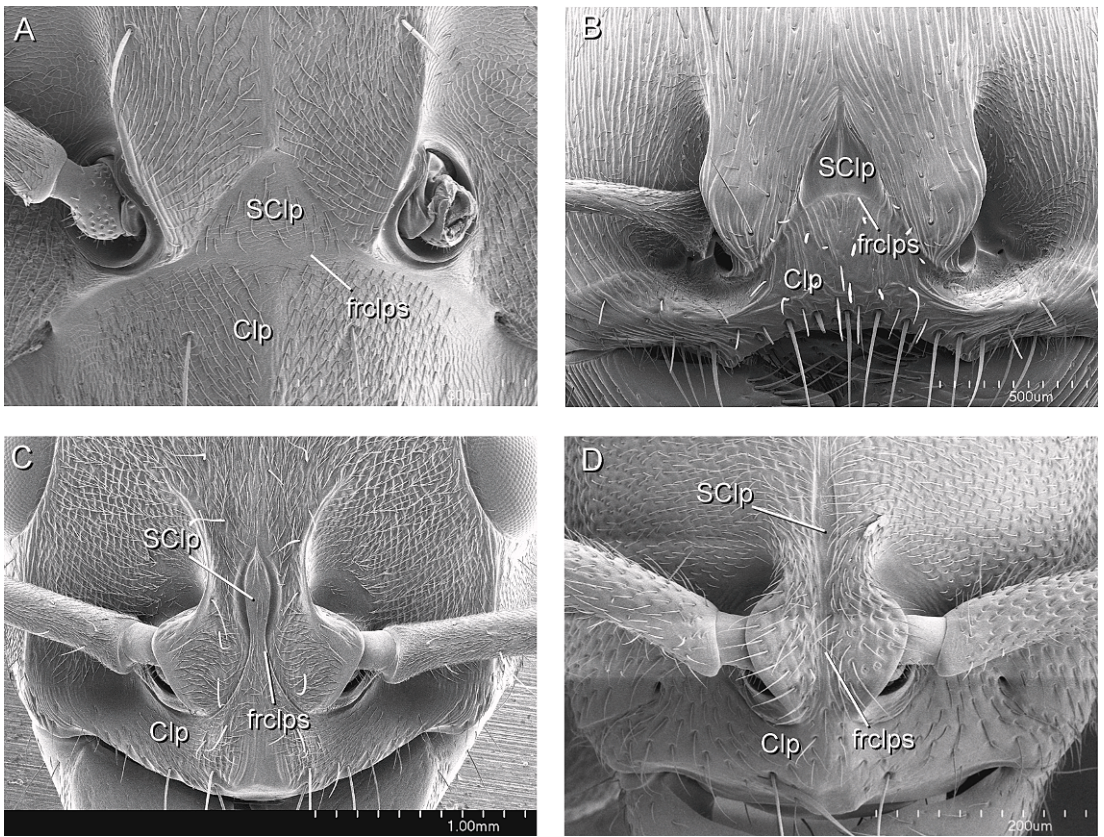


Fig. 8. Clypeus and supraclypeal area, full-face view. **A.** *Formica fusca* group, left antenna removed. **B.** *Pogonomyrmex barbatus*, left antenna removed. **C.** *Pachycondyla villosa*. **(D)** *Ponera pennsylvanica*. Abbreviations: Clp, clypeus; frcIps, frontoclypeal sulcus; SCIp, supraclypeal area.

1, as in *Cheliomyrmex morosus*, *Cerapachys nitidulus*). See also character 5.

5. *Median area of clypeus*: (0) not extending posterad between antennal sockets; (1) extending posterad between antennal sockets, frontoclypeal sulcus round; (2) extending posterad between antennal sockets, frontoclypeal sulcus acute; (3) extending posterad between antennal sockets as a narrow longitudinal strip, frontoclypeal sulcus acute.

In some taxa the *median area of the clypeus* (after Ettershank, 1966: 77) never extends posterad beyond an imaginary transverse line drawn at the anterior margins of the antennal sockets (fig. 8A), in which case the frontoclypeal sulcus forms an almost uninterrupted line or weak arc in front of the antennal insertions (state 0, as in *Formica*, *Tetraponera aethiops*). The supraclypeal area

is triangular and lies in front of or between the antennal sockets. An alternative condition is for the median area to extend posterad between the antennal insertions with the frontoclypeal sulcus forming a rounded line that reaches or surpasses the posterior margins of the antennal sockets (state 1, Ward, 1990: char. 11, in part). In this latter state the supraclypeal frontal area is perfectly triangular and lies behind the posterior margins of the antennal sockets (e.g., *Pogonomyrmex barbatus*, *Ectatomma tuberculatum*; fig. 8B). In another state the median area extends posteriorad between the antennal insertions and the frontoclypeal sulcus forms an acute line, in which case the supraclypeal area is longitudinally oblong (state 2, as in *Pachycondyla villosa*, *Cheliomyrmex morosus*; fig. 8C). Finally, the median area may extend

posterad as a narrow longitudinal strip between the closely approximated antennal insertions and the supraclypeal area appears as a short longitudinal depression (state 3, as in *Ponera pennsylvanica*, *Prionopelta antillana*; fig. 8D).

Discothyrea oculata, *D. testacea* and *Probolomyrmex guineensis* are coded as unknown (?) for this character because the high degree of fusion and modification of the frontoclypeal sclerites in these taxa makes assessment of this condition impossible.

This character combines the information about the position of the antennal sockets relative to the median clypeal area with the position of the sockets relative to each other since no satisfactory way was found to treat these two features independently without causing overlapping and contradiction of their various possible states. On the other hand, expressing the distance between the antennal sockets in terms of the degree of "compression" of the median clypeal area and supraclypeal area proved to be a successful way of translating an apparent continuum into discrete and unambiguous states. The distance between the antennal sockets and the anterior margin of the head at the clypeo-labral articulation is best represented independently in terms of the relative anteroposterior size of the lateral areas of the clypeus (see char. 4). Finally, the relative separation of the antennal sockets from the epistomal sulcus as a whole can be coded as a separate character (see char. 6).

6. *Antennal socket*: (0) situated at epistomal sulcus; (1) situated posterior to the epistomal sulcus.

The anterior margin of the antennal socket may be immediately at the epistomal sulcus, in which case the supraclypeal area lies between the sockets or behind the posterior margin of the sockets (state 0, as in *Formica fusca*, *Ponera pennsylvanica*). Otherwise the antennal socket may be situated at a distance from the epistomal sulcus, so that its anterior margin is behind the triangular supraclypeal area (state 1, as in *Oecophylla smaragdina*, *Camponotus*).

7. *Frontoclypeal shelflike projection*: (0) absent; (1) present.

In *Discothyrea* and *Probolomyrmex*, the clypeus and the anterior part of the frons are

fused together and extend anterad over the clypeo-labral articulation forming a shelflike projection or platform (fig. 9B). This shelflike projection overhangs the mandibles and supports the antennal sockets that lay well beyond the anterior tentorial pits (state 1, as in *Probolomyrmex guineensis*; coded after Brown (1958; 1978) and Taylor (1965)). In some species within *Proceratium*, the antennal sockets are situated at the anteriormost part of the cranium, slightly overhanging the clypeo-labral articulation, but they are never forward beyond the anterior tentorial pits (fig. 9A).

Antennal socket apparatus: The following nine characters (chars. 8–16) pertain to the different parts of the antennal socket apparatus and their associated structures: the torular arches, the antennal acetabula, the posttorular flanges and the frontal lobes. These interrelated structures together form one of the most complex sets of cuticular features found in ants. Given the variation in shape, size, and position of these structures and the differential levels of fusion and reduction among them it is not possible to code the observed diversity for each structure into completely independent binary or multistate characters. To complicate matters, the homology and consequent terminology of the different parts has been confused in the literature pertaining to identification keys, diagnoses, and descriptions of new taxa. For example, the term *frontal lobes* is commonly applied to either the lateral projections of the frontal carinae over the toruli or to the lateral expansions of the median arch of the toruli themselves, thus denoting nonhomologous structures in different taxa. Part of this confusion arises from the fact that establishing the correct correspondence among the different parts in distantly related groups is possible only through the examination of some key taxa with intermediate states, many of which are rare in collections and often dismissed as aberrant in taxonomic treatments. The characters presented here are an attempt to translate this variation into variables suitable for cladistic analysis, some of which may be partially correlated.

8. *Median arch of torulus*: (0) simple rim; (1) lobate, continuous with lateral arch; (2)

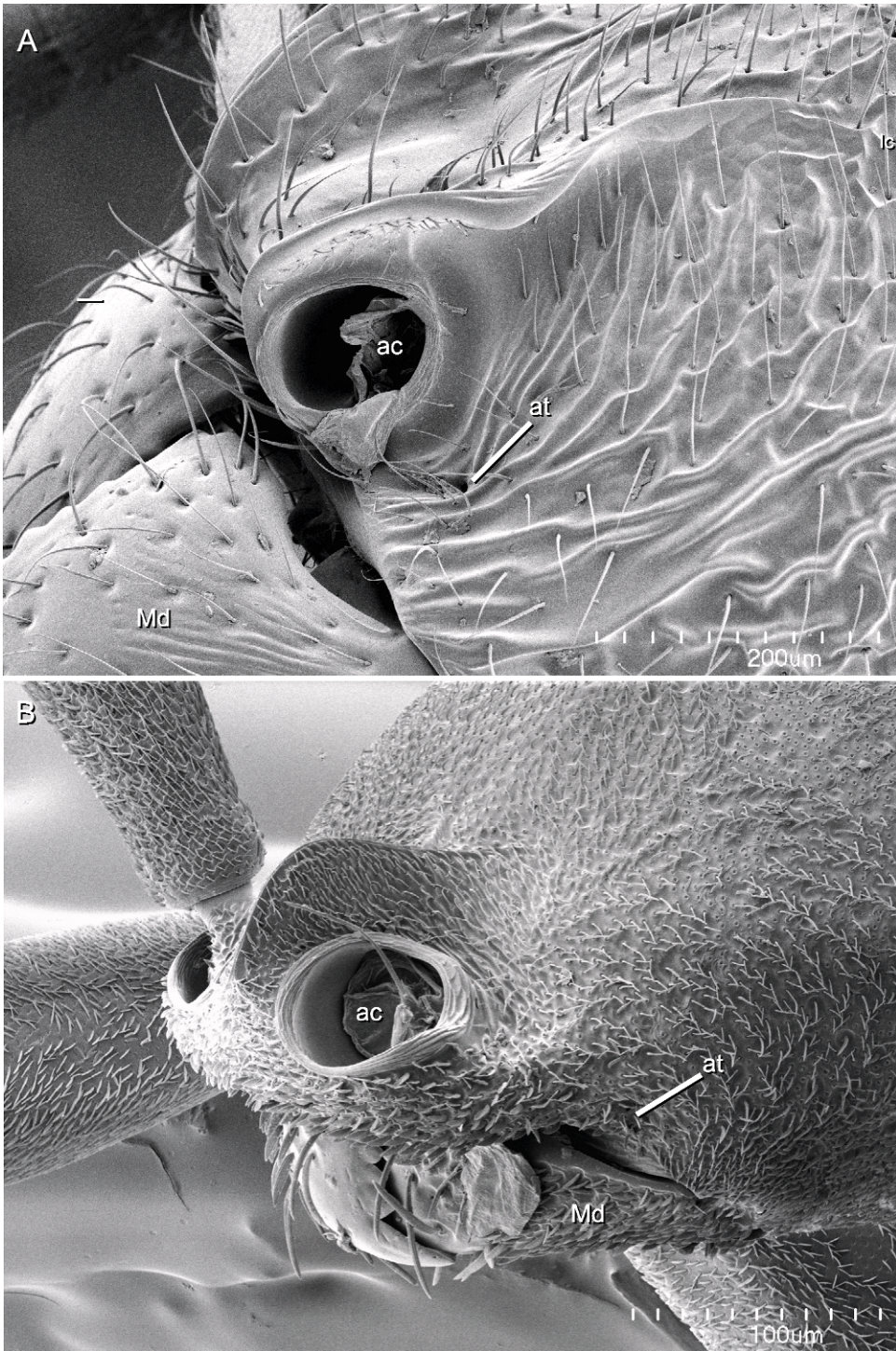


Fig. 9. Frontoclypeal area, left anterolateral view. **A.** *Proceratium croceum*. **B.** *Probolomyrmex guineensis*, showing shelflike projection. Abbreviations: ac, acetabulum of antennal socket; at, anterior tentorial pit; Md, mandible.

lobate, discontinuous with lateral arch; (3) hypertrophied. Additive.

In its simplest form (e.g., *Formica*) the torulus is a circular sclerite with a well-marked annular rim that can be divided into halves for convenience: the half closest to the midline of the cranium is the *median arch*,* and the laterad curving half is the *lateral arch** of the torulus (fig. 10; see also char. 9). The toruli are inclined in most ant taxa, so that the median arch is usually higher on the head relative to the lateral arch. In most ants the annular rim runs uninterrupted encircling the antennal acetabulum, thus making it impossible to draw a natural division between the median and lateral arches (fig. 10A–C). However, in some poneromorph taxa the arches become increasingly disassociated as a result of the expansion of the highest part of the median arch into a laterad lobate projection, the *torular lobe** (= dorsal lobe, median lobe, Ward, 1990; Lattke, 2004). The torular lobe varies from small (e.g., *Pseudomyrmex gracilis*) to a hypertrophied massive structure that conceals the acetabulum antennisalis and lateral arch completely in dorsal view (e.g., *Loboponera obeliscata*, fig. 10F). In this latter state the two arches of the torulus are discrete and easily recognized as independent structures.

The projection of the median arch into a torular lobe can be individuated as follows: the median arch may consist of a simple nonprojecting rim continuous with the lateral arch (state 0, as in *Dolichoderus laminatus*, *Oecophylla smaragdina*; fig. 10A); or the highest part of the median arch expands into a posterolateral projecting lobe that covers the antennal acetabulum in dorsal view either partially (e.g., *Tetraponera attenuata*, *Myrmecia nigriscapa*; fig. 10B) or completely (e.g., *Amblyopone pallipes*, *Paraponera clavata*; fig. 10C), but the arch forms a continuous rim with the lateral arch (state 1); or the highest part of the median arch expands laterad into a strong lobate projection that covers the antennal acetabulum almost completely in dorsal view, the posterior part of which extends posterad forming an horizontal free margin that surpasses the lateral arch without connecting to it (state 2, as in *Anochetus emarginatus*, *Pachycondyla villosa*; while some taxa show a faint carina

connecting the posterior ends between the median and lateral arches, the degree of connection between the anterior ends of the arches varies greatly; fig. 10D–E); or the median arch extends into an anterolateral horizontal massive lobe that overhangs the lateral arch on all directions and thus covers the antennal acetabulum completely in dorsal view (state 3, as in *Pachycondyla pachyderma*, *Plectroctena*, *Psalidomyrmex*, *Loboponera*; fig. 10F). In this last state there is no connection, either anterior or posterior, between the margins of the median and lateral arches. Taxa with torular-posttorular complex have been coded as inapplicable “–” for this character since the median arch is fused with the posttorular flange and it is not possible to homologize this structure unambiguously (see char. 15).

9. *Lateral arch of torulus*: (0) simple rim; (1) barrel shaped.

The lateral arch (see char. 8 for definition of this structure) usually delineates the outer half of the acetabulum as a simple low rim (state 0, as in *Paraponera clavata*, *Pachycondyla berthoudi*; fig. 10C). In some ponerine taxa with a disassociated torular arch (see char. 8), the lateral arch encloses the acetabulum almost completely and forms an elevated barrel-shaped base for the insertion of the antenna (state 1, as in *Diacamma ceylonense*, *Loboponera*; fig. 10E–F).

10. *Acetabulum of antennal socket apparatus*: (0) dishlike; (1) spherical; (2) hemispherical.

The antennal socket acetabulum consists of a depression of the central part of the torular sclerite and an outgrowth of the torular arch forming a concave surface for the reception of the bulbus of the scape. Although the depth of depression and shape of the acetabulum varies greatly among ants, the antennifer always sits in the center of the concavity, projecting upward, and anterior to the antennal socket foramen that opens within the lower wall of the acetabulum (see also char. 11; but see char. 13 for the only known exception). For this reason it is problematic to characterize the antennal socket as vertical or horizontal (e.g., Bolton, 1990b: 1353–1354) since the variation in the apparent opening direction of the sockets can be due to differences in shape of either the acetabulum or the torular arch, rather than

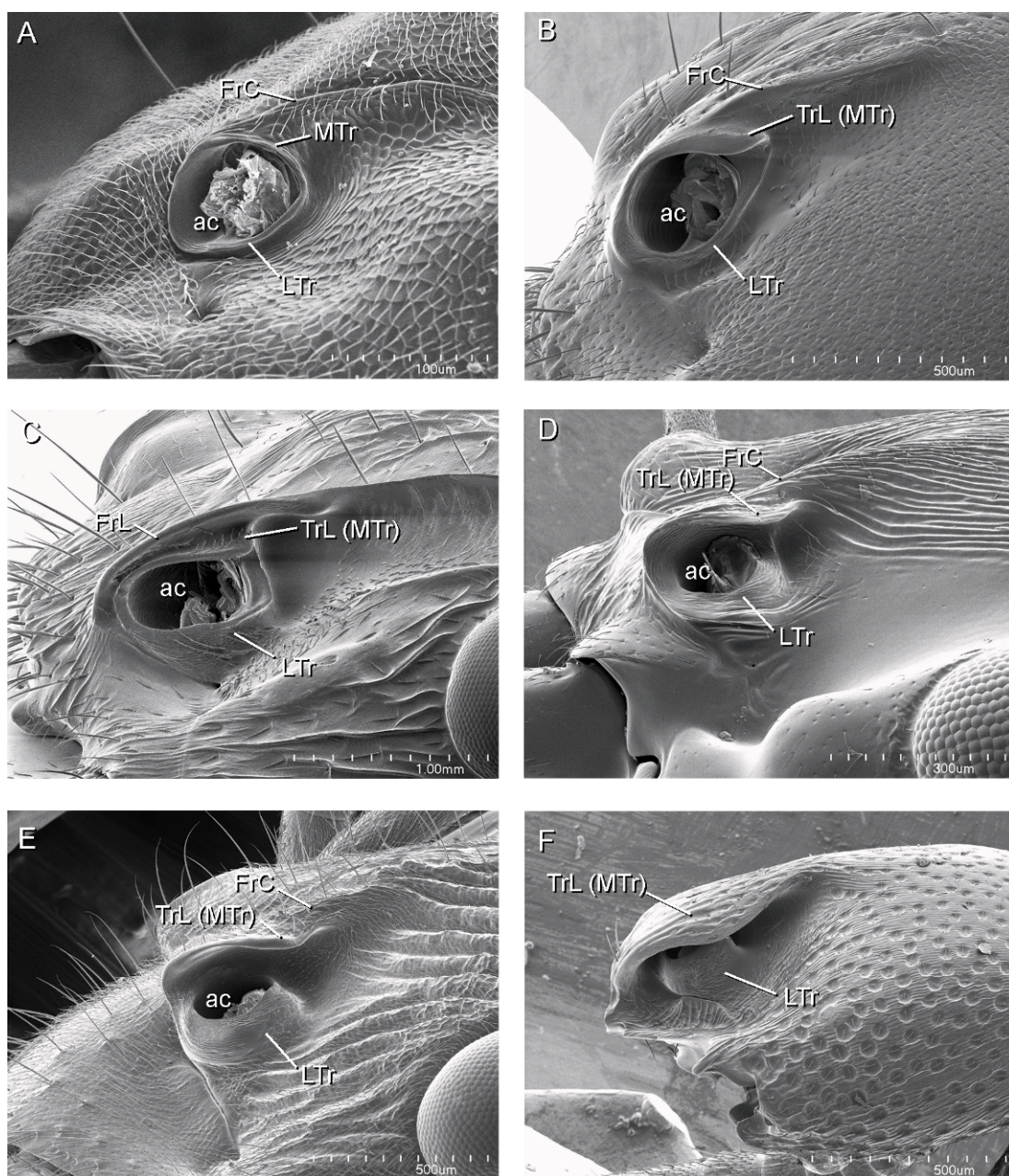


Fig. 10. Antennal socket apparatus, left lateral view. Antenna removed to expose acetabulum. **A.** *Technomyrmex albipes*. **B.** *Tetraponera aethiops*. **C.** *Paraponera clavata*. **D.** *Anochetus emarginatus*. **E.** *Diacamma ceylonense*. **F.** *Loboponera obeliscata*, mouthparts removed. Abbreviations: ac, acetabulum of antennal socket; FrC, frontal carina; FrL, frontal lobe; TrL, torular lobe; LTr, lateral arch of torulus; MTr, medial arch of torulus.

to a translocation of the entire socket relative to the cranial axis. An apparent horizontal socket can occur in analogy when the acetabulum is hemispherical (e.g., *Cerapachys nitidulus*; see below) or when the median arch of the torulus lies in a plane parallel to the lateral arch (e.g., *Probolomyrmex guineensis*). It is therefore better to conceptualize the differences found in the antennal socket in terms of the shape of the acetabulum per se (i.e., the shape of the concavity that forms the articulatory surface of the socket apparatus).

In its more generalized form, the antennal acetabulum consists of a shallow dishlike concavity with a short articulatory surface anterior to the antennal socket foramen and antennifer (state 0, as in *Formica fusca*, *Dolichoderus laminatus*; fig. 10A). The bulbus sits in the middle of this dishlike sclerite and is clearly visible since it is not enclosed by it. Or the torulus may form a closed spherical acetabulum, consisting of a large domed articulatory surface formed by the torular lobe with a lateral opening to receive the scape (state 1, as in *Nothomyrmecia macrops*, *Myrmica americana*). The bulbus articulates inside the spherical acetabulum and it is enclosed partially (e.g., *Tetramorium aethiops*; fig. 10B) or completely (e.g., *Paraponera clavata*; fig. 10C) by it. Alternatively, the acetabulum consists of a hemispherical concave depression of the lower torulus, with a large bowl-shaped articulatory surface and a horizontal circular opening for the reception of the scape (state 2, as in *Diacamma ceylonense*, *Myopopone castanea*, *Eciton hamatum*; figs. 10E, 11B–C). In this state the torular lobe does not form part of the articulatory surface. The bulbus is almost completely sunken inside the hemispherical acetabulum and only the bulbus neck is clearly visible.

11. *Antennal socket foramen location*: (0) posteroventral; (1) lateral.

The acetabulum of the antennal socket (see char. 10) opens to the inside of the cranium via an orifice, the *antennal socket foramen** proper, immediately posterior to the antennifer to which the bulbus of the scape actually articulates by way of the bulbus corium (see also char. 17). In most ants this foramen is located posteroventrad from the antennifer on the floor of the acetabulum,

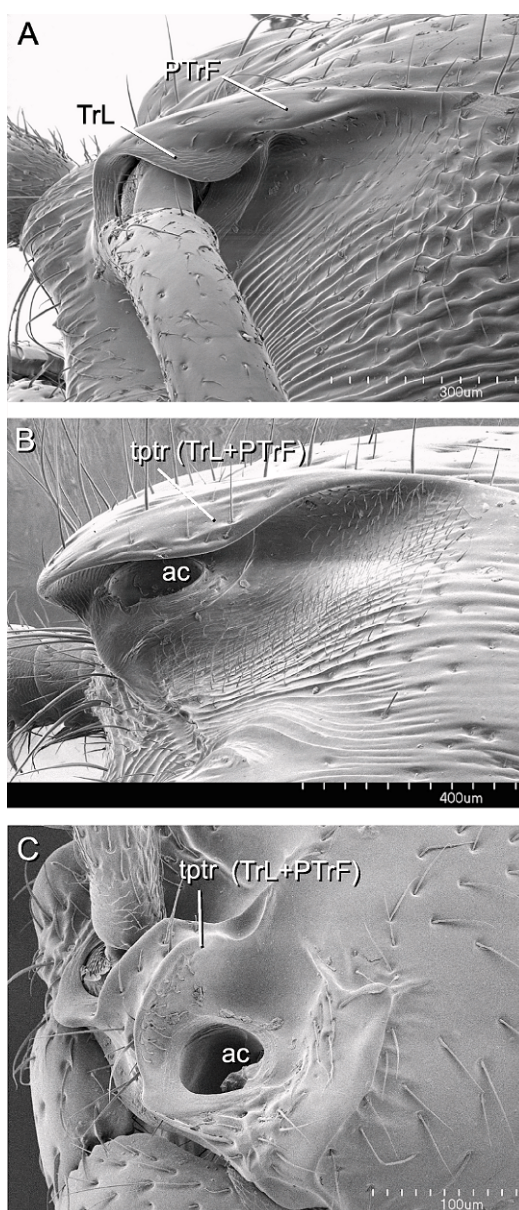


Fig. 11. Antennal socket, left lateral view. **A.** *Amblyopone mercovichii*. **B.** *Myopopone castanea*, antenna removed. **C.** *Cerapachys nitidulus*, left antenna removed. Abbreviations: ac, acetabulum of antennal socket; PTrF, posttorular flange; TrL, torular lobe; tptr, torular-posttorular complex.

forming a round to oval opening (state 0, as in *Formica*, *Pachycondyla*). In *Pseudomyrmex* and *Tetraponera* the foramen is located on the lower lateral wall of the acetabulum, with an oblong opening (state 1). *Tatuidris tatusia*

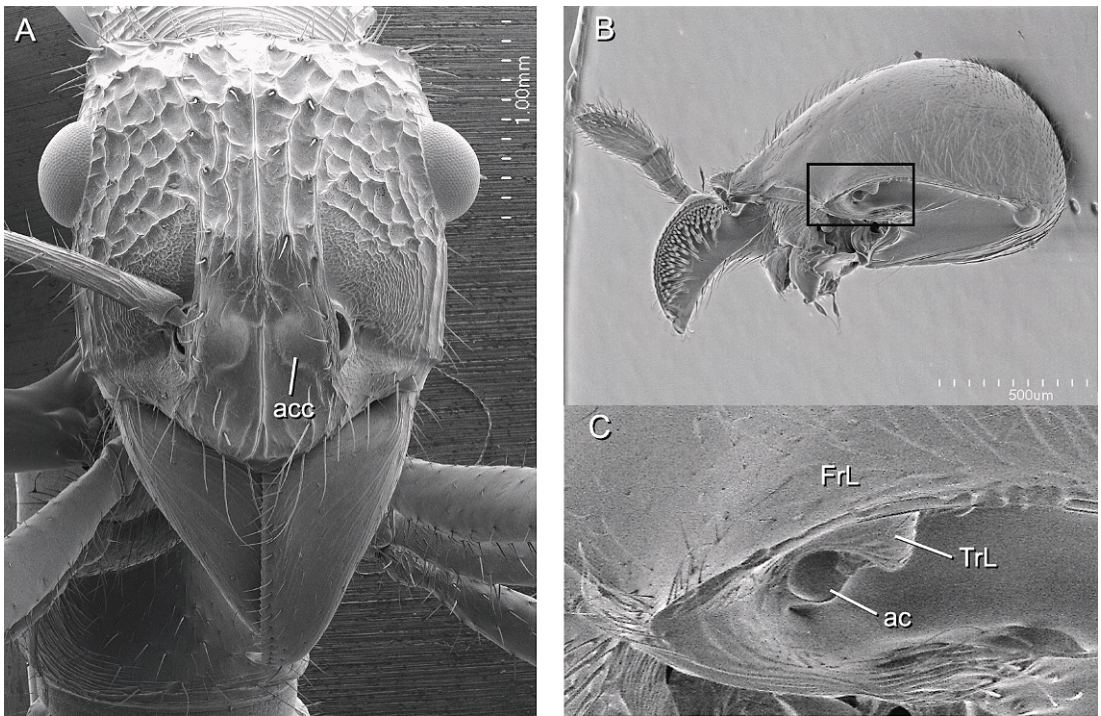


Fig. 12. **A.** Head of *Ectatomma tuberculatum*, full-face view, left antenna removed. **B–C.** Detached head of *Tatuidris tatusia*, anterolateral view, left antenna and left mandible removed. **C.** Close-up of antennal socket apparatus. Abbreviations: ac, antennal acetabulum; acc, accessory chamber of antennal socket; FrL, frontal lobe; TrL, torular lobe.

is coded as having “posteroventral” foramina since this is the location of the openings relative to the antennifer within the otherwise translocated torulus (see char. 13).

12. *Accessory chamber of antennal socket:* (0) absent; (1) present.

The antennal apparatus may possess an *accessory chamber** located mesad from the socket acetabulum (see char. 10). This accessory chamber is composed of a blind cuticular vesicula attached internally to the roof of the cranium in the area corresponding to the frons between the antennal insertions, and opening into the acetabulum by way of an aperture slightly smaller than the cavity itself. The vesicula may be ovate, as in *Tetraponera*, or spherical, as in *Ectatomma*. In this latter genus the chamber is larger than the socket itself and in some of its species (e.g., *Ectatomma tuberculatum*) it can be seen externally as a conspicuous translucent bulla located between the antennal sockets (fig. 12A). The accessory chamber is connected to the

outside by way of the socket acetabulum and is thus filled with air. In cases in which the antennal sockets are closely approximated to each other (e.g., *Pseudomyrmex gracilis*) the accessory chambers meet medially but are not connected. The function of these apparently blind chambers is unknown.

13. *Antennal socket apparatus orientation:* (0) dorsal; (1) ventral.

Despite the great diversity found across Formicidae in the antennal socket apparatus, this complex structure retains its relative orientation within the cranium; the central basal portion of the socket sits on a horizontal plane on the cranial dorsum and the antennifer points upward. This state can be described as dorsal (state 0). The only known exception occurs in *Tatuidris tatusia*, where the socket apparatus sits upside-down on the roof of the greatly expanded frontal lobe and the antennifer points almost downward (state 1). As a consequence the median arch of the torulus curves laterad and the torular

lobe projects ventrad, while the lateral arch is closer to the midline of the cranium (fig. 12B–C).

14. *Posttorular flange*: (0) absent; (1) present, unfused to torular lobe; (2) present, fused to torular lobe. Additive.

The *posttorular flange** is the lateral expansions of the frontal carina that run posterad from the middle of the torular lobes forming a longitudinal flange with a more or less straight margin. Unlike the frontal lobe (see char. 16), the posttorular flange never extend forward beyond the middle of the median arch or laterad surpassing the lateral arch. When unfused, the anterior margin of the flange run posterad as an independent structure from the free margin of the torular lobe and dorsal to it (fig. 11A), partially concealing the posterior half of the lobe in full-face view (state 1, as in *Tetraponera aethiops*, *Amblyopone mercovichii*). When fused to the torular lobe, the lateral margin of the flange run posterad as a single margin continuous with the free margin of the torular lobe (fig. 11B), forming the paired *torular-posttorular complex** in which the posttorular flange cannot be discriminated as an independent structure from the torular lobe (state 2, as in *Myopopone castanea*, *Simopone schoutedeni*). This completely fused complex is usually mistaken for the true frontal lobe, but see char. 16 for a discussion. The torular-posttorular complex may extend laterad and horizontally forming an antennal scrobe (e.g., *Cylindromyrmex*) or may be vertical and show various degrees of reduction (e.g., *Cerapachys*, *Dorylus*; see char. 15).

15. *Torular-posttorular complex*: (0) horizontal; (1) vertical.

When the torular-posttorular complex is present it may expand laterad in the horizontal plane partially or completely covering the antennal acetabulum in full-face view (state 0, as in *Myopopone castanea*, *Cylindromyrmex*, and *Acanthostichus*; fig. 11B). Alternatively, the torular-posttorular complex may project upward on a vertical plane leaving the hemispherical antennal acetabulum completely exposed in full-face view (state 1, as in *Cerapachys nitidulus*, *Eciton hamatum*; fig. 11C). This complex shows various degrees of reduction across the taxa possessing the latter state: it may be present

as a pair of standing, round lobes between the antennal sockets that continue posterad as carinae (e.g., *Cerapachys*) or the whole structure may be reduced to short arched carinae that delineate the antennal sockets anteriorly and meet medially between them (e.g., *Leptanillodes biconstricta*). Taxa lacking a torular-posttorular complex have been coded as inapplicable “-” for this character.

16. *Frontal lobe*: (0) absent; (1) present.

In the present study the term frontal lobe is strictly applied to the cuticular rounded flange formed by the dorsolateral expansion of the anterior section of the frontal carina, running posterad from the frontoclypeal sulcus and often covering the torular arches and antennal acetabulum in full-face view. Although this definition is similar to the one normally given in taxonomic treatments and identification keys (e.g., Bolton, 1994; Shattuck, 1999; Wilson, 2003), in practice the term is loosely applied to any kind of lobate structure either covering the antennal sockets in full-face view or present between the antennal sockets regardless of its true origin and topological correspondence. Commonly the term is mistakenly applied to the large and expanded torular lobe (see char. 8) found in many Ponerinae genera (e.g., Bolton and Brown, 2002; Baroni Urbani and de Andrade, 2003b), or to the fused torular-posttorular complex (see char. 14) found mostly among members of the Doryline section (e.g., Brady and Ward, 2005). Examples of a true frontal lobe occur in *Myrmecia*, *Paraponera* (fig. 10C), and most Myrmicinae. When a frontal lobe is present (state 1), the torular lobe (i.e., median arch of the torulus) may always be seen as a distinct structure underneath the lateral margin of the lobe. The short lateral expansion of the posterior section of the frontal carina is treated as a separate character (see char. 14).

17. *Bulbus shape*: (0) spherical; (1) hemispherical.

In adult Formicidae the radicle of the antennal scape can be divided into a basal round swelling, the *bulbus*, and a distal short constriction to which the base of the scape shaft attaches, the *bulbus neck* (fig. 13A–F; see also char. 18). The bulbus articulates inside the antennal socket acetabulum and thus serves as the scape condyle proper.

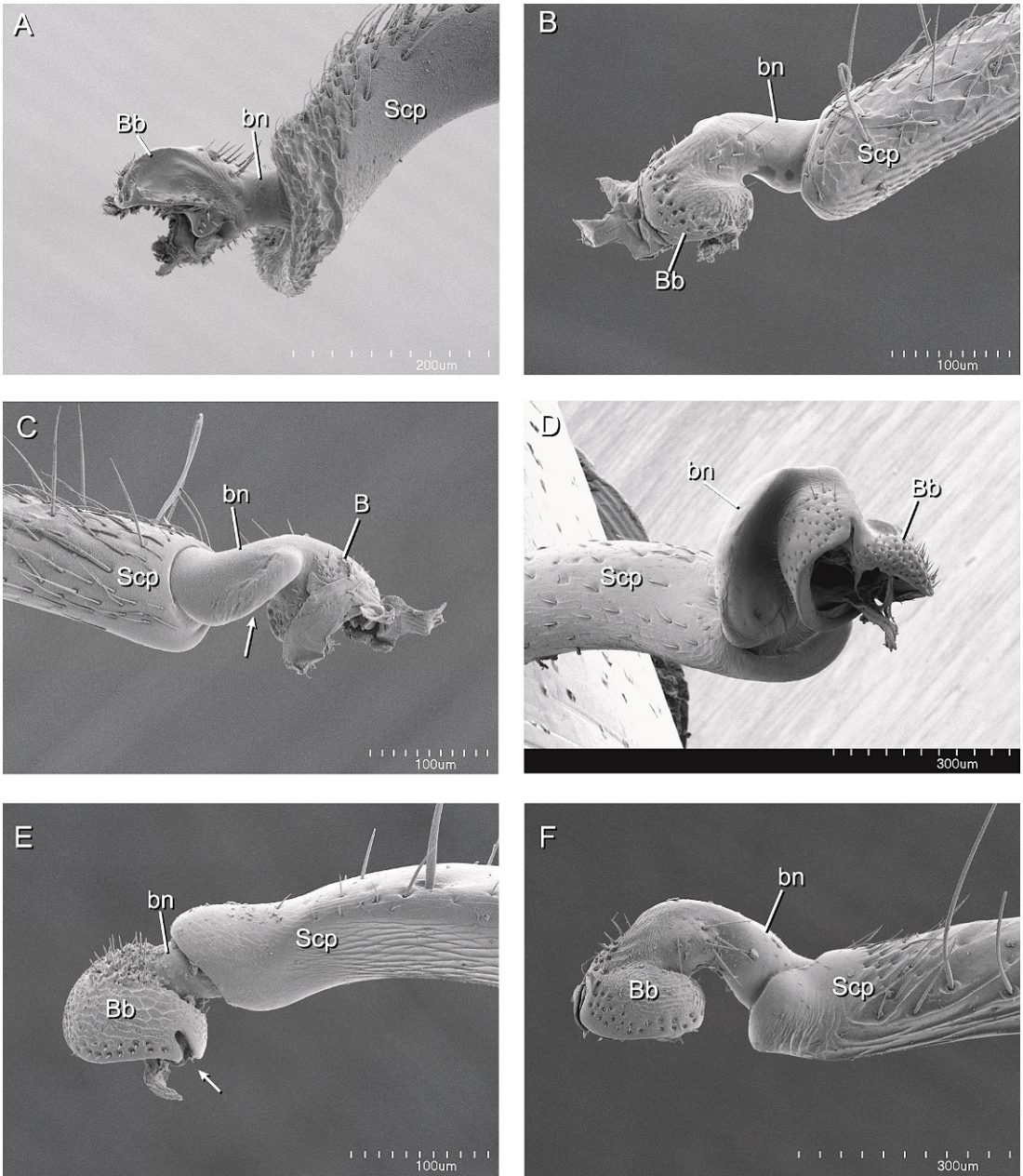


Fig. 13. Radicle of the left antenna. **A.** *Manica rubida*, anterior view. **B.** *Amblyopone pallipes*, anterior view; **C.** posterior view with arrow pointing at lobe. **D.** *Plectroctena mandibularis*, posterior view. **E.** *Acanthostichus serratulus*, anterior view with arrow pointing at lateral notch. **F.** *Myopopone castanea*, anterior view. Abbreviations: Bb, bulbus; bn, bulbus neck; Scp, scape.

The bulbus is a quasispherical structure with a posteroventral basal opening that aligns with the antennal socket foramen and connects to it by way of the bulbus corium (see also char.

11). In general, the shape of the bulbus is that of a sphere missing a $\frac{1}{4}$ section (i.e., a wedge-shaped cut) forming the basal opening, so that the two arced lips of the opening meet at an

approximate 90° angle. For practical purposes a bulbus in this state can be termed *spherical* (state 0, as in *Nothomyrmecia macrops*, *Manica rubida*; fig. 13A–D). In some taxa the shape of the bulbus is almost *hemispherical* since the basal opening corresponds to a missing ½ section of the bulbus sphere (state 1, as in *Acanthostichus serratus*, *Cheliomyrmex morosus*; fig. 13E–F).

18. *Bulbus neck insertion*: (0) lateral, perpendicular; (1) anterodorsal, oblique.

The place and plane of insertion of the neck into the body of the bulbus varies as follows: the neck may insert on the lateral side of the bulbus and perpendicular to it (state 0, as in *Nothomyrmecia macrops*, *Cerapachys nitidulus*; fig. 13A); or the insertion is anterodorsal and at an oblique plane so that the neck directs laterad (state 1, as in *Amblyopone pallipes*, *Ectatomma tuberculatum*; fig. 13B–C). While the neck is usually short and straight in the former type, in the latter the neck varies from short and slightly curved (e.g., *Belonopelta deletrix*, *Cylindromyrmex brevitarsus*; fig. 13E) to twice as long and strongly downward curved (e.g., *Myopopone castanea*; fig. 13F; see also Bolton, 1990b: 1353–1354, in part).

19. *Bulbus neck shape*: (0) tubular; (1) with posterior lobe; (2) discoidal.

The bulbus neck may be a simple tubular structure either straight or bent (state 0, as in *Nothomyrmecia macrops*, *Diacamma ceylonense*; fig. 13A, E–F); or the neck may bear a longitudinal posterior protuberance forming an elongated lobe (state 1, as in *Adetomyrma venatrix*, *Amblyopone pallipes*; fig. 13C); or the neck may have large anterior and posterior lobate projections that together form a disk-shaped structure with a convex dorsum (state 2, as in *Plectroctena mandibularis*, *Platythyrea punctata*; fig. 13D; see also Lattke, 2004: 35, 38).

20. *Anterior basal margin of bulbus*: (0) entire; (1) with a notch.

In most ants the anterior basal margin of the bulbus possesses a deep elongate notch toward the lateral side (state 1, as in *Paraponera clavata*, *Cerapachys nitidulus*; fig. 13E). This basal notch is associated with the depressor muscle of the scape, one of the four muscles responsible for the movement of the antenna (Snodgrass, 1956; Ehmer and Gronenberg,

1997). The long tendon of the depressor muscle attaches to the rounded end of the notch: when the muscle contracts the tendon is pulled through the notch, causing the scape to rotate forward along its longitudinal axis thus bringing the apex of the angled flagellum downward. Otherwise the anterior basal margin is entire at the place of attachment of the depressor muscle (state 0, as in *Myopopone castanea*; fig. 13F).

21. *Antenna*: (0) nongeniculate; (1) geniculate between scape and funiculus.

Coded after Bolton (2003: 15), geniculate antenna occurs in all ants and in the Vespidae used here as outgroup.

22. *Median longitudinal cephalic carina*: (0) absent; (1) running from supraclypeal area to vertex; (2) running from clypeus to vertex.

When present, the cephalic dorsum bears a strong medial longitudinal costa or carina distinct from other sculpture. The carina may run posterad from the supraclypeal area to the vertex (state 1, as in *Typhlomyrmex rogenhoferi*); or it may run uninterrupted from the anterior part of the clypeus to the vertex (state 2, as on *Acanthoponera minor*). Coded in part after Brown (1958) and Lattke (1994).

23. *Genal tooth*: (0) absent; (1) present.

When the genal tooth is absent the surface of the genal angle is flat and continuous with the pleurostoma. Otherwise the anterior genal angle bears a strongly developed tooth that projects anterolaterad from the cranium surpassing the pleurostoma (Wilson, 1958: state 1 as in *Myrmica*; Brown, 1960). Brady and Ward (2005: char. 1) treated this feature and the clypeal tooth found in leptanilloidine genera as part of the same character under the assumption that they are corresponding structures positioned differently within the anterior border of the head at the clypeo-labral articulation (overhanging or not the mandibles). However, a close comparison in terms of shape and position of both types of tooth among Amblyoponinae and Leptanilloidinae, and the reduced clypeus in related members within the Doryline section, shows that they are not homologous (see also char. 3).

24. *Laterobasal lobe on labrum*: (0) absent; (1) present.

When present, the lateral margin of the labrum expands outward, parallel to the external labral surface, forming a rounded

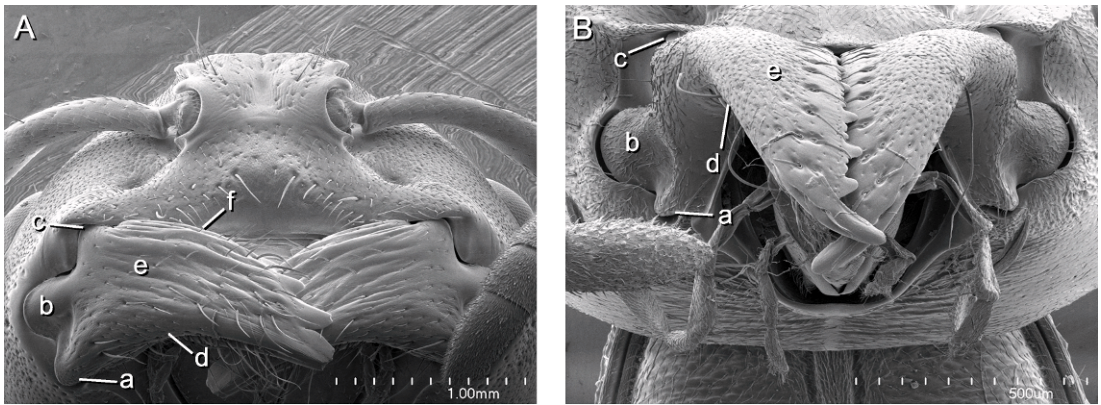


Fig. 14. Mandibles, anterior view. **A.** *Tetraponera aethiops*. **B.** *Nothomyrmecia macrops*. Abbreviations: a, ventral articulation; b, abductor apodeme; c, clypeal articulation of mandible; d, external margin; e, external face; f, basal margin.

basal lobe on the lateral side of the labrum (state 1, as in *Myrmecia nigriscapa*). These laterobasal lobes sit above the lateral labral arms, concealing the maxillo-labral articulation (see char. 32) when the maxillo-labial complex is retracted. Otherwise the lateral margins of the labrum extend more or less uninterrupted into the distal margin.

25. *Paired tuberculi on distal labral margin*: (0) absent; (1) present.

When present, the tuberculi, either peglike or spinelike, occur on the external surface of each of the labral lobes just behind the distal margin (Gotwald, 1969). *Amblyopone mercovichii* shows a transverse bilobate ridge on the labrum not considered homologous to the tuberculi given its difference in shape and position (see char. 27). See also char. 26.

26. *Unpaired tubercule on distal labral margin*: (0) absent; (1) present.

This is a single, median cuticular projection present dorsally in the cleft of the distal margin. This feature is coded as an independent character from the presence of paired tuberculi (char. 25) because both types of tuberculi occur in conjunction in some species (e.g., *Dorylus dentifrons*). See Gotwald (1969: 55) for a discussion on labral ornaments in Dorylinae.

27. *Transverse bilobate ridge on labrum*: (0) absent; (1) present.

Present only in *Amblyopone mercovichii* for this matrix, the transverse bilobate ridge is a blunt elevation of the cuticle on the middle of the external labral surface (Brown, 1960).

The ridge bears multiple small peglike setae similar to the ones present on the clypeus.

28. *Dentiform labral setae*: (0) absent; (1) present.

The stout setae are usually arranged in a single, unevenly spaced transverse row at the middle of the exterior labral surface. Their apices are blunt to acute, and when hypertrophied (e.g., *Apomyrma*) they are similar to the hypertrophied setae found on the clypeus (e.g., *Amblyopone phuto*). Although coded here as a present/absent character, variation in shape and arrangement holds potential for a more detailed cladistic analysis within Amblyoponinae if more exemplars are included. Presence of dentiform setae in the labrum and/or clypeus has been cited as a synapomorphy for Amblyoponinae (Ward, 1994; Bolton, 2003; Saux et al., 2004). See also char. 2.

29. *Mandibular type*: (0) planar; (1) torqued.

In the planar type, the corpus of the mandible runs distally without any twist or bend, so that the external face of the mandible extends in a flat semivertical plane (fig. 14A). The external margin originates basally at the ventral articulation (= posterior articulation) and runs parallel to the basal margin (state 0 as in *Tetraponera aethiops*). In the torqued type, the corpus of the mandible twists dorsally, around 90°, toward the internal margin (fig. 14B). As a result, the external face is vertical basally but runs increasingly horizontal and dorsal toward its distal end, and the external margin

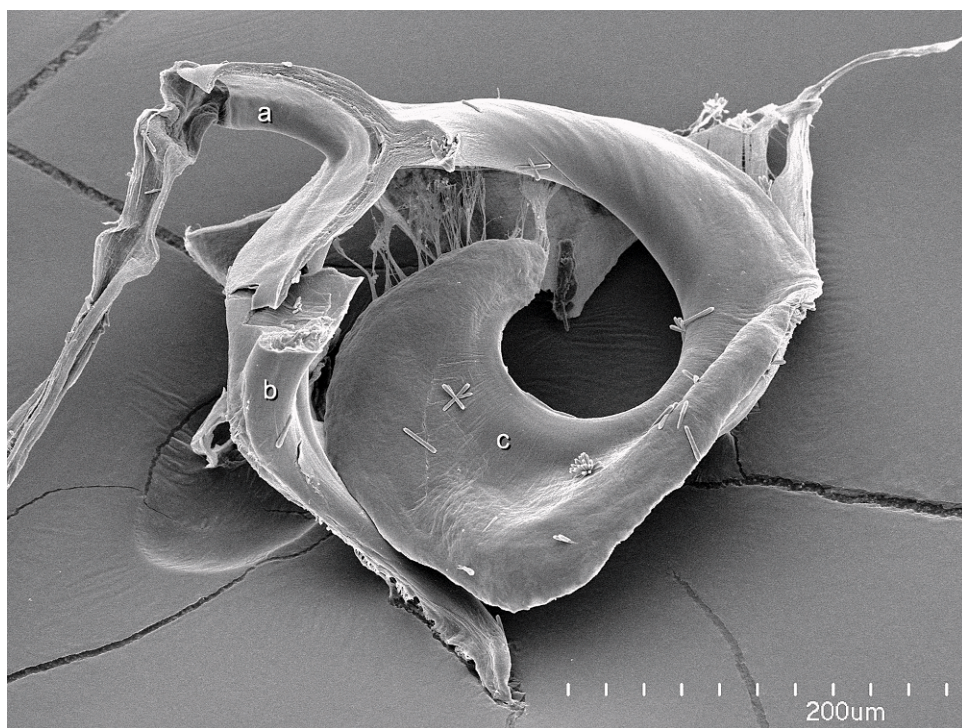


Fig. 15. Left mandibular adductor apodeme of *Anochetus emarginatus*, muscles removed. Note the wide sclerotized surface for muscle attachment. Abbreviations: a, apodeme medial branch; b, apodeme ligament; c, apodeme lateral branch.

originates basally at the lateral abductor apodeme (state 1 as in *Nothomyrmecia macrops*). The torqued mandible is the prevalent type among adult female ants, and it occurs regardless of the shape of the mandible.

30. *Dorsolateral face of mandible*: (0) without a groove; (1) with an oblique outward curved groove.

This groove runs laterapicad from the mandalus to the external margin forming a diagonal line across the external mandibular surface. The groove may be well marked (e.g., *Platythyrea punctata*, *Plectroctena strigosa*) to weak (e.g., *Pachycondyla porcata*). Some taxa (e.g., *Pachycondyla apicalis*, *Streblognathus peetersi*) show a shallow depression covered by small sparse setae that follow the same pattern described above and may represent a possible vestigial groove.

31. *Mandibular adductor apodeme*: (0) straight; (1) hooklike.

The mandibular adductor apodeme is a cuticular structure inside the cranium that connects to the base of the mandible on

its anterior end and serves as attachment site for the adductor muscle that closes the mandible when contracted (Snodgrass, 1935: 139). In most ants the apodeme consists of a sclerotized short stemlike base that branches posterad into lateral, central, and median straight branches (Paul and Gronenberg, 1999). In *Anochetus* and *Odonotomachus* the lateral branch is massive and heavily sclerotized and projects anterad as a hooklike structure (fig. 15. Gronenberg, 1995; Gronenberg and Ehmer, 1996); the modified hooklike apodeme is part of the specialized trap-jaw mechanism present in these genera (Brown, 1976; Carlin and Gladstein, 1989; Gronenberg et al., 1993).

32. *Articulation of labrum with maxillae*: (0) labro-palpal type; (1) labro-stipital type; 0) absent.

In both articulation types the maxillae interact with the labrum by way of the lateral labral arms. When a labro-palpal articulation is present, the lateral arms are perpendicular to the labrum and lock with the proximal

maxillary palpus joint that sits on the distal-most part of each stipes (state 0, as in *Formica fusca*; fig. 16A). In the labro-stipital articulation type, the stipes interacts directly with the labral arms, which extend in the same plane as the labrum. When the mouth-parts close, the stipes presses against the labral arms locking and securing the labrum on top of the retracted maxillo-labial complex (state 1, as in *Pachycondyla villosa*; fig. 16B–C). The area of articulation in the stipes appears as a weaker, pallescent part of the cuticle under the microscope on dissected maxillae.

33. *Labro-stipital articulation type on maxillae*: (0) apical and acute; (1) apical and flat; (2) apical and projecting beyond palpal socket; (3) lateral.

While the labrum always articulates with the maxillae by way of the labral arms, the position and shape of the stipital articulation is variable but falling into four main types: the stipes may articulate by way of a short acute process just lateral (to the exterior) to the palpus insertion (state 0, as in *Tetraponera aethiops*; fig. 17A); the articulation area may consist of a flat distal margin that extends lateral and to the exterior from the palpus insertion (state 1, as in *Manica rubida*; fig. 17C); the stipes may bear a strong tooth-like cuticular process that projects distad beyond the palpus insertion (state 2, as in *Pachycondyla villosa*; fig. 17D); or the stipes may articulate via a lateral extension (= lateral shoulder, Gotwald, 1969) midway on the lateral margin (state 3, *Eciton hamatum*; fig. 17B).

34. *Maxillary stipes, outer margin*: (0) without lateral expansion; (1) expanded laterad and arched.

The outer margin of the maxillary stipes is normally straight to slightly outwardly curved (fig. 17A–D). However, in taxa in which the mandibular articulations are widely separated (e.g., *Leptogenys*, *Thaumatomyrmex*), the outer stipital margin expands laterad on its distal half forming a strong arc that, when the maxillo-labial complex is retracted, effectively closes the corners of the fan-shaped oral foramen (fig. 18A–B).

35. *Transverse stipital groove*: (0) absent; (1) present, proximal face not projecting beyond

inner margin; (2) present, proximal face projecting beyond inner margin. Additive.

The external surface of the stipes may bear a diagonal groove across its middle, the transverse stipital groove, which divides the stipes into a *proximal external face* and a *distal external face* (Gotwald, 1969: 8). The proximal face is raised in relation to the distal face (fig. 17A–B) and the groove accommodates the distal labral margin when the maxillo-labral apparatus is retracted and the labrum rest against it, concealing part or all of the distal external face (Gotwald and Levieux, 1972: 388). In most taxa where the groove is present (e.g., *Ectatomma tuberculatum*, *Odontoponera transversa*), the proximal face does not extend beyond the inner margin of the stipes (state 1; fig. 17A). In some taxa, the proximal face extends beyond the inner margin as a raised shelllike projection (state 2, as in *Mystrium voeltzkowi*, *Dorylus helvolus*; fig. 17B). When the maxillo-labral apparatus is retracted the basal inner borders of each stipes meet, concealing the prementum underneath the extended proximal faces (see also Gotwald, 1969: 132). Otherwise the stipes bears no groove, and the external face extends as an uninterrupted, flat surface (state 0, as in figs. 17D, 18A–B). The condition described for state 2 has been treated in identification keys, diagnoses, and cladistic analyses in terms of the visibility of the prementum (Bolton, 2003; Brady and Ward, 2005) rather than in anatomical terms relating to the presence of stipital processes and therefore its identity with the processes described here as state 1 have been missed. In addition, the condition described here as state 2 has been proposed as a universal and unique synapomorphy for the dorylomorph subfamilies (Bolton, 2003; Brady and Ward, 2005); however, among dorylomorph taxa stipital processes covering the prementum are absent in *Aenictus* species and outside this group this condition is present among some Amblyoponinae (e.g., *Mystrium*, *Amblyopone pluto*).

36. *Maxillary palp number*: (0) 6; (1) 5; (2) 4; (3) 3; (4) 2; (5) 1; (6) 0.

The unique basal arrangement of maxillary palpi found in *Discothyrea* (see char. 39) has led some authors to miscount the number of palpomeres. Species in this taxon are

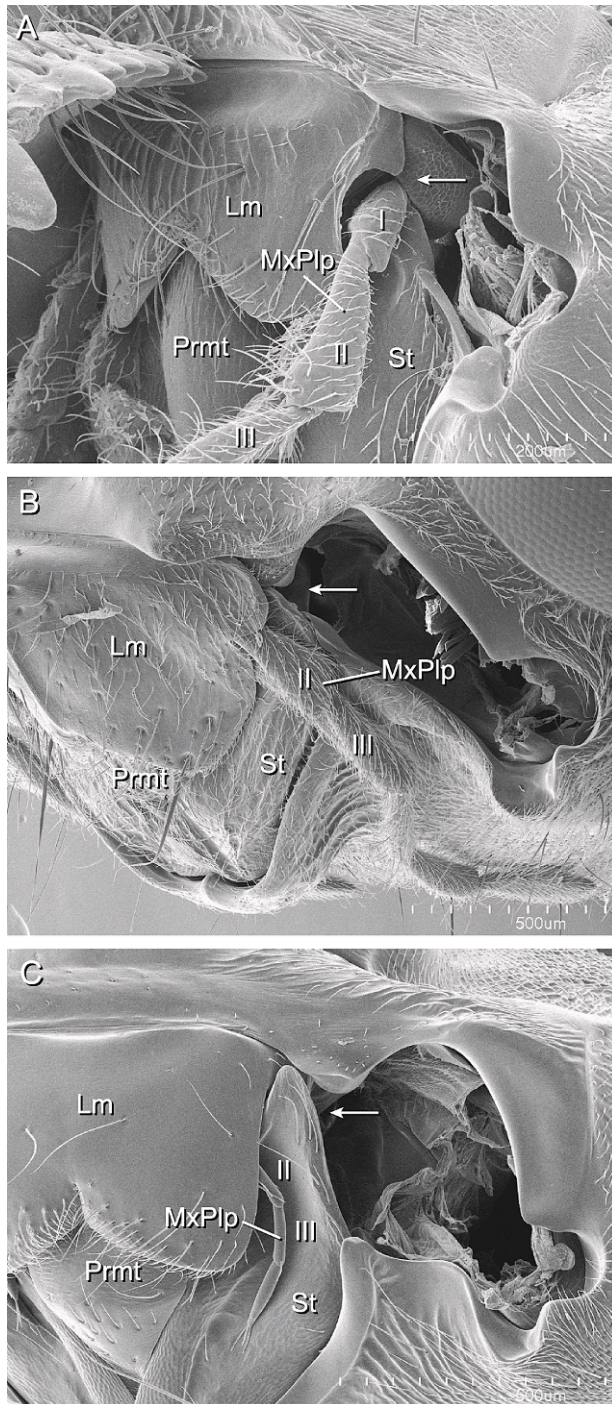


Fig. 16. Labro-maxillary articulation, left anterolateral view. Left mandible removed. The first three segments of the maxillary palpus are labeled when visible (I–III). Arrow points to the place of articulation. See text for explanation. **A.** *Formica fusca* group. **B.** *Myrmecia brevinoda*. **C.** *Pachycondyla apicalis*. Abbreviations: Lm, labrum; MxPlp, maxillary palpus; Prmt, prementum; St, stipes.

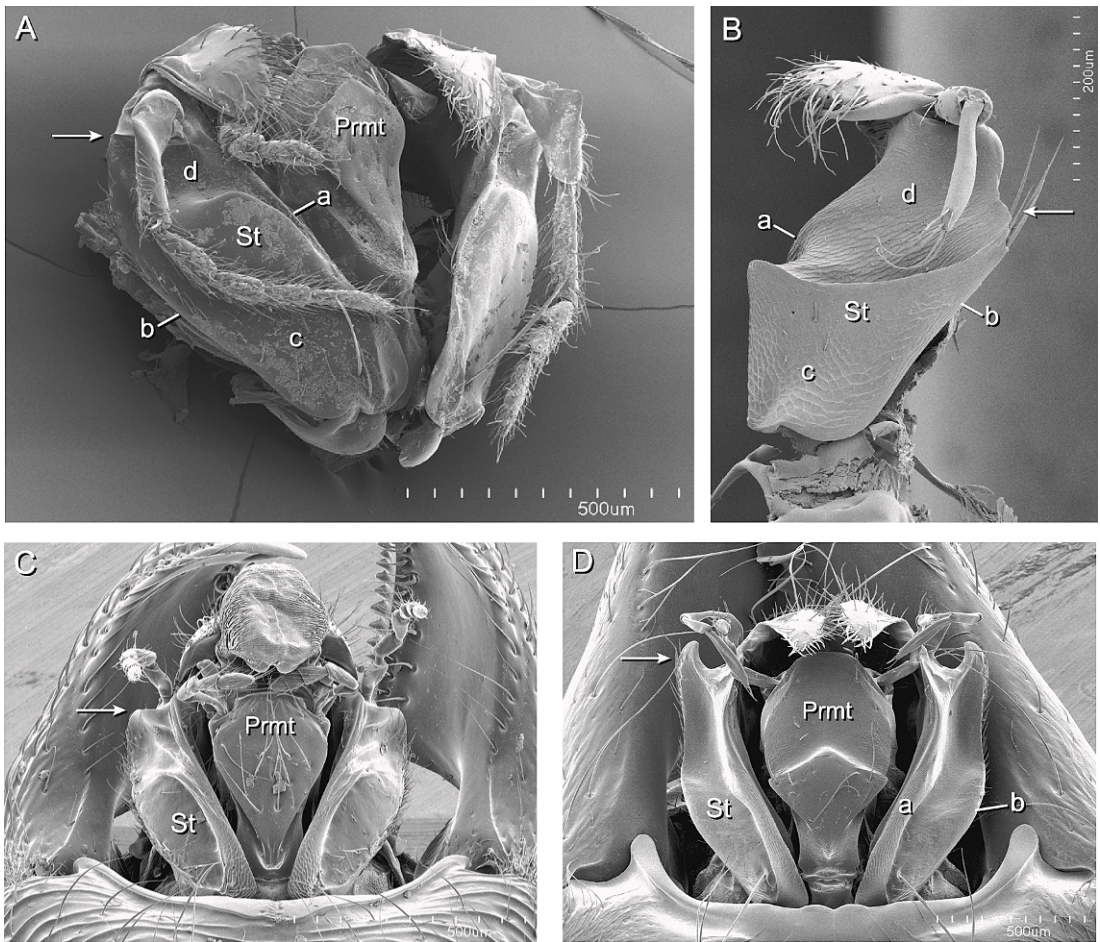


Fig. 17. Labro-stipital articulation types. Arrow indicates articulatory area on the stipes. **A.** Maxillae and labium of *Tetraponera aethiops*, right view. **B.** Left maxilla of *Eciton hamatum*. **C.** Maxillae and labium in situ of *Manica rubida*. **D.** Maxillae and labium in situ of *Pachycondyla villosa*. See text for explanation. Abbreviations: a, inner margin of stipes; b, outer margin of stipes; c, proximal face of stipes; d, distal face of stipes; Prmt, prementum; St, stipes.

usually reported as having one joint less and the genus as having no more than five joints (e.g., Bolton, 2003; de Andrade and Baroni Urbani, 2003).

37. *Labial palp number*: (0) 4; (1) 3; (2) 2; (3) 1.

The maximum number of labial palp joints known in ants is four. This number is often assumed to be a plesiomorphic condition with respect to lower numbers and loss of palpomeres is presumed to have occurred multiple times independently (e.g., Lattke, 1994).

38. *Maxillary palpi second palpomere*: (0) tubular; (1) hammer shaped.

Pointed out first by Brown (1958: 330 [84]) as a synapomorphy for *Proceratium* (fig. 19A), the hammer-shaped palpomere is discussed in detail by Baroni Urbani and de Andrade (2003a: 52). This peculiar feature is reported here to be shared also by *Probolomyrmex* species (fig. 19B).

39. *Maxillary palpus basal zigzag arrangement*: (0) absent; (1) present.

In *Discothyrea* the first two proximal palpomeres are highly reduced, partially fused, and transverse in relation to each other, so that the second palpomere articulates perpendicular to the first and the third palpo-

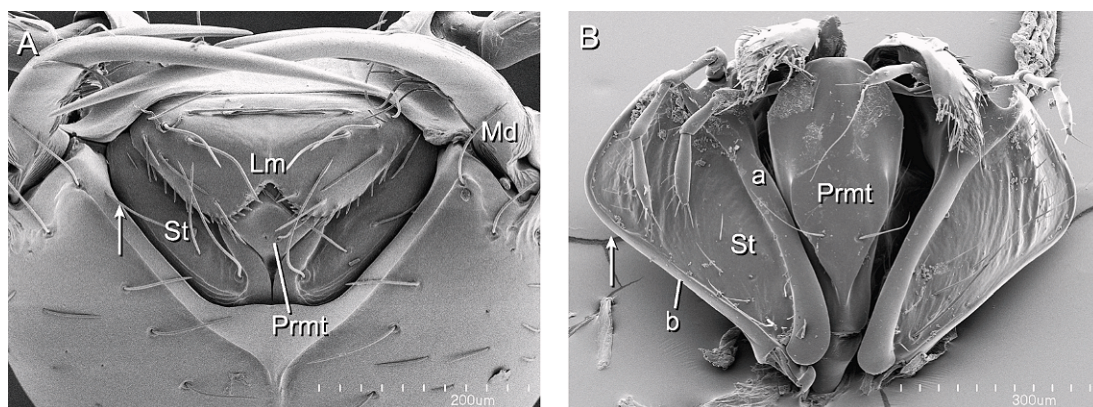


Fig. 18. Mouthparts, ventral view. Arrow points to lobate projections in the stipes. **A.** Closed mouthparts in situ of *Thaumatomyrmex atrox*. **B.** Maxillae and labium of *Leptogenys* sp. 1. Abbreviations: a, inner margin of stipes; b, outer margin of stipes; Lm, labrum; Md, mandible; Prmt, prementum; St, stipes.

mere perpendicular to the second forming a zigzag arrangement (fig. 19C). Otherwise the palpomeres articulate following each other's axis in a more or less linear arrangement (see also char. 36).

40. *Galeal comb*: (0) absent; (1) present.

The galeal comb is a row of large flat peglike setae that runs along the free margin of the galea (Gotwald, 1969: 8). The comb sits on the dorsal (outer) surface of the galea right opposite to the maxillary comb located on the ventral (internal) surface (fig. 20A–B). The galeal comb may be composed of multiple setae (as in *Amblyopone armigera*) or just a couple of hyperthrophied setae (as in *Eciton hamatum*).

41. *Spatulate stout setae on galeal crown*: (0) absent; (1) present.

The galeal crown, the distalmost part of the galea (Gotwald, 1969), may bear numerous spatulated setae along its dorsal (outer) margin (state 1, as in *Discothyrea oculata*; fig. 20C). Unlike the galeal comb, these spatulated setae sit well beyond the place where the maxillary comb is located (see char. 40). Otherwise the galeal crown has numerous undifferentiated setae (state 0, as in *Pachycondyla berthoudi*; fig. 20D).

42. *Ventral comb on galeal crown*: (0) absent; (1) present.

The galeal crown may bear an elongate comb formed by a row of closely spaced flat setae arising from its ventral surface (fig. 20A). State 1, as in *Amblyopone armigera*

(see also Gotwald and Levieux, 1972: 384).

43. *Galeal crown*: (0) flattened; (1) produced into a conical prominence.

The distalmost part of the galea, the galeal crown (Gotwald, 1969), is usually a flat continuation of this spatulate structure ending in a broad curved margin. In some *Dorylus* species (e.g., *Dorylus helvolus*) the crown forms a hollow conical prominence with a narrow base and a blunt apex (see also Gotwald, 1969).

44. *Premental shield*: (0) convex and oblong; (1) flat and rhomboidal.

In most Formicinae, Dolichoderinae, *Myrmecia*, and *Nothomyrmecia* the ventral surface of the prementum is convex and the shield is longitudinally elongate and oblong overall (state 0). Otherwise the premental surface is flat and the shield is rhomboidal to diamond shaped, sometimes with well-marked laterally rounded corners (fig. 17A,C–D; fig. 18B); this latter type also presents a high degree of sclerotization. A weak longitudinal medial crest may sometimes be present on either type of shield. In taxa where the labium is concealed under stipital projections when retracted (e.g., *Dorylus*, see char. 35) the premental shield is transversally compressed on its proximal half, but still flat and well sclerotized.

45. *Premental shield transverse groove*: (0) absent; (1) present.

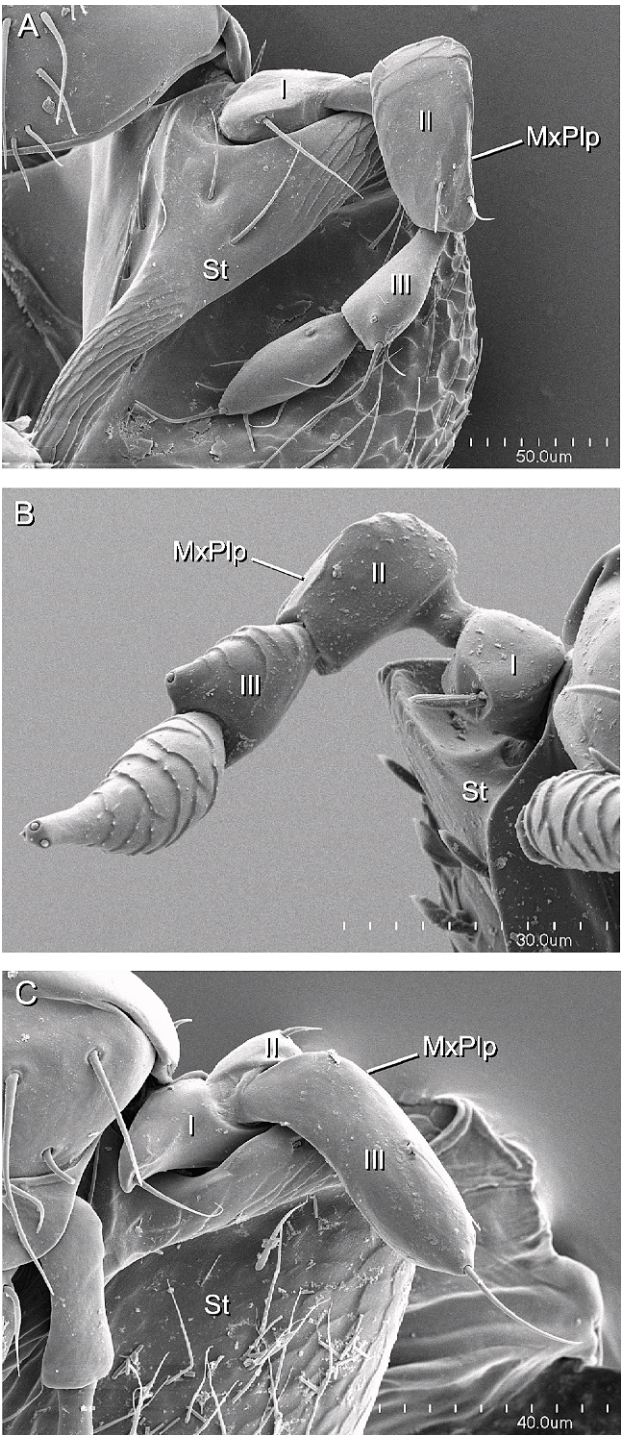


Fig. 19. Maxillary palpus. The first three segments of the palpus labeled (I–III). A. *Proceratium pergandei*, left palpus. B. *Probolomyrmex guineensis*, right palpus. C. *Discothyrea antarctica*, left palpus. Abbreviations: MxPlp, maxillary palpus; St, stipes.

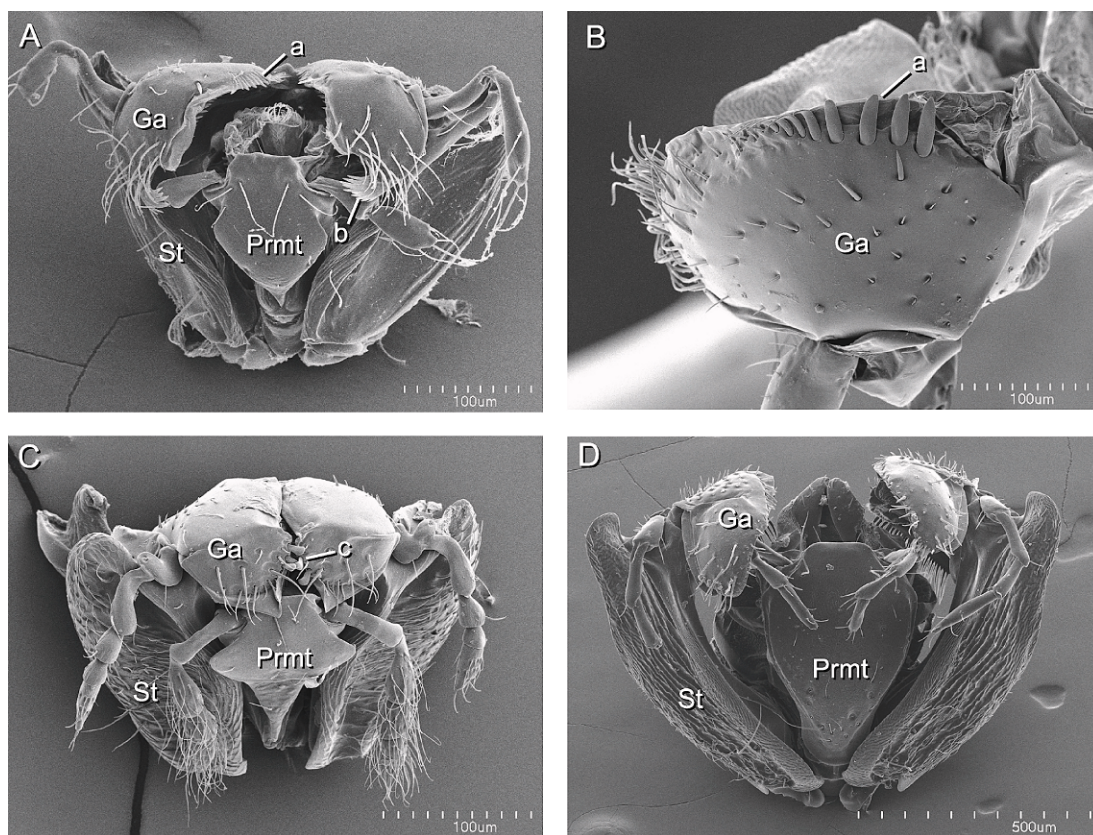


Fig. 20. Galeal armament. **A.** *Amblyopone armigera*, maxillae and labium. **B.** *Eciton hamatum*, left galea. **C.** *Discothyrea oculata*, maxillae and labium. **D.** *Pachycondyla berthoudi*, maxillae and labium. Abbreviations: a, galeal comb; b, ventral comb on galeal crown; c, spatulate stout setae on galeal crown; Ga, galea; Prmt, prementum; St, stipes.

The premental shield may bear a transverse groove analogous to the one found in the maxillary stipes (see char. 35), dividing the shield into a proximal and a distal external face (state 1; fig. 17D). The groove fits the median part of the distal labral margin when the maxillo-labral apparatus is retracted, concealing the distal face of the prementum. In general, the distal margin of the proximal face forms an acute arch that accommodates the median cleft of the labrum. Commonly, the transverse groove cuts the premental shield across the middle, so that the proximal and distal faces are of equal size (*Pachycondyla villosa*; fig. 17D). In some taxa (*Pseudomyrmecinae*, *Oecophylla*) the groove occurs near the distal margin of the premental shield and the distal face is longitudinally narrow.

46. *Specialized paraglossa*: (0) absent; (1) present.

Paired ant paraglossae consist of lobe-like structures that flank the glossa on either side, located at the membranous area between the subglossal brush and the insertion of the labial palpus (Gotwald, 1969). The paraglossa may be highly developed or much reduced and bear 1 to 3 pegs. Although its presence has been reported for only a few ant groups, in all the taxa studied during this survey (i.e., in most subfamilies) there seems to be some cuticular folding that may be attributed to the paraglossa. A major problem in determining the presence of this structure is that for the most part it is completely membranous and, unless the labium is preserved with the glossa fully expanded,

the small paraglossa may be mistaken for a folding of the cuticle on this area. An exception to this is found in the exemplars representing Myrmicinae in this study (e.g., *Manica rubida*). These taxa have large specialized paraglossa that are barrel shaped and bear multiple long spinelike microtrichia on their distal end. Such specialized paraglossa are slightly sclerotized except for a longitudinal dorsal strip that remains membranous. The slight degree of sclerotization relative to the rest of the surrounding membrane makes this structure easy to spot even when the soft parts of the labium are collapsed and gives a palpomerelike appearance to the paraglossa from lateral and ventral view. The function of this specialized structure is unknown and its homology with the true paraglossa found in other Hymenoptera is questionable (Gotwald, 1969; Baroni Urbani et al., 1992).

47. *Compound eye*: (0) absent; (1) present; (2) present, corneal facets fused into a single lens.

Compound eye in Formicidae may be large and formed by a few hundred ommatidia (e.g., *Myrmecia*, *Harpegnathos*), small with just a few facets (e.g., *Acropyga*, *Cryptopone*), or completely absent (e.g., *Leptanilla*, *Pachycondyla* [= *Wadeura*] *guianensis*). In some taxa (e.g., *Eciton*, *Simopelta*) the facets of the compound eye are fused into a single strongly convex cornea that acts as a single lens for the cluster of reticular cells lying under it (Werringloer, 1932). The fused ommatidia form a structure analogous to a true ocellus; however, vestiges of the multiple facets may normally be seen on the corneal surface under the scanning electron microscope. Brady (2003) and Brady and Ward (2005) treated the absence/presence and modification of the compound eye as separate characters, causing the paradoxical situation where presence of compound eye was treated as homologous to eye absence.

48. *Ocelli*: (0) absent; (1) present.

Universally present among ant males and queens, ocelli among workers are absent for the most part, but are present in some taxa, especially within Formicinae. Workers of *Asphinctopone silvestrii* may bear an apparent median ocellus, but this taxon has been coded as absent for this character.

Mesosoma

49. *Promesonotal junction*: (0) articulated; (1) sutured; (2) fused, indistinct. Additive.

The promesonotal junction is defined here explicitly as the point of confluence between the posterodorsal margin of the pronotum and the anterior margin of the mesonotum. The mesothoracic spiracles are used as landmarks: the posterior pronotal margin usually projects posterad at these spots forming spiracular lobes (= pronotal lobes, Gibson, 1985. See also char. 56) that functionally act as lateral hinges when the pronotum is articulated with respect to the mesothorax (fig. 21). Thus, the promesonotal junction pertains only to the confluent margins that run dorsad from one spiracle to the other. Since the pronotum extends ventrolaterad and therefore the posterior margin extends below the location of these lateral hinges at the spiracles, there is a paired secondary articulation or junction formed with the mesepisterna. These paired junctions, which show fusion to various degrees, are treated as a separate character (char. 50).

The promesonotal junction may be articulated and highly movable (state 0, as in *Harpegnathos saltator*; fig. 21A), or it may be fused into an immovable but well marked suture (state 1, as in *Rhytidoponera confusa*, *Paraponera clavata*), or it may be completely fused with no trace of suture forming a promesonotal complex (state 2, as in *Eciton hamatum*, *Myrmica americana*; fig. 21B–C).

50. *Pronotomesepisternal junction*: (0) articulated; (1) sutured; (2) fused, indistinct.

The *pronotomesepisternal junction** is the point of confluence between the posterolateral margins of the pronotum and the anterior margin of the mesepisternum laying in direct opposition (specifically the area corresponding to the anepisternum). The *posterolateral margins of the pronotum** are defined here as the part of the posterior margin that extends below the level of the mesothoracic spiracles down to the ventral margin of the pronotum on each side of the thorax (fig. 21A–B; see also char. 49). These paired junctions may form movable articulations (state 0, as in *Nothomyrmecia macrops*, *Formica fusca*; fig. 21A); may be fused into immovable sutures (state 1, as in *Ectatomma tuberculatum*, *Acanthostichus ser-*

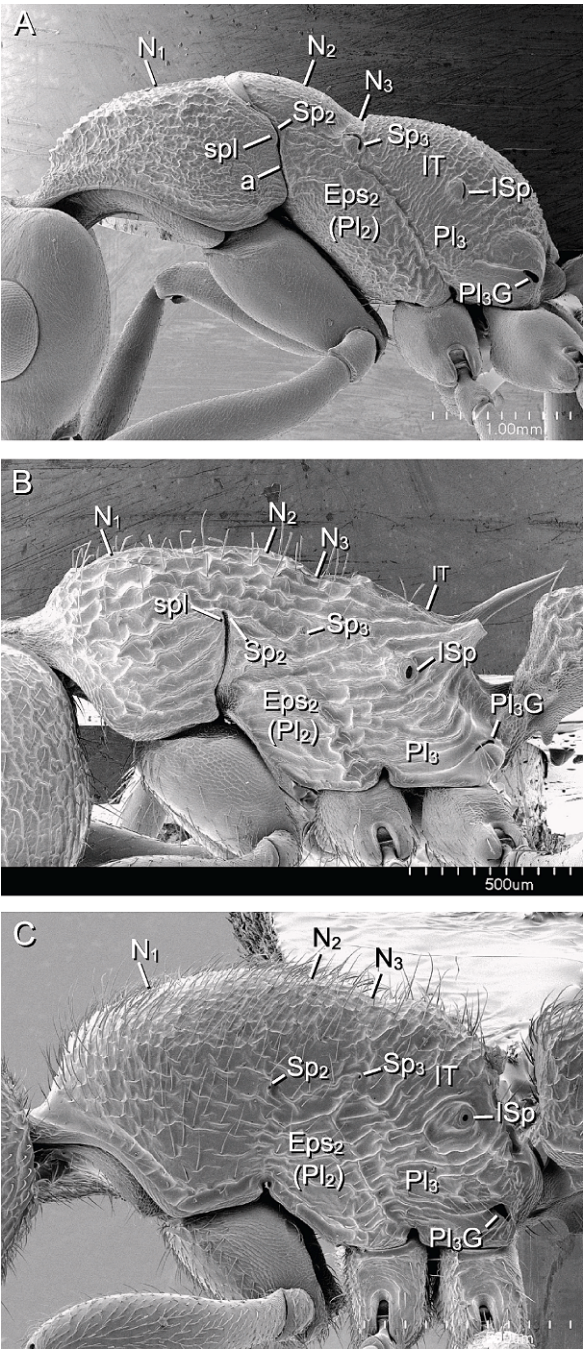


Fig. 21. Mesosoma showing different degrees of thoracic fusion, left lateral view. **A.** *Nothomyrmecia macrops*. **B.** *Myrmica americana*. **C.** *Proceratium croceum*. Note that the boundaries of notal and tergal plates in B–C can be inferred only relative to the position of the spiracles. Abbreviations: a, posterolateral margins of pronotum; Eps₂, mesepisternum; N₁, pronotum; N₂, mesonotum; N₃, metanotum; Pl₂, mesopleuron; Pl₃, metapleuron; Pl₃G, metapleural gland opening; Sp₂, mesothoracic spiracle; Sp₃, metathoracic spiracle; ISp, propodeal spiracle; spl, spiracle lobe; IT, propodeum.

ratulus; fig. 21B); or may be completely fused with no external sign of a suture (state 2, as in *Proceratium croceum*; fig. 21C). This character is coded separately from the preceding character (char. 49, unlike Brady, 2003) to emphasize the different anatomical relation between the structures involved.

51. *Stout, peglike setae on pronotal disc*: (0) absent; (1) present.

A putative autapomorphy of *Concoctio*, the pronotum raises abruptly to form a well-marked anterior border followed by a flat disc (Brown, 1974). This surface bears numerous stout, peglike setae anteriorly directed (state 1, *Concoctio concentra*).

52. *Mesonotum*: (0) round and dome shaped; (1) longitudinally narrow and flat; (2) continuous or near continuous with metanotum and propodeum in profile.

The worker mesonotum may be a very prominent and distinctly delineated sclerite within the mesosoma or it may be completely fused with the propodeum and the rest of the thoracic structures to the point where its delimitation can only be inferred from the position of the paired mesothoracic and metathoracic spiracles (see also char. 57). When most prominent (e.g., *Ectatomma* and *Formica*), the mesonotum is round in dorsal view, dome shaped and well delineated by impressed sutural lines (state 0), creating an interrupted dorsal mesosomal profile. The mesonotum may also be shaped as a longitudinally narrow transverse oval in dorsal view and flat in profile (e.g., *Amblyopone pallipes* and *Ponera alpha*), while still delineated from the metanotum and propodeum (state 1). Alternatively, the mesonotum may be fused and continuous with the metanotum and propodeum (e.g., *Paraponera clavata* and *Proceratium pergandei*), forming an uninterrupted dorsal mesosomal profile (state 2).

53. *Notopleural suture on mesothorax*: (0) present; (1) absent.

The mesonotum can be delineated from the mesopleura by a groovelike suture that runs slightly above and in between the mesothoracic and metathoracic spiracles on each side of the mesothorax (state 0, as in *Centromyrmex brachycola*). Alternatively, the mesonotum may be completely fused with the mesopleura forming a continuous structure

without any trace of suture or groove (state 1, as in *Prionopelta antillana*).

54. *Mesonotal lateral margins*: (0) parallel to subparallel; (1) posteriorly tapering, dorsum triangular.

The sides of the mesonotum are normally parallel to subparallel in dorsal view, and when delineated this structure has an oval appearance in dorsal view (state 0, as in *Nothomyrmecia macrops*). Alternatively, the mesonotum may be posteriorly tapering by lateral constrictions of the upper region of the mesopleura, resulting in a triangular dorsum. Brown (1974) mistakenly described this constriction as similar to the one found in some Ponerini genera (e.g., *Centromyrmex*, *Cryptopone*); however, in these taxa the constriction pertains to the anterior part of the propodeum (see char. 63). State 1 is a putative autapomorphy of *Concoctio concentra*.

55. *Median sulcus on mesepisterna*: (0) absent; (1) present.

The median mesepisternal sulcus consists of a horizontal to oblique groovelike sulcus running from the anterior margin of the mesepisternum, just below the pronotomese-pisternal junction (see char. 50), to the endoapodemal pit of the mesopleural arm. When absent the mesepisternum consists of a single undivided plate (state 0, as in *Platythyrea punctata*). When the median sulcus is present, the mesepisternum is divided into an upper anepisternum and a lower katepisternum (state 1, as in *Pachycondyla apicalis*).

56. *Mesothoracic spiracle*: (0) concealed by a spiracular lobe; (1) exposed.

The mesothoracic spiracle is usually concealed underneath a round lobe formed by a posterior projection of the posterolateral margin of the pronotum (= pronotal lobes Snodgrass, 1956: 236. State 0, as in *Pachycondyla crassinoda*; Gibson, 1985; fig. 21A–B). This spiracular lobe is absent in some taxa and the opening of the spiracle is exposed and clearly visible in lateral view (state 1, as in *Discothyrea testacea*; fig. 21C). Whether the lobe is present or absent is independent of the degree of fusion between the pronotal posterolateral margin and the anterior mesepisternal edge (i.e., independent of char. 50). Both the meso- and metathoracic spiracles may be much reduced and difficult to see in the smallest species (e.g., *Probolo-*

myrmex, *Leptanilloides*), but they were always present in all the taxa examined during this study. The spiracular lobe cannot be closed and is not homologous to a true spiracular operculum.

57. *Metanotum*: (0) discernable on dorsal mesosoma as a transverse striplike sclerite; (1) present only as a groove; (2) obliterated. Additive.

In worker ants the metanotum can be discernible as a dorsal transverse striplike sclerite (fig. 22A), delineated from the mesonotum and propodeum by anterior and posterior groovelike sutures respectively (state 0, as in *Nothomyrmecia macrops* and *Tetraponera aethiops*); or present as a single transverse groove (state 1, as in *Typhlomyrmex pusillus* and *Amblyopone pallipes*; fig. 22B). Otherwise the metanotum is completely obliterated and the mesonotum and metanotum form a continuous dorsal surface with the propodeum (state 2, as in *Platythyrea turneri*; fig. 22C). In the latter state, the relative position of this fully fused sclerite can only be inferred from the position of the metathoracic spiracles (see also char. 52). Workers of some *Odontomachus* species show a narrow, raised transverse area delineated by grooves similar in overall appearance to a metanotum in state 0, but lying anterior to the metathoracic spiracles. However, comparisons with ergatoid queens of the same genus show that this area corresponds to a vestigial scutellum (Keller, unpubl. data), and thus *Odontomachus bauri* has been scored as state 1.

58. *Metathoracic spiracle*: (0) concealed by a spiracular lobe; (1) exposed, opening round to oval.

A serial homolog of the mesothoracic spiracle (char. 56), the second thoracic spiracle may be concealed underneath a round and raised spiracular lobe formed by a posterior projection of the much reduced mesepimeron (= piastra stigmatica, Emery, 1900: 106). This spiracular lobe is delineated anteriorly by a sulcus (= pleural sulcus?) that sets it apart from the rest of the mesopleural episternum, forming a bulla or scale (state 0, as in *Ectatomma tuberculatum*, *Tetraponera aethiops*; figs. 21A, 22A–C). The lobe may be absent in which case the spiracle is exposed and clearly visible in profile (state 1, as in *Myrmica americana*; fig. 21B–C).

59. *Metathoracic spiracle orientation*: (0) dorsad; (1) posterolaterad; (2) anterolaterad.

The metathoracic spiracles may be situated high on the mesosoma, close to each other, and opening into the mesosomal dorsum (state 0, as in *Formica fusca* and *Aneuretus simoni*). Otherwise they are situated lower on the mesosoma laterad, with the opening directed either posteriorad (state 1, as in *Myopopone castanea* and *Myrmica americana*), or anterad (state 2, as in *Dorylus helvolus* and *Leptanilloides biconstricta*).

60. *Metapleural gland*: (0) absent; (1) present.

The metapleural gland (Brown, 1968) is a gland found exclusively in ants and it is believed to be involved in the secretion of antibiotic substances (Hölldobler and Wilson, 1990). Internally the glandular cells are arranged in a pair of large clusters occupying the mesosomal cavity formed by the metathorax and propodeum. Each cell cluster sits on a membranous collecting sac located at the end of an internal cuticular storage chamber (Hölldobler and Engel-Siegel, 1984), which lays immediately dorsal to the socketlike acetabulum of the metacoxa and opens to the exterior at the lower posterior corner of the metapleura (figs. 21, 23). The size and shape of the cuticular chamber varies greatly across the family.

61. *Ventral flap on metapleural gland opening*: (0) absent; (1) bulla shaped and unarmed; (2) oblong and armed with a keellike projection.

The ventral flap corresponds to a thin cuticular extension of the ventral margin of the external aperture of the metapleural gland chamber. It projects dorsad freely over the opening, appearing convex on its external surface. The flap covers the opening almost entirely (fig. 23B–C), leaving an oblique curved slit aperture directed dorsad to posterodorsad (Bolton, 2003: 45). The structure may be a simple round to oval projection appearing as a bulla in the lower posterior corner of the metapleuron, usually bearing a set of setae directed dorsad (state 1, as in *Ectatomma tuberculatum*, *Myrmica americana*; fig. 23B); or it may be a dorsally oblong extension, armed with a thick keellike posterolaterad projection that runs vertical through its center (state 2, as in *Amblyopone australis*, *Apomyrma stygia*; fig. 23C). The

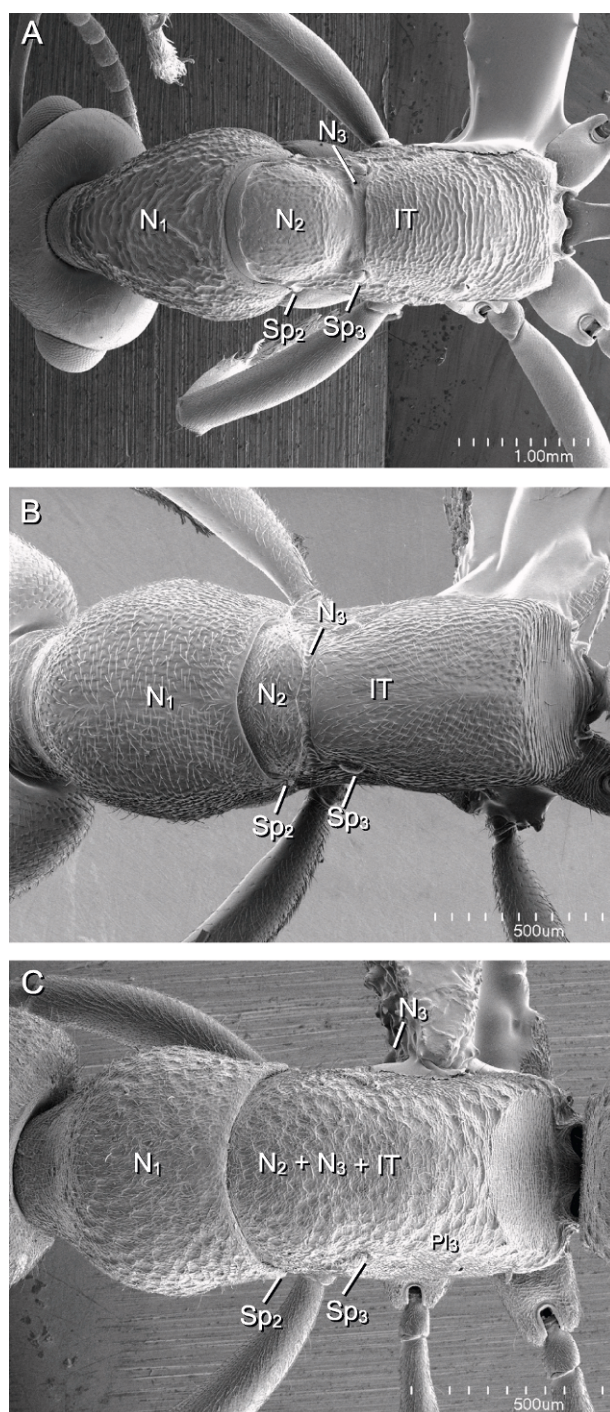


Fig. 22. Mesosoma showing different degree of fusion of dorsal sclerites, dorsal view. **A.** *Nothomyrmecia macrops*. **B.** *Amblyopone pallipes*. **C.** *Platythyrea turneri*. See text for further explanation. Abbreviations: N₁, pronotum; N₂, mesonotum; N₃, metanotum; Sp₂, mesothoracic spiracle; Sp₃, metathoracic spiracle; IT, propodeum.

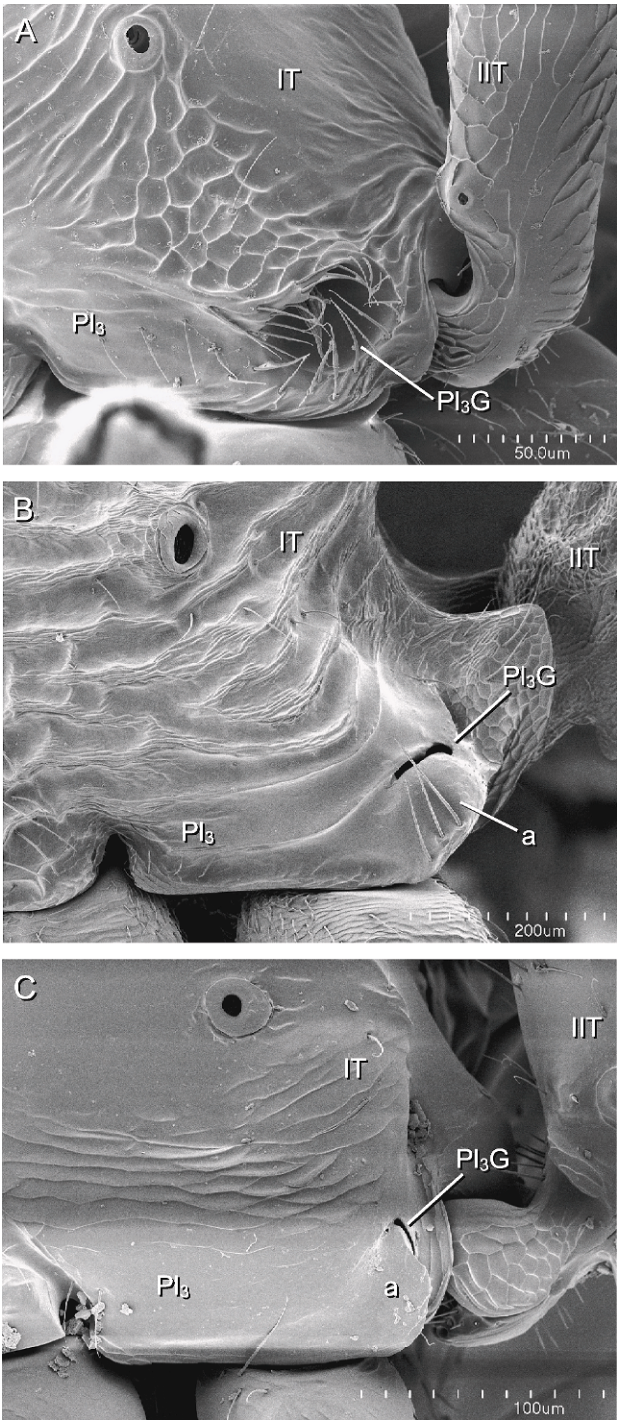


Fig. 23. Metapleural gland opening, left lateral view. **A.** *Aneuretus simoni*. **B.** *Myrmica americana*. **C.** *Prionopelta antillana*. Abbreviations: a, ventral flap projection; Pl₃, metapleuron; Pl₃G, metapleural gland opening; IT, propodeum; IIT, tergum of petiole.

keellike projection may be a small, well-defined carina or a large structure concealing the propodeal lobe in profile (e.g., *Mystrium*). State 0 is as in *Formica fusca* and *Nothomyrmecia macrops*. Taxa lacking the metapleural gland have been coded as inapplicable for this character.

62. *Metapleural longitudinal flange*: (0) absent; (1) projecting laterad; (2) projecting ventrolaterad, concealing the metapleural gland opening.

This carina runs parallel to subparallel to the body long axis through the metapleuron, from the middle lower side of the sclerite to the dorsum of the metapleural gland opening. In many taxa (e.g., *Nothomyrmecia macrops*) a weak carina may be present, running as a low ridge that delineates dorsally a shallow impression immediately anterior to the metapleural gland opening (see Bolton, 1990b, for a detailed description). In such cases, the carina simply merges into the dorsal margin of the gland aperture without forming a flap or flange. Alternatively, this carina may project laterad increasingly toward the back forming a flap or flange with a round ending dorsal to the metapleural gland opening without concealing its aperture (state 1, as in *Acanthoponera minor*, *Tetraponera aethiops*). Alternatively, the carina may form a strong ventrolaterally projected flange extending posterad beyond the metapleural gland opening and concealing its aperture in lateral view (Bolton, 1990b, as in *Acanthostichus serratus*). In some taxa (e.g., *Cheliomyrmex morosus*) the flange extends further posterad from the posterior limit of the metapleuron before curving down to merge with the ventral carinate margin of this pleuron.

Bolton (2003: 16) describes a state in which a flangelike carina is "reduced anteriorly and extended posteromedially" as a putative synapomorphy for the formicomorph subfamilies (Aneuretinae + Dolichoderinae + Formicinae). Dissection of the metapleural gland storage chamber, however, reveals that there is no projecting cuticular flange. Rather, the chamber meets the external surface of the metapleuron at a narrow angle dorsally, thus forming a well-marked dorsal rim to the chamber's opening. The presence of a weak carina in some formicomorph taxa (e.g., *Aneuretus simoni*) merging dorsally with the

opening, as described previously, further gives the impression of a flange, but nonetheless no such structure exists in those taxa.

63. *Propodeal lateral margins*: (0) parallel to subparallel; (1) upper anterior part strongly constricted.

The sides of the propodeum may run parallel to each other (state 0, as in *Nothomyrmecia macrops*), or the propodeum may be anteriorly tapered on its upper region by lateral constrictions of the mesosoma starting at the upper part of the metapleura just behind the metathoracic spiracles (state 1). In the latter case the propodeum has a triangular appearance in dorsal view (e.g., *Cryptopone gilva*). See also char. 54.

64. *Propodeal spiracle*: (0) with bulla; (1) without bulla.

The propodeal spiracle may bear a swollen bulla in the form of a round convexity of the cuticle, immediately anterior to the opening, reminiscent of the spiracular lobe found at the metathoracic spiracle (see char. 56). The bullate condition is best assessed in dorsal view (state 0, as in *Nothomyrmecia macrops*, *Tetraponera aethiops*). Otherwise the spiracle is not preceded by a shallow blister or convexity of the cuticle (state 1, as in *Pachycondyla villosa*, *Amblyopone pallipes*).

65. *Propodeal spiracle atrial opening*: (0) slit shaped; (1) round to oval.

The outer atrial opening of the propodeal spiracle may be in the shape of an oblique slit, more than twice as long as wide, from straight (e.g., *Centromyrmex brachycola*) to slightly arched (e.g., *Pachycondyla berthoudi*; state 0). Alternatively, the opening may be round (e.g., *Typhlomyrmex pusillus*) to vertical oval (e.g., *Formica fusca*; state 1).

66. *Propodeal spines*: (0) absent; (1) present.

Considered present when the propodeum is armed with strong cuticular spines directed posterad (state 1, as in *Acanthoponera minor*, *Myrmica americana*). Otherwise the propodeum is unarmed or bears only short tubercles (state 0, as in *Rhytidoponera confusa*, *Anochetus emarginatus*).

67. *Propodeal lobe*: (0) absent; (1) present.

These paired lobes that flank the propodeal foramen (= petiolar foramen, Bolton, 2003) on each side vary greatly in size from well developed and conspicuous (e.g., *Myrmica*) to reduced (e.g., *Labidus*). Although

commonly reported as present in all Ecitoninae ants (e.g., Brady and Ward, 2005), the lobe is absent in *Cheliomyrmex*; in this genus the cuticular flange above the metapleural gland orifice projects posterad forming a large lobe that can be misidentified as belonging to the propodeum. *Aneuretus simoni*, *Apomyrma stygia*, and *Leptanilloides* have been described as lacking propodeal lobes (e.g., Bolton, 1994; Brandão et al., 1999; Bolton, 2003); however, in both *A. simoni* and *A. stygia* the lobes are reduced but nevertheless present and coded as such here. *Leptanilloides* on the other hand shows a unique condition among ants wherein the propodeal lobes are fused to form a tubular structure (see discussion of next character, char. 68).

68. *Propodeal foramen*: (0) free and visible; (1) enclosed in a tubular projection.

In *Leptanilloides* the propodeal lobes extend dorsad and ventrad meeting each other and fusing to form a tubular structure surrounding the foramen inside which the petiole articulates with the propodeum (state 1). Otherwise the propodeal foramen is free and visible on its dorsum and ventrum (state 0).

69. *Metacoxal cavity*: (0) open; (1) closed.

When open, the metathoracic acetabulum inside which the condyle of the metacoxa articulates is connected internally to the propodeal foramen (state 0, as in *Nothomyrmecia macrops*). When closed, the cavity of the metathoracic acetabulum is completely independent of the propodeal foramen (state 1, as in *Formica fusca*). Note that this way of coding is different from the one used previously in the literature. For example, Bolton (2003: 41) considers the cavity closed when there is an overlapping of external cuticle between the opening of the acetabulum and the propodeal foramen, even though the internal cavities are connected internally. After Baroni-Urbani et al. (1992: char. 13).

Legs

70. *Protibial anterior sulcus*: (0) absent, (1) present.

This is a longitudinal sulcus present on the anterior face of the protibia, running distad from its midlength and terminating near the calcar socket. This is a putative autapomorphy of *Aneuretus simoni*.

71. *Stout setae on posterior apex of protibia*: (0) absent; (1) one; (2) two.

The protibia may be armed by one (state 1, as in *Amblyopone australis*; fig. 24A) or two (state 2, as in *Nothomyrmecia macrops*) spiniform stout setae at the posterior apex, close to the place of insertion of the strigil calcar (Lattke, 1994: char. 10).

72. *Stout setae on posterior surface of probasitarsal notch*: (0) absent; (1) single; (2) row parallel to strigil comb.

The posterior surface of the probasitarsus may bear one or a row of stout setae aligned with the comb of the strigil notch (Schönitzer and Lawitzky, 1987). When single, the stout setae are present near the proximal end of the notch (state 1, as in *Typhlomyrmex rogenhoferi*; fig. 24B). Or multiple setae may be arranged in a single row parallel to the comb of the notch (state 2, as in *Amblyopone australis*; fig. 24A). Coded after Lattke (1994) characters 11 and 12 in part.

73. *Basal projection on inner portion of probasitarsus*: (0) absent; (1) rounded; (2) acute.

The probasitarsus may bear a projection on its inner basal portion. When present, this projection is the starting point for the notch and comb of the strigil. The projection may be rounded (state 1, as in *Pachycondyla apicalis*), or protrude dorsally acutely (state 2, as in *Loboponera vigilans*; fig. 24C). Otherwise the base of the probasitarsus continues into the notch of the strigil without protruding (state 0, as in *Amblyopone australis*; fig. 24A).

74. *Calcar of strigil*: (0) fully pectinated; (1) with a basal lamella; (2) fully lamellated.

The calcar of the strigil may be pectinated over its whole length (state 0, as in *Typhlomyrmex rogenhoferi*; fig. 24B), or the basal half may bear a transparent lamella (= velum, Schönitzer and Lawitzky, 1987; state 1 as in *Amblyopone australis*; fig. 24A), or it may consist entirely of a transparent lamella (state 2, as in *Myopopone castanea*; fig. 24D).

75. *Lamella of strigil calcar*: (0) entire; (1) with a notch.

When present, the lamella on the strigil is usually entire (state 0, as in *Amblyopone australis*; fig. 24A). In *Odontomachus* and *Anochetus* the lamella bear a distinct notch on its proximal end (state 1, as in *Odontomachus bauri*; fig. 24E).

76. *Brush on posterior surface of strigil calcar*: (0) absent; (1) present.

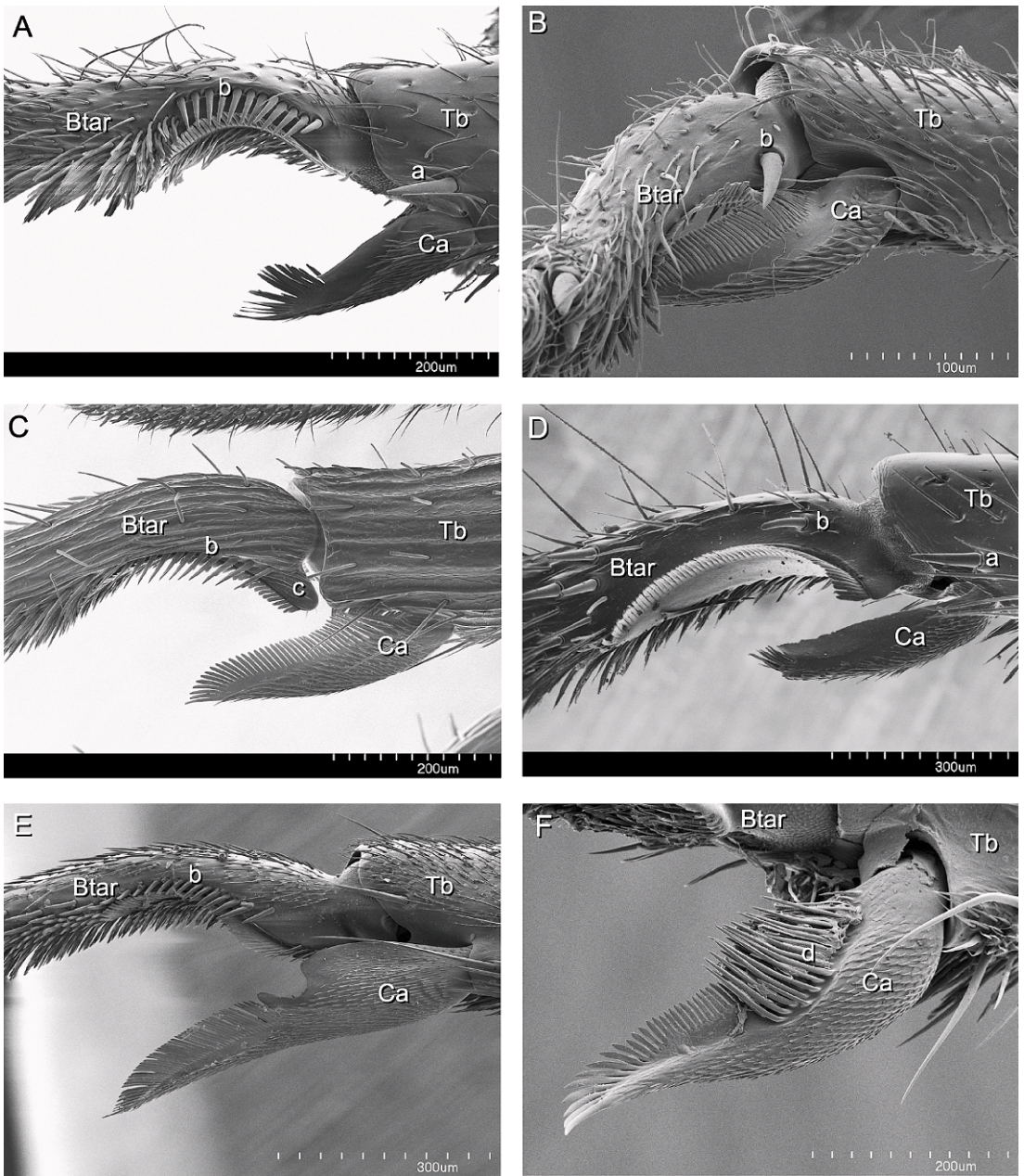


Fig. 24. Antenna cleaner, left foreleg, posterior view. **A.** *Amblyopone australis*. **B.** *Typhlomyrmex rogenhoferi*. **C.** *Loboponera vigilans*. **D.** *Myopopone castanea*. **E.** *Odontomachus bauri*. **F.** *Ectatomma tuberculatum*. Abbreviations: a, stout setae on tibial apex; b, stout setae on posterior surface of probasitarsal notch; c, basal projection on inner portion of probasitarsus; d, calcal posterior brush; Btar, basitarsus; Ca, calcar; Tb, tibia.

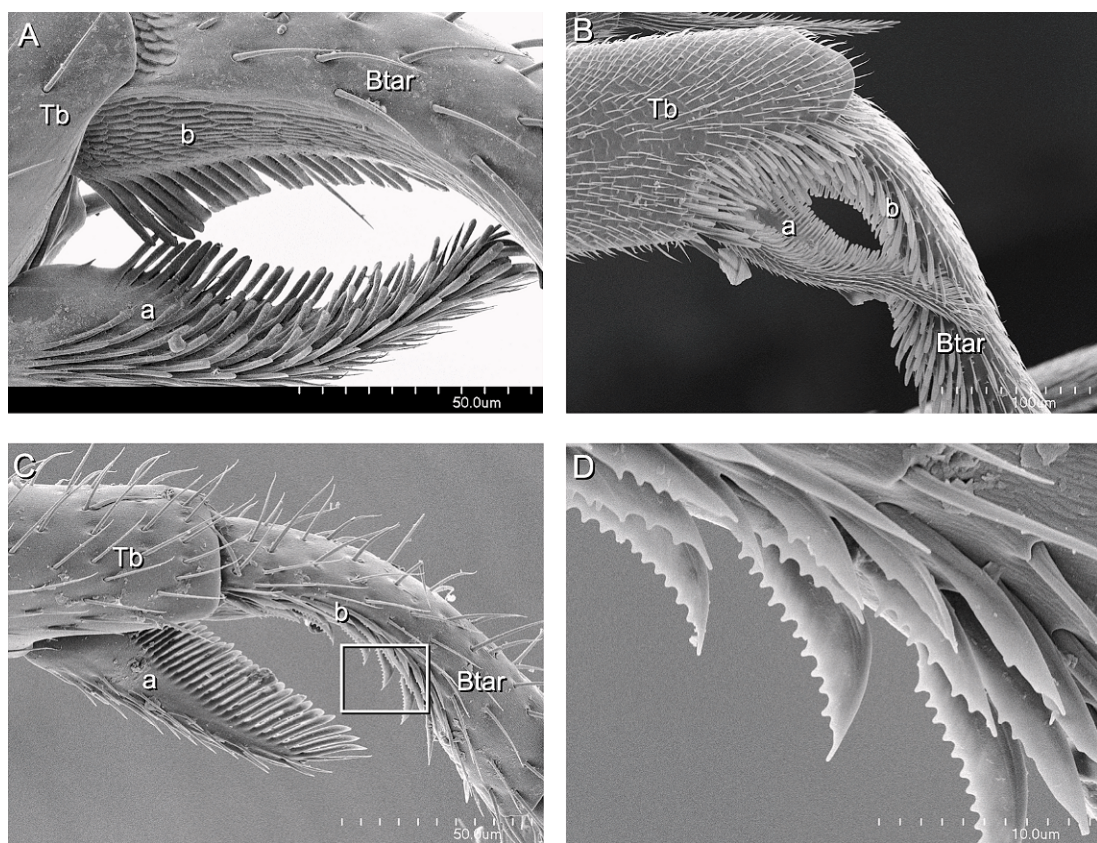


Fig. 25. Antena cleaner, left foreleg, anterior view. **A.** *Apomyrma stygia*. **B.** *Tapinoma erraticum*. **C.** *Leptanilloides biconstricta*; **D.** close-up on basitarsal notch. Abbreviations: a, calcar; b, notch on basitarsus; Btar, basitarsus; Tb, tibia.

The posterior surface of the calcar may bear a brush made of stout setaelike cuticular projections that arise just parallel to the lamellated or combed edge and project beyond it (state 1 as in *Ectatomma tuberculatum*; fig. 24F).

77. *Longitudinal sulcus on probasitarsal posterior surface*: (0) absent; (1) present.

Paraponera clavata bears a longitudinal sulcus devoid of setae along the entire length of the posterior surface of the probasitarsus.

78. *Squamiform brush on calcar anterior surface of strigil*: (0) absent; (1) present.

The brush may consist of few, widely spaced, straplike and truncate microtrichia (e.g., *Apomyrma stygia*; fig. 25A); it may be a very dense, tightly spaced arrangement of microtrichia that start as sword shaped at the bottom and transform into tapelike and truncate at the top (e.g., *Tapinoma erraticum*;

fig. 25B); or it may be made up entirely of sword-shaped microtrichia (e.g., *Thaumatomyrmex atrox*). Otherwise the anterior face of the calcar may be devoid of microtrichia (e.g., *Leptanilloides biconstricta*; fig. 25C). The brush covers the anterior surface of the calcar and differs from the spinelike and distally oriented microtrichia commonly present on the ventral margin of this spur (fig. 25A–C). Presence of this brush is a putative autapomorphy of Formicidae (Schönitzer and Lawitzky, 1987; Francoeur and Loiselle, 1988; Basibuyuk and Quicke, 1995).

79. *Setae on anterior surface of probasitarsal notch*: (0) absent, (1) paddle shaped, (2) serrated. Additive.

The notch on the ventral (inner) surface of the foreleg basitarsus (Snodgrass, 1956: 108) usually bears multiple flattened setae along its anterior surface (Schönitzer and Lawitzky,

1987). Rarely among Formicidae are such setae absent (state 0, as in *Apomyrma stygia*; fig. 25A). The setae may be paddle shaped, with a narrow peduncle and a round tip (state 1, as in *Tapinoma erraticum*; fig. 25B), or the ventral interior edge may be serrated (state 2, as in *Leptanilloides biconstricta*; fig. 25C–D).

80. *Protarsus fourth tarsomere*: (0) with lateral lobate projections; (1) conical; (2) cylindrical. Additive.

The fourth tarsomere of the protarsus may have a pair of lateral lobes that extend distally to a distance equal to the main body of the segment itself (state 0, as in *Nothomyrmecia macrops*; fig. 26A); or the fourth tarsomere may have a truncate, inverted conical shape, with the proximal part being narrow and becoming wider distad without lateral lobate projections (state 1, as in *Cerapachys nitidulus*; fig. 26B); or the diameter may be equal along the length of the tarsomere, being cylindrical in shape (state 2, as in *Ponera pennsylvanica*; fig. 26C). Tarsomeres on most ants are armed with stout setae on their lateroventral distal margins that can be mistaken for lobate extensions, but the character pertains only to the shape of the tarsomere body. Although this variation may be observed in the second to fourth tarsomeres, it is in the latter joint where the distinction is most characteristic and hence has been used as reference for this character.

81. *Propretarsal manubrium*: (0) flat and discoidal; (1) protruded distad.

The manubrium is the unpaired pretarsal sclerite located between the claws and supporting the arolium from above (Snodgrass, 1956; Federle et al., 2001). In most ants, the manubrium is a flat, discoidal to elliptical sclerite that usually bears a pair of long setae (= manubrium macrosetae, Orivel et al., 2001). Within the exemplars included in this analysis *Amblyopone mutica* departs from this arrangement by having the manubrium of the forelegs protruded distad as a finger-like structure as long as the extended arolium and bearing a distal pair of long setae plus several smaller setae along its dorsal surface.

82. *Claws in propretarsus*: (0) simple; (1) with preapical tooth; (2) pectinate; (3) with basal spines.

The pretarsal claws on the prothoracic leg may be simple (state 0, as in *Oecophylla*

smaragdina; fig. 27A); or the inner surface may bear a single tooth that may be short (state 1, as in *Cheliomyrmex morosus*) or as long as the main body of the claws (as in *Harpegnathos saltator*; fig. 27B); or the inner surface may bear multiple blunt teeth in a single row (state 2, as in *Leptogenys*; fig. 27C); or the inner surface of the claws may be armed with a set of small spiniform projections at the base (state 3, as in *Pachycondyla pachyderma*; fig. 27D).

83. *Arolium in propretarsus*: (0) vestigial to absent; (1) present.

Freeland et al. (1982) surveyed the presence of arolium across various ant species and across sexes, noting that in some taxa lacking a functional arolium a small membranous structure is still present between the manubrium and the ungular plate that may correspond to a vestigial arolium. This observation is confirmed in the extended taxon sampling surveyed here, although the difference between a vestigial arolium and its complete absence cannot be established unambiguously. Therefore state 0 correspond to cases in which no fully developed arolium is observed (fig. 27C D). Orivel et al. (2001) surveyed some *Pachycondyla* species for this character, looking for correlations with arboreal lifestyle (see also Federle, 2002; Orivel and Dejean, 2002). Finally, Federle et al. (2001) studied the biomechanics of this adhesive pretarsal organ. This propretarsal feature is coded as a separate character from the presence of arolium in the mid- and hind legs because of its independent pattern of variation (see char. 84).

84. *Arolium in mesopretarsus and metapretarsus*: (0) vestigial to absent; (1) present.

This feature is coded as a separate character from the foreleg due to its independent variation across taxa. See char. 83 for discussion.

85. *Spinellike setae on midleg*: (0) absent; (1) present on tibia and basitarsus; (2) present on basitarsus only.

The middle leg may be armed with multiple heavy, conical, spinellike setae on the extensor surface of both the tibia and basitarsus (state 1, as in *Cryptopone gilva*, *Myopopone castanea*; Brown, 1960: 171; 1963: 3); or the basitarsus alone (state 2, as in *Pachycondyla stigma*). Otherwise such setae are absent (state 0). See also char. 86.

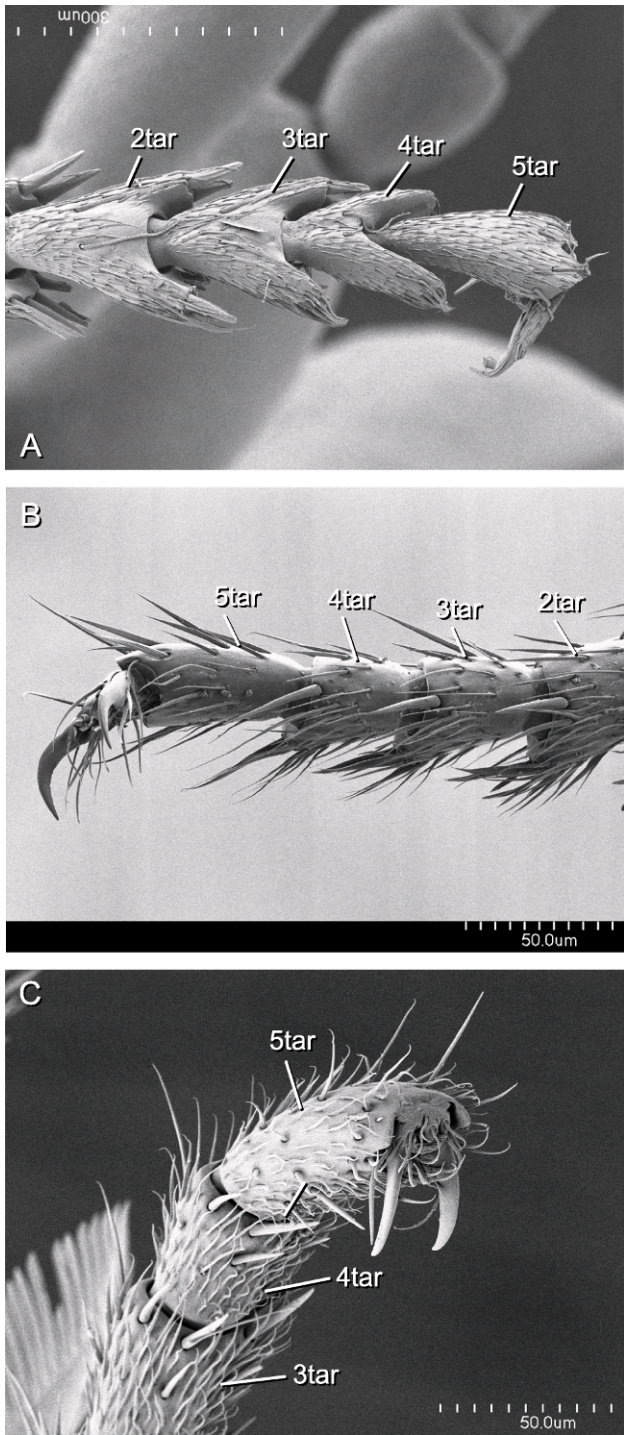


Fig. 26. Tarsus of foreleg. **A.** *Nothomyrmecia macrops*. **B.** *Cerapachys nitidulus*. **C.** *Ponera pennsylvanica*. Abbreviations: 2tar, second tarsomere; 3tar, third tarsomere; 4tar, fourth tarsomere; 5tar, fifth tarsomere.

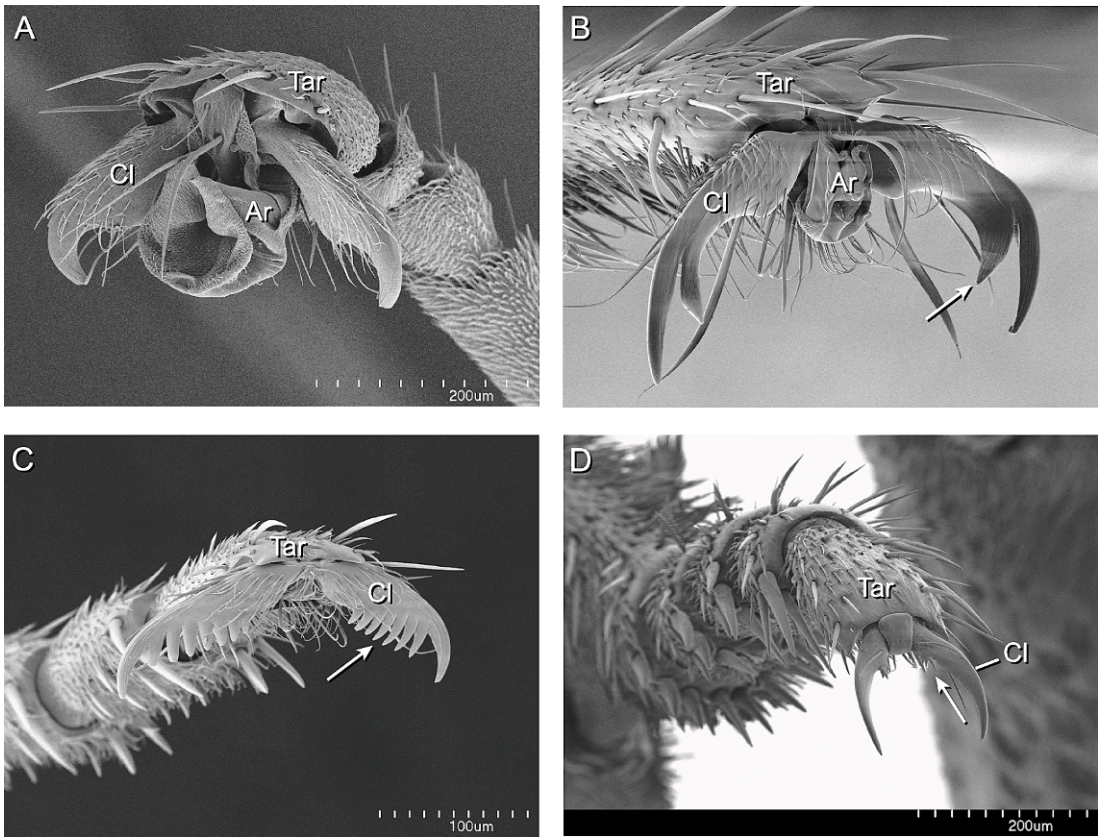


Fig. 27. Pretarsal claws of foreleg. Arrows point at claw armament. **A.** *Oecophylla smaragdina*, simple claws. **B.** *Harpegnathos saltator*, single tooth. **C.** *Leptogenys* sp., pectinated claw. **D.** *Pachycondyla pachyderma*, spiniform basal projections. Abbreviations: Ar, arolium; Cl, pretarsal claw; Tar, tarsus.

86. *Spinelike setae on metabasitarsus*: (0) absent; (1) present.

The metabasitarsus extensor surfaces may be armed with heavy, conical, spinelike setae (state 1, as in *Centromyrmex brachycola*). Otherwise the metabasitarsus are devoid of such stout setae (state 0). These heavy setae are similar to the ones present on the tibia and basitarsus of the middle leg (char. 85), but is coded here as a separate character because it shows independent variation.

87. *Metacoxal dorsum*: (0) unarmed; (1) armed with a tooth or spine.

The dorsal surface of each metacoxa may be armed with a tooth, spine, or tubercle (Brown, 1958: 223; Lattke, 1992, 2003, 2004: char. 56).

88. *Anterior metatibial spur*: (0) absent; (1) simple; (2) pectinate.

The metatibia may bear one or two spurs at the inner region of its distal end (fig. 28). Each spur has been coded here as a separate character on the ground that similarity and position support treating each structure as independent both biologically and logically. Both spurs may be of similar size and shape (as in *Amblyopone australis*; fig. 28A), but most often the one located in an anterior position is smaller and simpler than the most posterior one (as in *Pachycondyla crassinoda*; fig. 28B). Furthermore, the posterior spur is always located at the innermost region of the metatibia, while the anterior spur lies immediately in front of it off center. This also supports the conclusion that an anterior spur is present only in conjunction with the posterior spur, i.e., no cases were observed in which a single spur was located at the place

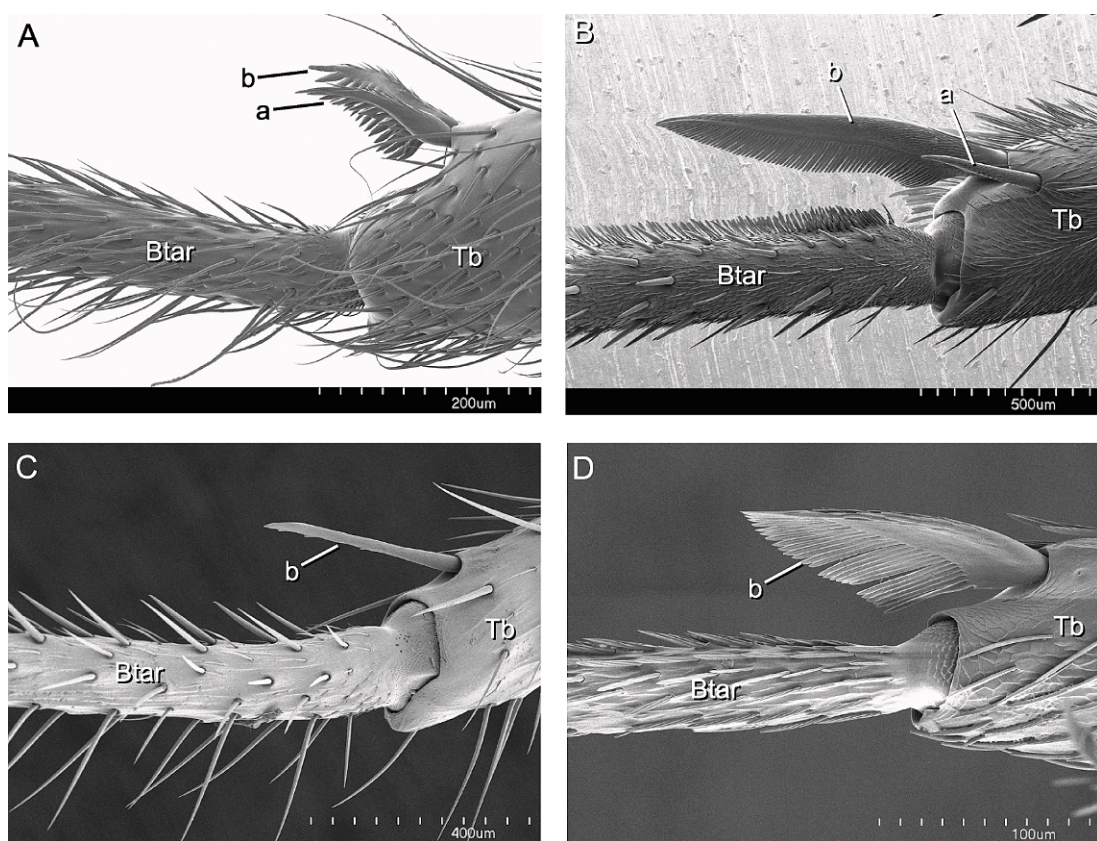


Fig. 28. Tibial spurs on hindlegs, anterior view. **A.** *Amblyopone australis*. **B.** *Pachycondyla crassinoda*. **C.** *Ectatomma tuberculatum*. **D.** *Thaumatomyrmex atrox*. Abbreviations: a, anterior spur on tibia; b, posterior spur on tibia; Btar, basitarsus; Tb, tibia.

where the anterior spur normally occurs in taxa bearing two of these structures. The anterior spur may be spearlike and devoid of projections (state 1, as in *Pachycondyla crassinoda*); or it may bear a single row of teethlike projections along its outer margin (i.e., in opposition to the basitarsus, state 2, as in *Amblyopone australis*). See also character 89.

89. *Posterior metatibial spur*: (0) absent; (1) simple; (2) pectinate.

The posterior spur may be a simple and spearlike (state 1, as in *Ectatomma tuberculatum*; fig. 28C); or it may bear a single row of teethlike projections along its outer margin (state 2, as in *Thaumatomyrmex atrox*; fig. 28D). See character 88 for discussion.

90. *Microtrichia on metatibial spur posterior face*: (0) absent; (1) present, simple; (2) present, antlerlike.

The posterior face of the main metatibial spur may bear a brush of microtrichia similar to the one found on the protibial calcar (char. 78). When present, the microtrichia may be simple sword-shaped to tapelike projections (state 1, as in *Platythyrea punctata*; fig. 29A), or each microtrichia may have multiple distal branches and be antlerlike (state 2, as in *Amblyopone armigera*; fig. 29B). The brush covers the posterior surface of the spur and differs from the spinelike and distally oriented microtrichia commonly present on the ventral edge. When the spur is absent the character has been coded as inapplicable ("–").

91. *Mesobasitarsal sulcus*: (0) absent; (1) present.

When present it appears as a longitudinal impression situated on the anterodorsal face of the basitarsus (state 1, as in *Amblyopone*

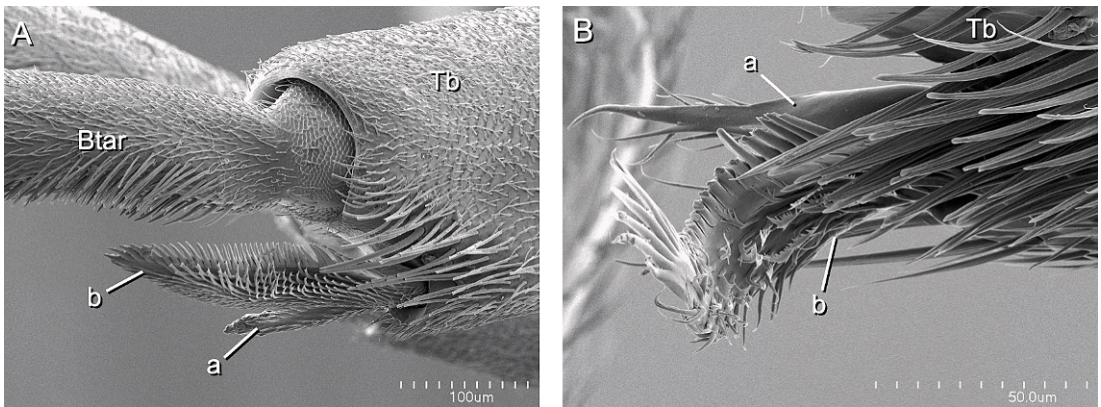


Fig. 29. Tibial spurs on hindlegs of two worker ants, posterior view. **A.** *Platythyrea punctata*. **B.** *Amblyopone armigera*. Abbreviations: a, anterior spur on tibia; b, posterior spur on tibia; Btar, basitarsus; Tb, tibia.

pallipes). A serial homolog may be found in the hindlegs (see char. 92).

92. *Metabasitarsal sulcus*: (0) absent; (1) present.

When present it appears as a longitudinal impression situated on the anterodorsal face of the metabasitarsus (state 1, as in *Nothomyrmecia macrops*). The presence of this sulcus in the mesobasitarsus (char. 91) and metabasitarsus has traditionally been coded as an exclusive character for the hindlegs (i.e., Ward, 1990: char. 23; Baroni Urbani et al., 1992: char. 15), presumably because these sulci often occur on both leg pairs simultaneously. Nevertheless, it may be present in either the mesobasitarsus or the metabasitarsus exclusively, proving its independent variation and hence coded as such here (see also char. 93).

93. *Metabasitarsal ventral longitudinal groove*: (0) absent; (1) present.

This is a deep, broad, elliptical groove running half the length of the ventral surface of the metabasitarsus. The inner surface is granulose in appearance and seems to be glandular (see also Brown, 1975: 79). The edge of the groove is lined exteriorly on all sides by a row of modified spatulate setae. This feature, apparently unique to some *Simopone* species, has been coded as a non-homologous character separate from character 92, due to the peculiarities described above (see also Baroni Urbani et al., 1992: char. 15).

94. *Basitarsal gland on metatarsus*: (0) absent; (1) present.

This gland opens at the distal end of the ventral flexor surface of the basitarsal hind leg. The opening consists of a small slit-shaped structure or circular pocket covered by a membranous villiform brush and a pair of setae (probably mechanoreceptors) coming out at the distal end of the slit or depression (Hölldobler and Palmer, 1989; Hölldobler et al., 1992). Secretion of this gland acts as a trail pheromone and its presence has been studied in *Onychomyrmex* species and *Prionopelta* (op. cit.). The ventral surface of the metabasitarsus of *Concoctio concentra* bears a small slitlike depression on the cuticle with a pair of setae similar to the condition found in *Prionopelta* and has thus been coded as present for this character but awaiting histological confirmation. It is possible that the large groovelike opening found in the metabasitarsus of most *Simopone* species (char. 92) is homologous with this basitarsal gland. However, due to its marked differences, it is reasonable to code it as a separate character as has been done here.

Metasoma

95. *Petiolear levator process*: (0) complete; (1) with lacuna.

The *petiolear levator process** is the ligamentary process located dorsally and medially on the anterior articulatory end of the petiolear tergite (median ridge, Snodgrass, 1956: 138; = vertical plate, Prentice, 1998:

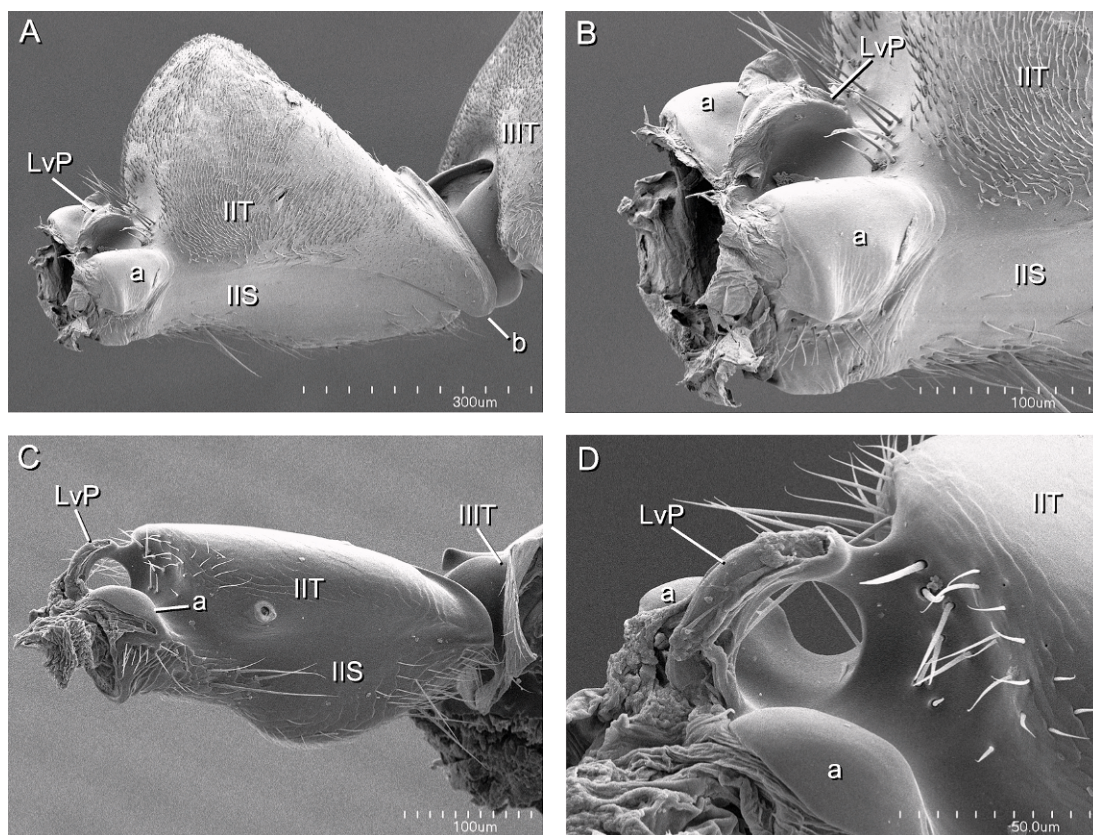


Fig. 30. Petiole, detached from mesosoma, left lateral view. **A.** *Leptomyrmex pallens*, **B.** close-up of anterior articular end. **C.** *Tapinoma erraticum*, **D.** close-up of anterior articular end. Abbreviations: a, anterior condyle of tergum; b, posterolateral lobe; LvP, levator process of petiole; IIS, petiolar sternum; IIT, tergum of petiole; IIIT, tergum of third abdominal segment.

702). This process sits between the well-developed pair of anterior tergal condyles that articulate within the acetabula of the propodeal foramen (fig. 30). The process itself fits within the levator foramen of the propodeum (after Ettershank, 1966: 79) and receives the ligament of the median levator muscle that elevates the petiole (Snodgrass, 1956: 138–139). In its complete state (state 0, as in *Formica fusca*) the levator process is an elongated cuticular structure with a thick dorsal edge and a pair of basal longitudinal grooves (one on each side) that serve as acetabula for the propodeal teeth (fig. 30A–B, see also Prentice, 1998: 492). In many taxa the cuticle in the middle of the basal grooves is thin and appears as a circular fenestra visible in transmitted light on lateral view. In most Dolichoderinae genera the levator

process has a large transverse basal round lacuna (state 1, as in *Dolichoderus laminatus*; fig. 30C–D). In the latter case the propodeal teeth extend posterad with their rounded apices almost touching each other through the lacuna. The function of the lacunate levator process is unknown, but it seems that it allows for some lateral movement of the metasoma while preventing the petiole from disengaging.

96. *Petiole*: (0) sessile to subsessile; (1) pedunculated.

When sessile, the main body of the petiole starts immediately after its anterior articular section, in which case the anterior face of the tergal node or scale rises upward just behind the paired condyles (state 0, as in *Formica fusca*). The petiole may have a narrow and elongated peduncle

between its anterior articulatory section and its main body, as long as or longer than the tergal node or scale (state 1, as in *Nothomyrmecia macrops*; see also Bolton, 1994: 198). *Aneuretus simoni* shows a very peculiar pedunculated petiole: the peduncle is twice as long as the round node and projects upward at an almost 90° angle. Also, unlike other ant taxa with peduncles, the spiracles are located anterior to the peduncle, just behind the articulatory section, rather than posterior to it at the tergal node. However, this taxon has been coded conservatively as having a peduncle homologous to the other taxa.

97. *Petiolar tergite anterior carina*: (0) absent; (1) with lateral dorsoventral carina; (2) with lateral carina extending posterad above the spiracles. Additive.

First described cladistically by Ward (1990: char. 29), the petiolar tergite may be flanked by a pair of dorsoventral, lobate carinae located immediately behind the anterior tergal condyles (see char. 95) and anterior to the spiracles (state 1). The carinae usually meet dorsally and may be independent from the petiolar node (e.g., *Myrmecia nigriscapa*) or are completely fused to it (e.g., *Platythyrea punctata*). In some taxa the carina extends posterad and horizontally above the spiracle along the full length of the petiole (state 2, as in *Cerapachys nitidulus*). Otherwise there is no structural separation between the anterior articulatory section and the main body of the petiole (state 0, as in *Nothomyrmecia macrops*). In *Amblyopone mutica* and *Apomyrma stygia* the lateral dorsoventral carina is low on the tergum and meets ventrally but is otherwise present and coded here as such. This peculiar arrangement seems to be a result of the ventral fusion of the petiolar tergum in these taxa (char. 107).

98. *Petiolar spiracle orientation*: (0) opening laterad; (1) opening ventrad.

In most taxa, the petiolar spiracle opens within the lateral sides of the tergite (state 0, as in *Ectatomma tuberculatum*). In the *Gnamptogenys minuta* group and some Proceratiinae and *Tatuidris tatusia*, the spiracle is located on ventral folds on each side of the tergum and the opening is directed ventrad (state 1, as in *Gnamptogenys minuta*). Coded after Lattke (1992).

99. *Petiolar tergite*: (0) with an anterior, vertical to inclined face; (1) without an anterior face.

In general, the petiolar tergite dorsum rises upward, behind its area of propodeal articulation, forming an anterior face that may be flat and vertical (e.g., *Formica fusca*; figs. 30A, 31A–B) to rounded and inclined (e.g., *Pseudomyrmex gracilis*). In *Tapinoma* and *Techonomyrmex*, the tergite extends into a flat dorsal face immediately behind the anterior levator process, without rising dorsally into an anterior face or node (state 1, as in *Tapinoma erraticum*; fig. 30C).

100. *Petiolar tergite*: (0) with a dorsal face leading to petiolar foramen; (1) with a posterior face descending into petiolar foramen.

In some taxa, mostly Amblyoponinae, the highest part of the petiolar tergite extends posterad as a dorsal face, evenly reaching the posterior margin of the sclerite that forms the petiolar foramen dorsum (state 0, as in *Adetomyrma venatrix*; fig. 31A). In most ants in contrast, the petiolar tergite descends posterad into the posterior margin after reaching its summit (figs. 30A,C, 31B), thus forming a posterior vertical to inclined face above the petiolar foramen (state 1, as in *Ponera pennsylvanica*). Coded after Brown (1960; see also Ward, 1994, Bolton, 2003).

101. *Laterotergite on petiole*: (0) delineated by sutures; (1) fully fused, indistinct.

The laterotergite is a paired long and narrow striplike area of cuticle parallel to the ventral margin of the petiolar tergite. It flanks and partially overlaps the poststernite, starting at the narrow neck of the petiole and running to the posterior margin of the segment while gradually increasing in width (fig. 32A, C; see also Ward, 1994). The laterotergite may be distinct and well delineated from the rest of the tergite by a suture (state 1, as in *Myrmecia nigriscapa*, *Platythyrea punctata*), or may be fully fused and indistinct (state 0, as in *Nothomyrmecia macrops*; fig. 32B, D). In the latter case, the area occupied by the laterotergite can be often inferred by differences in surface sculpture (usually appearing as a smooth surface) and/or lack of pilosity (e.g., *Heteroponera relict*a, *Emeryopone buttelreepeni*), or by the corresponding place of articulation of the petiolar tergite with the lower side of the helcium tergite.

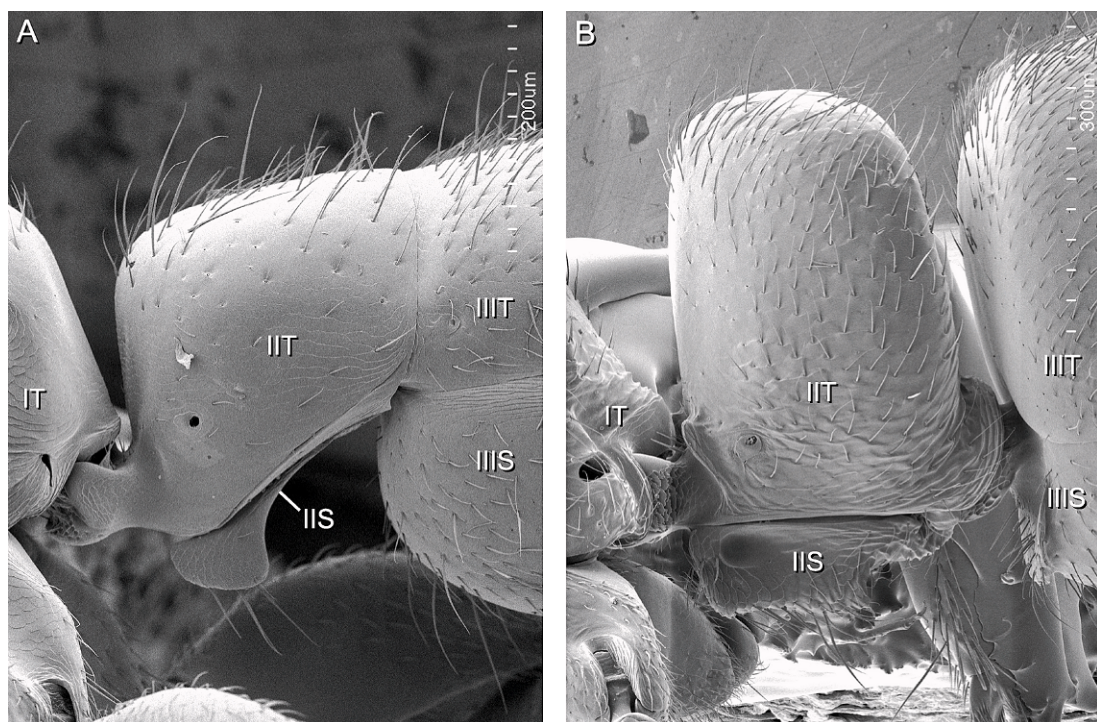


Fig. 31. Petiole, left profile view. **A.** *Adetomyrma* sp1. **B.** *Ponera pennsylvanica*. Abbreviations: IIS, sternum of petiole; IIIS, sternum of third abdominal segment; IT, tergum of propodeum; IIT, tergum of petiole; IIIT, tergum of third abdominal segment.

102. *Posteroventral margin of petiolar tergite*: (0) straight, continuous with ventral margin; (1) projecting posteroventrally as a rounded lobe.

On each side of the petiolar tergite, the posterior end of the ventral margin usually runs straight from its anterior section before curving dorsally to form the top arch of the posterior petiolar foramen (fig. 31). As such, the lateral posterior corner of the tergite does not project ventrad or posterad (state 0, as in *Pseudomyrmex gracilis*, *Acanthoponera minor*). By contrast, in Formicinae and Dolichoderinae the lateral posterior corner projects posteroventrad forming a rounded lobe that overlaps the petiolar sternite in profile view (state 1, as in *Formica fusca*, *Leptomyrmex pallens*; fig. 30A).

103. *Posterior peduncle on petiolar tergite*: (0) absent; (1) present.

Generally, the posterior margin of the petiolar tergum is a narrow lip that forms the dorsal arch of the petiolar foramen (state 0). In *Apomyrma stygia* and *Leptanilla*, the

posterior margin projects posterad, forming a short tubular peduncle inside which the helcium articulates (state 1). In *Apomyrma* the tubular tergal peduncle is interrupted by a V-shaped ventral opening housing the reduced petiolar poststernite (see char. 108). In *Leptanilla* the tubular peduncle is entire: the ventral margins are completely fused without trace of sutures. Coded after Brown et al. (1971) and Bolton (1990c) in part.

104. *Proprioceptor zone on anterior disc of petiolar sternite*: (0) absent; (1) present as a small posterior depression; (2) present, arrow shaped; (3) present as a large circle or semicircle.

The anteriormost part of the petiolar sternite consists of a disc or fan-shaped area, here termed the *anterior disc*,* followed by a narrow neck immediately posterior to it (fig. 32). A central proprioceptor zone is usually present here in the form of a semicircular to narrow depression sharply delineated anteriorly and bearing numerous pressure sensitive sensilla. The size and shape

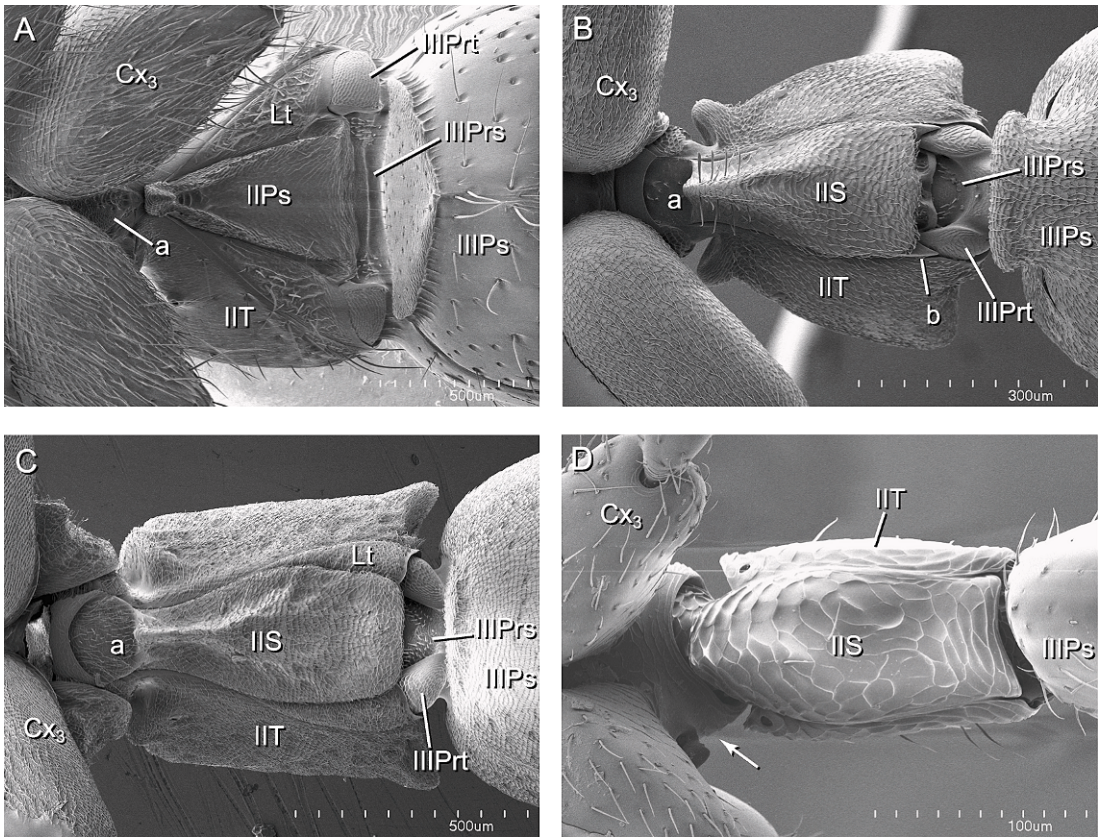


Fig. 32. Petiole, ventral view. **A.** *Myopopone castanea*. **B.** *Belonopelta deletrix*. **C.** *Platythyrea punctata*. **D.** *Leptanilloides biconstricta*, arrow pointing at tubular foramen of propodeum. Abbreviations: a, anterior disc of petiole; b, posterolateral condyle of petiolar sternum; Cx₃, metacoxa; Lt, laterotergite; IIPs, poststernite of petiole; IIPrs, presternite of third abdominal segment; IIPrt, pretergite of third abdominal segment; IIPs, poststernite of third abdominal segment.

of the depression is relative to the articulation surface that delineates it: in most ants, there is a large and round proprioceptor area delineated anteriorly by an arched articulating surface (state 3, as in *Ectatomma tuberculatum*; fig. 32B–C); in members of the *Plectroctena* genus group (sensu Bolton and Brown, 2002) the articulating surface expands laterad toward the ventral midline constricting the proprioceptor area into an arrow-shaped depression (state 2, see also Bolton and Brown, 2002); in some genera (e.g., *Adetomyrma*, *Myopopone*) the articulating surface is greatly expanded and the proprioceptor is reduced to a small depressed area on the posterior part of the anterior disc bearing just a few sensilla (state 1); or the articulating

surface may cover the anterior disc completely forming a convex uniform surface without any depression and no trace of pressure sensitive sensilla (state 0, see Bolton, 1990a, for a description of this state in Dorylinae).

105. *Anterior disc of petiolar sternite*: (0) undivided; (1) divided by a transverse groove.

In most taxa the anterior sternal disc (see char. 104) consists of a single piece continuous with the posterior part of the sternite after a necklike constriction (state 0, as in *Prionopelta antillana*). In *Probolomyrmex* the disc is divided by a transverse groove into a semicircular anterior part bearing most of the proprioceptor zone and a fan-shaped posterior part continuous with the rest of the sternite (state 1).

106. *Petiolar sternite*: (0) articulated with tergite over its entire length; (1) fused with tergite over its entire length.

As in all the external abdominal segments within the metasoma, in the highly specialized petiole the lateral margins of the sternite are overlapped by the ventral margins of the tergite. Generally, the petiolar sternite articulates fully with the tergite over the entire length of their joining margins (state 0, as in *Myrmecia nigriscapa*). Alternatively, the sternite may be completely fused to the tergite, from front to back, along the entire length of their joining margins (state 1). In the latter case, a semiparallel pair of sutures may be visible ventrally delineating the sternite (e.g., *Ectatomma tuberculatum*) or the sutures may be completely obliterated and the sternite may form an uninterrupted surface with the tergite (e.g., *Tapinoma erraticum*). See also character 107.

Leptanilla swani has been scored as unknown for this character because it is not clear whether the sternite is fully fused to the tergite and whether its boundaries are not discernable or are completely obliterated by the fusion of the lateral margins of the tergite ventrally with each other (see char. 107).

107. *Petiolar tergite lateroventral margins*: (0) not meeting ventrally; (1) partially fused to each other anteriorly; (2) fully fused to each other anteriorly. Additive.

In some taxa, particularly within Amblyoponinae, the ventrolateral margins of the tergite meet and fuse with each other ventrally at the narrow neck of the petiole, immediately posterior to the anterior disc (see char. 104). When this occurs, the petiolar sternite is obliterated at the meeting point and the anterior disc is fused to the tergite (Ward, 1994: 167), leaving a free poststernite plate posterior to the narrow neck (Perrault, 2004: 360). Fusion at the meeting point may be partial (state 1), often leaving a longitudinal suture (e.g., *Adetomyrma* sp.) or anteroventral "pinch-like" area of fusion (e.g., *Amblyopone armigera*). In some taxa (e.g., *Amblyopone mutica*, *Leptanilla swani*) the tergite is completely fused ventrally and extends longitudinal into a short peduncle exhibiting a reticulate sculpture (state 2).

The sternite is not obliterated in taxa with complete tergosternal fusion, even among

putative closely related taxa to the ones described above (e.g., *Onychomyrmex doddi*), and hence this character is treated as independent from character 106. Also among Amblyoponines, *Concoctio concenta* and the *Prionopelta* species examined in this study the sternite is fully articulated and not obliterated by the tergite at the narrow neck.

108. *Petiolar poststernite*: (0) broad from anterior to posterior; (1) reduced to an oval posteromedial sclerite.

A reduced and oval free poststernite (Bolton, 1990c) is a putative synapomorphy for *Amblyopone mutica* and *Apomyrma stygia*. The petiolar ventrum of these two species also shares similarities unique among ants in the structure of the narrow neck, as recognized by previous authors (Brown et al., 1971; Ward, 1994: 170; Bolton, 2003: 39).

109. *Posterolateral condyle of petiolar sternite*: (0) absent; (1) present.

In some taxa, the posterolateral corner of the petiolar sternite projects laterally over the helcium tergite, forming a lobelike condyle (state 1, as in *Nothomyrmecia macrops*, *Belonopelta deletrix*; fig. 32B). In this configuration, the posteromedial part of the petiolar sternite articulates with the helcium sternite, while the condyle form an incision inside which the thick, round ventral margin of the helcium tergite articulate. Otherwise the petiolar sternite articulates exclusively with the helcium sternite, on its entire posterior margin (fig. 32A). The posterolateral corner does not expand laterally, and the ventral margin of the helcium tergite articulates against the laterotergite instead (state 0, as in *Myopopone castanea*; see also char. 101).

This character corresponds in part to the "lateral lobes" of Ward (1990: char. 31) and Lattke (1994: char. 23), but it is here coded independent of tergosternal fusion of the petiole (see char. 106). In taxa with complete fusion, it is possible to infer the presence/absence of the lateral condyle by the position of the petiolar tergosternal sutures relative to the place of articulation of the helcium. When the latter assessment is not possible (e.g., *Leptanilla*), the taxon has been coded as unknown. Note that the posterolateral condyles do not necessarily correspond to the "expansions latérosternales" described by Perrault (2004). See also character 110.

110. *Posteromedial margin of petiolar sternite*: (0) entire; (1) incised.

The petiolar sternite articulates with the helcium sternite through the medial part of its posterior margin. The posteromedial part of the margin may be entire (state 0), being straight (e.g., *Adetomyrma venatrix*; fig. 32A), slightly convex (e.g., *Acanthostichus serratus*), or slightly concave (e.g., *Ectatomma tuberculatum*). Alternatively, the margin may be incised (state 1; fig. 32B) by a broad concave cut (e.g., *Formica fusca*) or deep notch (e.g., *Anochetus emarginatus*). See also character 109.

111. *Posterior spatulated projection on petiolar sternite*: (0) absent; (1) present.

When present, the posterior part of the petiolar sternite extends posterolaterad, immediately underneath and parallel to the true ventral face of the sternite, forming a wide and flat spatula-shaped projection (state 1, as in *Phrynoponera gabonensis*; fig. 32C). This projection extends beyond the true posterior margin of the sternite, thus concealing the articulation with the helcium in ventral view. Otherwise no such spatulalike projection occurs, and the sternal articulation between the petiole and the helcium is visible in ventral view (state 0, as in *Pachycondyla villosa*; fig. 32A–B).

112. *Maximum diameter of abdominal segment III*: (0) subequal to the minimum diameter of abdominal segment IV in sagittal plane; (1) smaller than abdominal segment IV.

This character codes for the presence of a postpetiole in workers. State 0 as in *Formica fusca*. State 1 as in *Manica rubida*. After Baroni Urbani et al. (1992), character 21.

113. *Helcium sclerites*: (0) located at posttergite; (1) located at posttergite and poststernite respectively; (2) located at poststernite.

The helcial sclerites (pretergite + pre-sternite) may be located at the posttergite of the third abdominal segment, in which case a distinct transverse tergosternal suture runs ventral and posterior to the helcium (state 0, as in *Formica fusca*); or the helcium may be situated along the anterior joint between the posttergite and poststernite, so that each helcial sclerite is continuous with its corresponding postsclerites (state 1, as in *Oecophylla smaragdina*); or the helcial sclerites may be situated ventrally

within the poststernite of the third abdominal segment, in which case the tergosternal suture runs dorsal and anterior to the helcium (state 2, as in *Tapinoma erraticum*). Coded after Agosti and Bolton (1990) and Agosti (1991).

114. *Helcium location*: (0) supraaxial; (1) axial; (2) infraaxial.

Location of the helcium within the third abdominal segment can be described in terms of its position relative to the longitudinal axis of the segment as follows: *supraaxial*, when the main corpus of the helcium occurs above the axis (fig. 33B), even though the ventrum is at the axis (state 0, as in *Adetomyrma venatrix*); *axial*, when the helcium is bisected by the axis (fig. 33C), usually with the sternal part immediately below it (state 1, as in *Myrmecia nigriscapa*); *infraaxial*, when the corpus of the helcium is well below the axis (state 2, as in *Odontomachus bauri*; fig. 33A). In the supraaxial state, the posttergite usually lacks an anterior face above the helcium, while the poststernite has a wide, rounded anterior face below it. This arrangement is reversed in the infraaxial state, where the posttergite ascends behind the helcium into a large, vertical anterior face, while the poststernite has little to no anterior face at all. Coded after Perrault (2004).

Note that this character is independent of the one describing the relation of connectivity between the pre- and postsclerites on this abdominal segment (i.e., char 113).

115. *Helcium tergite anterior margin*: (0) entire; (1) with a dorsal U-shaped emargination.

The anterior margin of the helcium tergite usually forms an uninterrupted entire arch (state 0, as in *Ectatomma tuberculatum*). In Dolichoderinae and most Formicinae the anterior margin is interrupted by a dorsal U-shaped emargination that may be as deep as the whole length of the helcium (state 1, as in *Dolichoderus laminatus*; Bolton, 1994: fig. 58).

116. *Medial tergal apodeme of helcium*: (0) absent; (1) present.

Internally, the anterior end of the helcium tergite may consist of a simple liplike margin (state 0, as in *Amblyopone pallipes*). In some taxa, the medial part of the internal margin projects as a cuticular lobe. This medial tergal apodeme (after Perrault, 2004: 314)

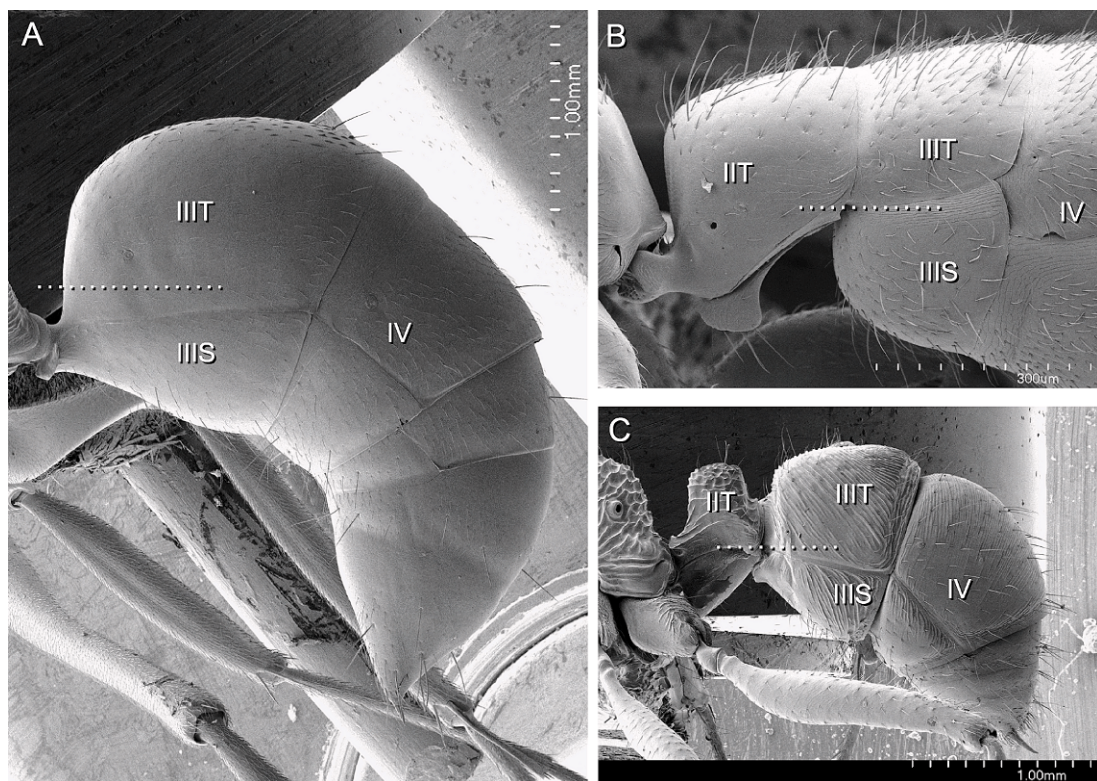


Fig. 33. Helcium location relative to postsclerites, left profile view. Dotted lines correspond to the position of the longitudinal body axis relative to the metasoma. **A.** *Odontomachus bauri*, infraaxial helcium. **B.** *Adetomyrma* sp. 1, supraaxial helcium. **C.** *Ectatomma tuberculatum*, axial helcium. After Perrault (2004), see text for explanation. Abbreviations: IIIS, sternum of third abdominal segment; IIT, tergum of petiole; IIIIT, tergum of third abdominal segment; IV, fourth abdominal segment.

serves as the place of origin for the dorsal retractor muscle of the fourth abdominal tergite that elevates the posterior part of the metasoma (Hashimoto, 1996).

Hashimoto (1996) and Ward and Brady (2003) reported this apodeme as absent in *Myrmecia*. However, Perrault (2004) reported the apodeme as present in this genus, noting that in this taxon the extension is weakly sclerotized and thus easy to break during dissection. The present study agrees with Perrault's observation.

117. *Helcium sternite*: (0) flat to slightly ventrally curved; (1) convex.

The helcium tergite may be a narrow plate either flat (e.g., *Onychomyrmex doddi*) or with a slight ventrally directed curvature in its center between the paired lateral proprioceptor zones (e.g., *Anochetus emarginatus*). Alternatively, the sternite may be well

developed and convex (state 1, as in *Labidus coecus*), bulging ventrally and clearly visible in lateral view (Bolton, 1990b: 1350).

118. *Helcium sternite lateral margin*: (0) overlapped by tergite; (1) meeting tergite along the ventrolateral margin.

In general, the helcium sternite is overlapped by the tergum, connecting directly to it without a membrane (as opposed to the remaining IVth–VIIth abdominal segments), and the sternite attaches directly to the tergite on its inner surface, slightly dorsal from the ventral margin on each side (state 0, Bolton, 2003: 52). In most Myrmicinae, the sternite is not overlapped by the tergite and instead the lateral margin of the helcium sternite meets the tergite along the apex of the ventral margin, forming a tubular structure (state 1, as in *Myrmica americana*). Character after Ward (1990: char. 35).

119. *Helcium tergosternal junction*: (0) articulated; (1) fused.

In some taxa, the helcial tergum and sternum are articulated and may be cleanly separated from each other by dissection, even though they fit tightly (state 0, as in *Tetraponera aethiops*, *Pogonomyrmex barbatus*). Alternatively, the sclerites may be fused to each other and cannot be teased apart by dissection (state 1, as in *Ectatomma tuberculatum*). Character after Ward (1990); see also Baroni Urbani et al. (1992) and references therein.

120. *Postsclerites of third abdominal segment*: (0) tergum articulated with sternum; (1) tergum and sternum fused, with sutured margins.

The posttergum and poststernum of the third abdominal segment may overlap increasingly posterad on each side, articulating fully with each other (state 0, as in *Oecophylla smaragdina*, *Pseudomyrmex gracilis*). Alternatively, the lateral margins of the sclerites may meet with little overlapping, showing complete fusion along the resulting lateral sutures (state 1, as in *Pachycondyla crassinoda*). After Kusnezov (1955a) and Gotwald (1969). See also Bolton (1990a: 58) on fusion of abdominal segments.

121. *Presclerites on fourth abdominal segment*: (0) forming an even surface with postsclerites; (1) delineated from postsclerites by a transverse constriction or groove.

Both the tergum and sternum of the fourth abdominal segment may consist of a trapezoidal plate with an even, uninterrupted surface (state 0, as in *Formica fusca*). In such cases, the limit of the presclerite is marked only by a change in surface sculpture of the anterior region of the sclerite to a semi-smooth, transversely reticulate surface devoid of pilosity. Alternatively, these sclerites may consist of a plate interrupted by a transverse constriction in the form of a depressed line or deep groove that delineates the presclerite from the postsclerites (state 1, as in *Amblyopone pallipes*). Coded after Taylor (1978; see also char. 123).

122. *Tergosternal joints of fourth abdominal segment*: (0) articulated along the anteroposterior edge; (1) with sutured presclerites; (2) fused along the anteroposterior edge.

The lateral margin of the tergum may overlap and articulate fully with the lateral margin of the sternum (state 0, as in *Oecophylla smaragdina*); or these sclerites may be fused together on their anterior sections, forming a suture in the joints between the pretergite and the presternite (state 1, as in *Myrmecia nigriscapa*); or the tergum and sternum may be fused along the whole length of their lateral joints, forming a pair of parallel sutures along each side of the segment (state 2 as in, *Platythyrea punctata*). Recoded as a multistate character after Ward (1990: char. 36, in part), Baroni Urbani et al. (1992: chars. 26 and 29) and Brady and Ward (2005: chars. 49 and 51).

123. *Presclerites on fifth abdominal segment*: (0) forming an even surface with postsclerites; (1) delineated from postsclerites by a transverse constriction or groove.

A serial homolog of the condition described in character 121, the sclerites may have an even surface (state 0), or bear a transverse groove that delineates the presclerite from the rest of the plate (state 1, as in *Dorylus helvolus*).

124. *Stridulitrum on fourth abdominal pretergite*: (0) absent; (1) present.

A dorsal stridulatory organ may be present between the third and fourth abdominal segments (Ward, 1990: char. 39; Baroni Urbani et al., 1992: char. 23). When present, a large oval to triangular stridulitrum occurs on the dorsalmost part of the fourth abdominal pretergite (state 1, as in *Pachycondyla villosa*). Markl (1973) investigated the absence/presence of this character among ants extensively and discussed its phylogenetic implications. See also character 125.

125. *Stridulitrum on fourth abdominal presternite*: (0) absent; (1) present.

A ventral stridulatory organ occurs between the third and fourth abdominal segments in *Nothomyrmecia macrops* (Taylor, 1978) and *Rythidoponera* (Baroni Urbani et al., 1992: char. 24). Additionally, in *Nothomyrmecia* the medial part of the posterior sternal margin is protruded into an external thickening associated with the internal pectrum of the stridulatory organ (Ward and Brady, 2003: char. 51). See also character 124.

126. *Abdominal segment IV*: (0) tubular; (1) vaulted 45°; (2) vaulted 90°. (additive)

When tubular, the abdominal tergite and sternite have similar lengths and the anterior and posterior openings of the segment are aligned following the main body axis (state 0, as in *Adetomyrma*). When vaulted 45°, the abdominal tergite IV is arched and enlarged in relation to the sternite, so that the longitudinal axis of the gaster bends downward 45° (state 1, as in *Ectatomma tuberculatum*); when vaulted 90°, the tergite is strongly arched and hypertrophied in relation to the reduced sternite. The main axis of the gaster bends downward almost 90° (state 1, as in *Proceratium croceum*). Coded after Bolton (2003: 49) in part.

127. *Location of spiracles of abdominal segments V–VII*: (0) pretergite; (1) posttergite.

Spiracles on abdominal segments V–VII are generally located well into the pretergite or close to the boundary between pretergite and posttergite, but nevertheless are concealed by the previous segments in a normally distended gaster (state 0, as in *Amblyopone australis*). Among members of the dorylomorphs taxa, these abdominal spiracles are located well into the posttergite, and are thus visible without distension or disarticulation of the gaster (state 1, as in *Dorylus helvolus*). Coded after Bolton (1990b), see also Brady and Ward (2005: char. 55).

128. *Orientation of spiracles of abdominal segments V–VII*: (0) lateral; (1) posterior.

The openings of spiracles of abdominal segments V–VII are generally oriented laterad in ants (state 0, as in *Rhytidoponera confusa*). In Ecitoninae, the opening of these spiracles is directed posteriorly (state 1, as in *Cheliomyrmex morosus*). Coded after Bolton (1990b); see also Brady and Ward (2005: char. 54). Note that the spiracles on abdominal segment IV in Ecitoninae open laterally (contra Bolton, 1990b).

129. *Median face of pygidial posttergite*: (0) even with pretergite; (1) strongly angled.

In its general state, the faces of the pygidial pretergite and posttergite extend into a relatively uniform plane, forming a continuous surface arranged parallel and telescopic relative to the preceding sixth abdominal tergite (state 0, as in *Formica fusca*; fig. 34A–D). In most Dolichoderinae, the median face

of the pygidial posttergite is bent downward more than 90° with respect to the narrow pretergite, with a carina marking the bending margin (state 1, as in *Tapinoma erraticum*; fig. 34E). Together with the pretergite, the lateral parts of the posttergite bearing the spiracles remain parallel to and overlapped by abdominal tergite VI (fig. 34F). Under this arrangement, only four gastral tergites (III–VI) are visible on dorsal view, and the posteriormost apical part of the abdomen consists of a slit formed by the junction of the dorsoposterior margin of the sixth abdominal tergite and the carinated bending margin of the pygidium (fig. 34F: VIT and VIIT). The secretions of the large pygidial gland (char. 135) empty through this slit-shaped pseudoapex of the abdomen. Additionally, all the pilosity of the median face points toward the pseudoapex (i.e., toward the sixth tergite), rather than to the posterior tergal margin as in all other taxa with unmodified pygidia.

Among Dolichoderinae, *Technomyrmex* seems to be the only genus without an angled pygidium. In this taxon the pygidium is longitudinally narrow as a whole and the pilosity points posterad (i.e., toward the posterior pygidial margin; fig. 30D), and thus has been scored as state 0. However, the weak sclerotization of the pygidial pretergite suggests that this may be a secondary development from an angled condition.

130. *Pygidial shape*: (0) large and arched; (1) reduced to a narrow U-shaped sclerite.

In state 1, as described by Bolton (1990b), the pygidium is reduced to a striplike, U-shaped sclerite dorsally overhung by the sixth abdominal tergum (fig. 34C). Baroni Urbani et al. (1992) treated the shape of the pygidium and its topological relation with the preceding tergite as separate characters (their chars. 33 and 34, respectively), arguing that while the former condition is shared between Leptanilloidinae and some of the army ants subfamilies, the latter is an autapomorphy for Leptanilloidinae (see also Bolton, 1994, 2003; Brandão et al., 1999). However, the pygidium is always overhung by the preceding tergite (i.e., the sixth abdominal segment) when reduced to a narrow U-shaped sclerite, being more apparent in Leptanilloidinae due to the short nonprotruding sting, but otherwise similar in all taxa sharing this feature. Brady (2003) treated this

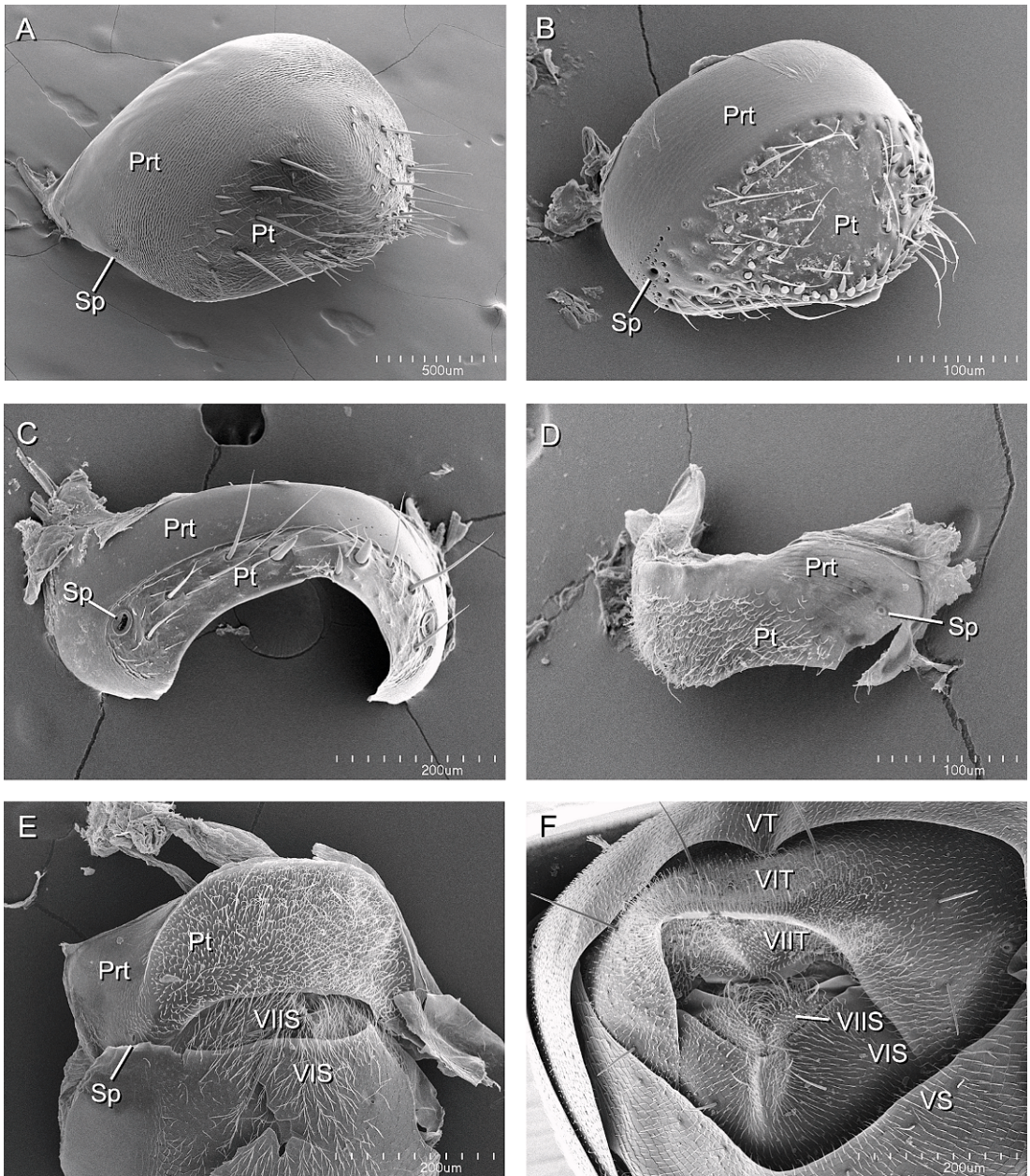


Fig. 34. Pygidium, posterolateral view. **A.** *Ectatomma opaciventre*. **B.** *Cerapachys nitidulus*. **C.** *Labidus coecus*. **D.** *Technomyrmex albipes*. **E–F.** *Tapinoma erraticum* (note pilosity directed anterad on angled posttergite); **F.** pygidium in situ. See text for explanation. Abbreviations: Prt, pretergite of pygidium; Pt, posttergite; Sp, spiracle; VS, sternum of fifth abdominal segment; VIS, sternum of sixth abdominal segment; VIIS, hypopygium; VT, tergum of fifth abdominal segment; VIT, tergum of sixth abdominal segment; VIIT, pygidium.

feature together with pygidial armature as a single character (his char. 52). Here pygidial shape (this character) and pygidial armament (char. 131) are treated as independent characters because different combinations of their states can be observed occurring in conjunction (e.g., *Labidus coecus* and *Cerapachys doryloides*). Previously reported as a putative synapomorphy of Aenictinae, Ecitoninae, and Leptanilloidinae (Bolton, 1990a, 1990b, 2003; Baroni Urbani et al., 1992; Brady, 2002), the reduced condition is also present in some *Cerapachys* species.

131. *Pygidial setal armament*: (0) absent; (1) present, posterior pair of dentiform setae; (2) present, posterolateral row of dentiform setae.

The armament may be present as a single posterior pair of prominent stout dentiform setae separated by a concave gap above the sting area (state 1, as in *Dorylus helvolus*); or as a continuous row of dentiform short, sharp setae bordering the pygidium laterally to posteriorly without a prominent concave gap above the sting area (fig. 34B–C, see also Brown, 1954, 1975; Bolton, 1990a, 2003). The row may consist of multiple dentiform setae to only a small pair above the posterior pygidial margin (state 2, as in *Acanthostichus serratulus* and *Labidus coecus*). Baroni Urbani et al. (1992) treated such armament states as separate characters (their chars. 31 and 32) possibly working under the argument that they are synapomorphies for Dorylinae and Cerapachyinae respectively (see also Bolton, 1990a, 2003). However, the similarity and topological correspondence of the dentiform setae suggest their homology as part of the same character (see also Bolton, 1990b: 1348), regardless of their status as synapomorphies a posteriori. Brady (2003) treated this character together with pygidial shape, but see character 130 for discussion.

132. *Pygidial posttergite dorsum*: (0) convex; (1) flattened to concave.

A large, simple and convex pygidial posttergite is the most common condition among ants (state 0, as in *Nothomyrmecia macrops*; fig. 34A). In some taxa, the posttergite dorsum may be longitudinally flattened to concave and marginated (state 1, as in *Dorylus helvolus*; fig. 34B–C). This feature is treated here independently of pygidial shape and armament (chars. 130 and 131,

respectively) because the different states of these three features occur in different combinations across the taxa considered in this study (i.e., they occur in conjunction).

133. *Posterior pygidial carina*: (0) absent; (1) present.

This is a transverse carina that rises gradually toward the apex of the pygidium forming a straight transverse edge just above the true posterior margin. It can be seen in profile as a shelflike structure that overhangs the posterior margin. The dorsal surface may be covered by a dense brush of tightly spaced setae on its entire area or just delineating the carinal margin, while the ventral rim is devoid of setae (state 1, as in *Ectatomma tuberculatum*, *Gnamptogenys annulata*).

134. *Pygidial pair of stout upcurved teeth*: (0) absent; (1) present.

A putative autapomorphy of *Pachycondyla crassinoda*, the pygidium bears a pair of prominent upcurved teeth or spines directed posterad (state 1). These cuticular projections are not homologous with the pair of dentiform setae present in other taxa (e.g., *Dorylus helvolus*; char. 131).

135. *Pygidial gland*: (0) absent; (1) present.

The pygidial gland is located under abdominal tergite VI and its duct opens in the intersegmental membrane between abdominal tergites VI and VII (= pygidium) (Hölldobler and Wilson, 1990). Assessment of its presence requires histological preparation that was not conducted for the present study, yet there are enough published records documenting its distribution throughout Formicidae and an attempt was made to code this character from the literature. When its presence/absence has been recorded in a species congeneric to a well-defined genus, the information has been extrapolated to the exemplar included in this study (e.g., recorded as present in *Dinoponera australis* coded as such for *Dinoponera lucida*). So far, the pygidial gland seems to be present in all ants surveyed but Formicinae (coded after Janet, 1898; Kugler, 1978b; Hölldobler and Engel, 1979; Jessen et al., 1979; Hölldobler and Traniello, 1980; Traniello and Jayasuriya, 1981; Hölldobler and Taylor, 1983; Traniello and Hölldobler, 1984; Billen, 1986; Hölldobler and Wilson, 1990; Hashimoto, 1991; Morgan et al., 2003).

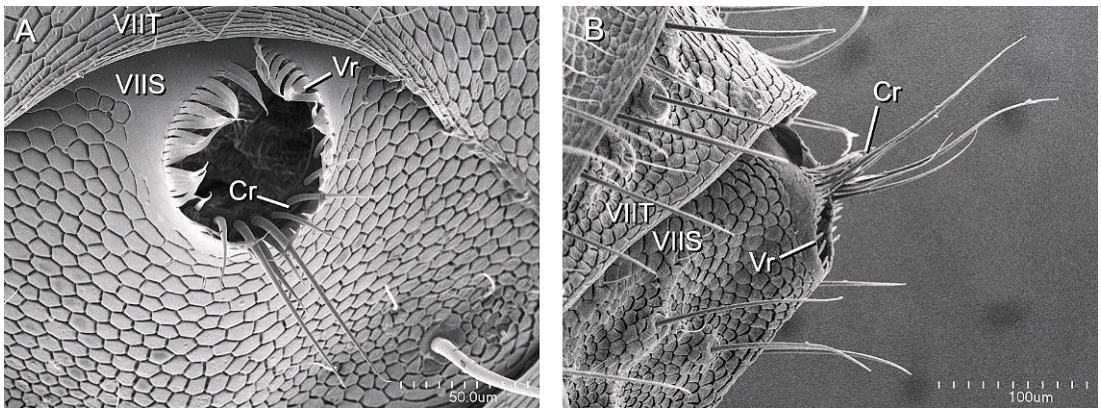


Fig. 35. Acidopore. **A.** *Formica fusca* group. **B.** *Oecophylla smaragdina*. Abbreviations: Cr, coronula; VIIS, hypopygium; VIIT, pygidium; Vr, verticillus.

136. *Acidopore on hypopygium*: (0) absent; (1) present.

Presence of an acidopore and its corresponding poison gland is the strongest synapomorphy of Formicinae. The opening of the formic acid producing gland is formed by the rolling of the apical portion of the hypopygium and is normally surrounded by a setal ring termed coronula (Hung and Brown, 1966). The coronula is in turn surrounded by a second ring of flat elongated cuticular projections here termed *verticillus** (fig. 35). The presence of an acidopore seems to be correlated with the occurrence of a particular well-marked foveolate sculpture on the terminal abdominal sclerites, especially the pygidium and hypopygium, not found anywhere else outside Formicinae. Such thick sculpture probably provides protection to the ant against its own secretion. The coronula and the verticillus show great variation across Formicinae in terms of position of setae and shape of the projections respectively with good potential as characters for further phylogenetic studies inside this subfamily.

137. *Apical hypopygial process*: (0) absent; (1) present.

This is a keellike process that extends posteroventrad from the hypopygial apex, just below the protruding sting (state 1). It is a putative autapomorphy of *Odontoponera transversa*.

138. *Sting apparatus*: (0) well developed; (1) vestigial.

Modification of the ovipositor into a sting apparatus is characteristic of aculeates. In

most ants the sting apparatus is well developed and functional (state 0, Hermann and Blum, 1966; Hermann and Blum, 1967a; Hermann and Blum, 1967b; Hermann, 1968a; Hermann, 1968b; Hermann, 1969b; Hermann, 1969a; Kugler, 1978a, 1979b, 1980, 1991, 1992). The sting is vestigial and not functional in Formicinae and Dolichoderinae among the exemplars in this study (state 1, as in *Formica fusca*).

139. *Lancets*: (0) articulated on sting; (1) disarticulated.

Within the sting apparatus, the paired lancets normally articulate with the sting shaft in all ants (state 0). In the vestigial sting apparatus of Formicinae, the lancets are disarticulated (state 1, Hermann and Blum, 1968). This feature has been coded as independent of character 138 because the lancets may remain articulated in some taxa even when the sting apparatus as a whole is nonfunctional (i.e., vestigial; see also Baroni-Urbani et al., 1992).

CHARACTERS EXCLUDED FROM THE ANALYSIS

Glands: There is an enormous body of literature on the subject of glands in ants, from labial glands to specialized trail pheromone glands in various parts of the abdomen. Unfortunately the published information is still too fragmentary to be useful in a phylogenetic context at the scope dealt with in the present study. An exception is the pygidial gland (char. 135), since it has been surveyed in enough species across Formicidae to justify an attempt to code its presence/

absence from published records alone. Some characters apparently related to glands included in the present study are restricted to specimens in which the cuticular openings of these structures can be distinctly observed without the need of histological preparations (e.g., the metapleural gland opening). Therefore, the characters pertain more to the actual presence, shape, and location of these cuticular openings rather than the gland per se.

Presence of the Pavan's gland has been used both in diagnoses and cladistic analyses as a feature shared between *Aneuretus simoni* and Dolichoderinae (Baroni Urbani et al., 1992; Shattuck, 1992a, 1992b; Bolton, 2003). Nevertheless, the gland has been reported as absent in some Dolichoderinae genera (Billen, 1986). Since the histological work necessary to assess the presences of this gland was beyond the scope of this study, this feature was not included in this analysis.

Presence of the metatibial gland has become a widely used as a diagnostic (e.g., Bolton, 2003) and phylogenetic character (e.g., Brady and Ward, 2005), especially among dorylomorph subfamilies. However, while its presence can be unambiguously assessed in some taxa by external inspection alone (e.g., Ecitoninae), in other groups where this gland has been noted only after histological investigation (e.g., *Pachycondyla crenata*, Hölldobler et al., 1996) external inspection was insufficient to assess its presence even with the use of scanning electron microscopy. This was specially the case within the diverse Ponerinae genera where this character appears to have great phylogenetic potential. Therefore, this character has been left out, awaiting broader histological consideration.

Socket of sensilla basiconica of antenna: Even with cuticular surface or raised above cuticular surface. Suggested first by Hashimoto (1991), the raised socket condition has been reported as synapomorphy for *Myrmecia* + *Nothomyrmecia* + *Pseudomyrmecinae* (see also Ward, 1994; Bolton, 2003; and Ward and Brady, 2003). The present survey found this character to be problematic because: its states cannot be delimited discretely, with many intermediate states between having a socket completely sunk relative to the cuticular surface to clearly raised above it; the

distribution of the states was found to be different and in some cases contradictory to what was originally reported (e.g., some *Myrmecia* species have a sunken socket while a clear raised condition is common throughout many taxa); and some taxa show both conditions on the same flagellomere. This last observation suggests that the different conditions of this membranous socket may be due to preservation artifacts.

Serration on sting: The presence of serration or dorsal barbules on the sting was first noted by Kugler (1992) as a prominent character with phylogenetic value among members of the Leptanillinae (sensu Bolton, 1990c, then including *Apomyrma*). Although the relative size of the barbules is very large in some Leptanillinae genera, presence of a serrated sting is common throughout the family and the relative size and number of the barbules proved to be too variable to be useful at the level of the present study.

RESULTS AND DISCUSSION

MORPHOLOGICAL ANALYSIS

The anatomical survey resulted in 139 characters, 17 of which are parsimony uninformative given the terminal taxa included in this study. These putative autapomorphies have been kept throughout the cladistic analyses and calculation of tree descriptive statistics since the principal aim of this study is the interpretation of the morphology through phylogeny, and because of their potential as synapomorphies in future studies. Eleven multistate characters are treated as additive. The matrix with the final scores for the 105 terminal taxa included in this study is given in appendix 2.

Of the 139 characters listed above, 54 (38.8%) are newly described and analyzed here; 27 (19.4%) were suggested from the literature (e.g., species descriptions, taxonomic keys) but coded here for the first time; 18 (13%) have been used before cladistically but were thoroughly reinterpreted (e.g., by merging, splitting, expanded with novel states or redescribed); and 40 (28.7%) were taken from previous cladistic analyses.

For the majority of characters taken from the literature, the current study expanded

their scope to many new taxa not scored before. As a result, all characters have been standardized throughout the taxon sample as much as possible so that they apply unambiguously across Formicidae as a whole.

CLADISTIC ANALYSIS

Analysis under equal weights resulted in 3192 most-parsimonious trees of 776 steps; the strict consensus is shown in figure 36. The large number of optimal trees is due to multiple alternative resolutions given the high level of homoplasy (CI = 0.24; RI = 0.73). In all trees, poneromorphs consistently form a paraphyletic assemblage with respect to myrmicomorphs (groups G and H), leptanillomorphs (groups L and M), and a clade comprising the five dorylomorph subfamilies (army ants and their closest relatives; group N). The alternative conflicting resolutions in this part of the tree involve the relationships between poneromorph subfamilies and these last three clades (i.e., myrmicomorphs, leptanillomorphs, and dorylomorphs), resulting in a large polytomy shown in the strict consensus (fig. 36). A particular source of conflict is the position of Paraponerinae (group F). This subfamily appears either as sister of the myrmicomorphs + Proceratiinae (groups G, H, and I) or as sister of Heteroponerinae + Ectatomminae (groups J and K).

Another large area of conflicting resolution involves the relationships within Ponerinae (group P), and revolves around a paraphyletic set comprised mostly of *Pachycondyla* species. Here, different terminals permute alone or in combination as sister to the rest of some Ponerinae genera.

Among the nonponeromorph subfamilies Formicinae (group A) is not resolved as monophyletic. This occurs because *Oecophylla smaragdina* clusters as sister to the rest of the subfamily plus Dolichoderinae according to these data.

The results of analyses under implied weights are summarized in table 2. Fewer trees "of best fit" are selected under all concavity values in comparison to those selected under equal weights. Concavities 1–2 (strong downweighting of homoplasious characters) selected tree topologies that differ markedly from the ones selected under both

equal weights and concavities 3–10 (mild to weak downweighting of homoplasious characters). Concavities 3–10 selected trees that differ only in minor rearrangements between them. Figure 37 shows a strict consensus of three best-fit trees under concavity 10, in which homoplasy is downweighted the least severely (see below).

In contrast with the equal-weights analysis, under implied weights ($K = 10$) there is little conflict between the alternative optimal trees and therefore greater resolution in the strict consensus. However, this resolution does not amount to the preference of some of the alternative topologies recovered under equal weights. Rather, under implied weights, even with little downweighting, the relationships between the poneromorph subfamilies are markedly different. Paraponerinae is now sister to a large clade composed of Proceratiinae, myrmicomorphs, and dorylomorphs. Also peculiar is the position of the leptanillomorphs (groups L and M), which are now nested within Amblyoponinae. Within Ponerinae, the different species of *Pachycondyla* cluster separately as sisters to different clades, still forming a large paraphyletic genus.

In some cases, implied weighting favors topological arrangements that are congruent with traditional taxonomic views and molecular studies. A good example is the position of the leptanillomorph subfamilies Apomyrminae (group L) and Leptanillinae (group M). In all analyses, under equal and implied weights, these subfamilies are sister groups as suspected previously (e.g., Bolton, 1990c, 2003), but not supported by current molecular data (and see below). Under equal weights, these subfamilies cluster as sister or closely related to the well-supported dorylomorph clade. In contrast, under implied weights (for all values of K) both subfamilies nest within Amblyoponinae (group O), specifically as sister to *Amblyopone mutica* (fig. 37).

That the monotypic *Apomyrma* belongs within Amblyoponinae has long been suspected: the genus was classified within this group (then the tribe Amblyoponini) when first described (Brown et al., 1971), but was subsequently placed in a suprageneric group of its own due to its specialized morphology related to a cryptobiotic way of life (Bolton,

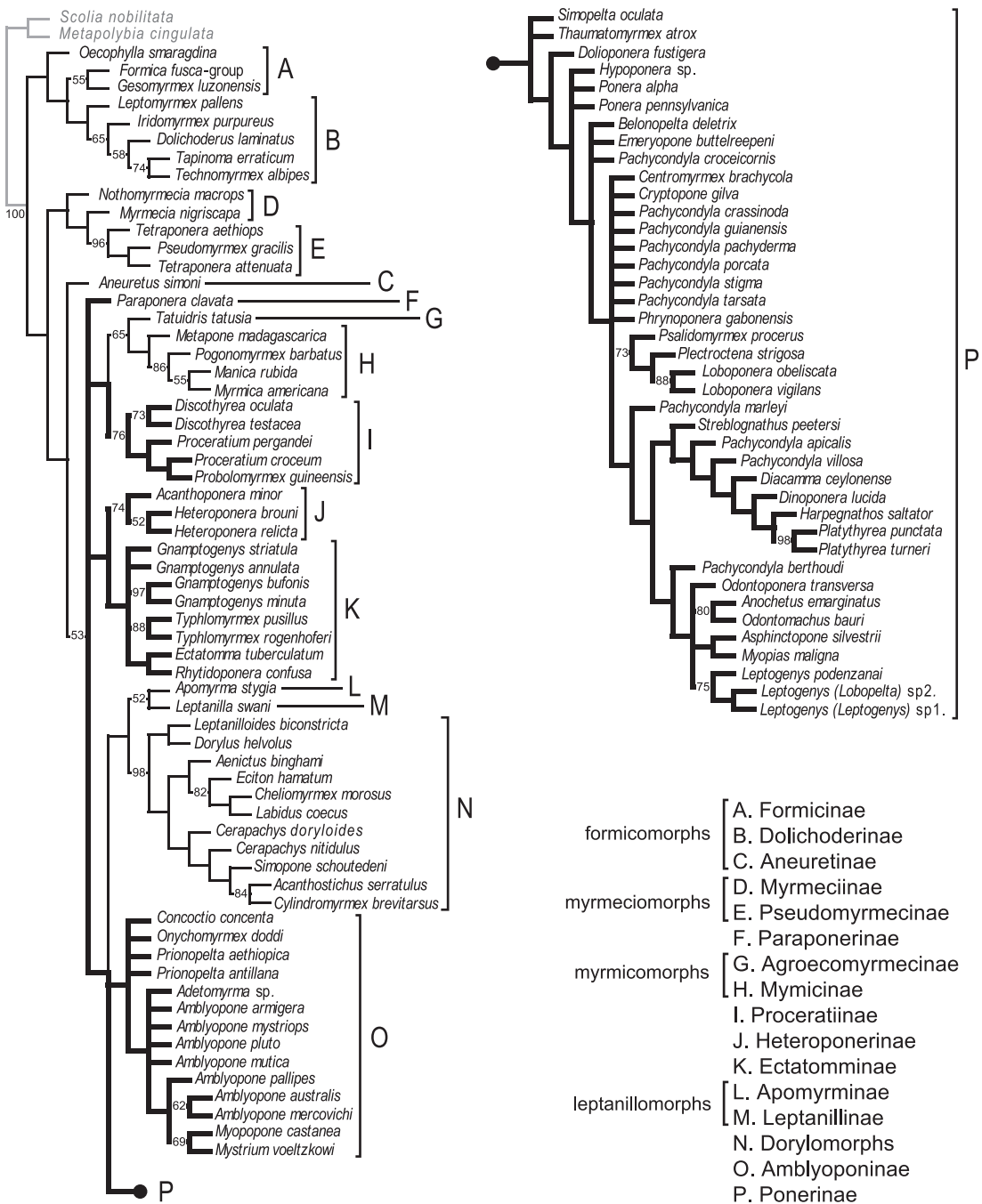


Fig. 36. Strict consensus of 3192 most-parsimonious trees obtained under equal-weights analysis (L = 776, CI = 0.24, RI = 0.73). Thick lines correspond to poneromorph taxa. Symmetric resampling values above 50 are shown on branches.

TABLE 2
Results of Parsimony Analysis Under Different
Weighting Schemes. K = Constant of Concavity.

Weighting scheme	No. of trees	Length
Equal weights	3192	776
$K = 10$	3	793
$K = 9$	3	793
$K = 8$	3	793
$K = 7$	3	795
$K = 6$	3	807
$K = 5$	3	819
$K = 4$	3	819
$K = 3$	3	826
$K = 2$	1	827
$K = 1$	1	847

1990c; Baroni Urbani et al., 1992; Bolton, 1994, 2003). Molecular-based analyses now consistently place this taxon back within Amblyoponinae (Saux et al., 2004; Brady et al., 2006; Moreau et al., 2006).

The case of Leptanillinae is less straightforward. These minute ants were hypothesized as close relatives to the army ant genus *Dorylus* at the time of description (Emery, 1870), transferred briefly to Myrmicinae due to the possession of a two-segmented waist (Emery, 1877), but placed back into army ants some years later after careful examination of the female mouthparts and genitalia with the then newly invented technique of insect clearing by potassium hydroxide (Emery, 1904). The taxon was later transferred to its own subfamily (Wheeler, 1923) in recognition that its unique, highly derived skeletal morphology makes inferring its exact affinities difficult. Recent molecular studies place the group as sister to the rest of the ants (Saux et al., 2004; Moreau et al., 2006), but it is now acknowledged that this pattern is an artifact of long-branch attraction, regardless of the method of analysis used, caused by high rates of evolution that the taxon experienced at the sequence level (Brady et al., 2006). The best molecular-based estimates, however, place Leptanillinae close to Amblyoponinae.

Another example of marked differences between results of equal weighting versus implied weighting involves cases of rerooting in some subclades. Within Ectatomminae (group K), equal weighting recovers trees

in which *Gnamptogenys* is paraphyletic with respect to *Ectatomma* + *Rhytidoponera* (fig. 36). Specifically, the *Gnamptogenys minuta* group (represented by *G. minuta* and *G. bufonis* here) is sister to a clade containing the rest of *Gnamptogenys* + (*Ectatomma*, *Rhytidoponera*). Conversely, under implied weighting *Ectatomma* + *Rhytidoponera* is sister to a monophyletic *Gnamptogenys* in which the *minuta* group takes a higher nested position. Within the well-studied dorylomorph clade (group L), equal weighting always favors army ants (here Aenictinae, Dorylinae, and Ecitoninae) as paraphyletic with respect to Cerapachyinae, even though relationships among the army ants vary and thus the consensus is unresolved. Under implied weighting the reverse is the case: Cerapachyinae is paraphyletic with respect to the army ant subfamilies, and the relationships among its constituent genera mirrors that obtained in simultaneous analysis of morphology and molecules (Brady, 2003; Brady and Ward, 2005).

The significant differences in topology between optimal trees selected by the two weighting strategies occur even under high-concavity values (e.g., $K = 8-10$), that is, even when characters with extra steps are only weakly penalized (downweighted). Table 3 shows the weight (fit) assigned to characters up to 4 steps longer under the different concavity values used in this study, as calculated by the weighting function $F = K/(K + ES)$ (Goloboff, 1995, 1997b). Whereas under $K = 1$ a character with one extra step on a given tree receives 50% of the weight of a character with perfect fit, under $K = 10$ the same character is downweighted only by 10%. More drastically, under $K = 1$ a character implying three extra steps is downweighted by 75% of the weight of a character with perfect fit, whereas under $K = 10$ the same character is downweighted only by 23%. In other words, high values of K consider characters to be nearly equally influential (Goloboff, 1995), as does analyses under equal weights, while still correcting for the fact that extra steps in highly homoplasious characters should have less influence in selecting between alternative topologies than extra steps in characters close to perfect fit (Farris, 1969; Carpenter, 1988; Goloboff,

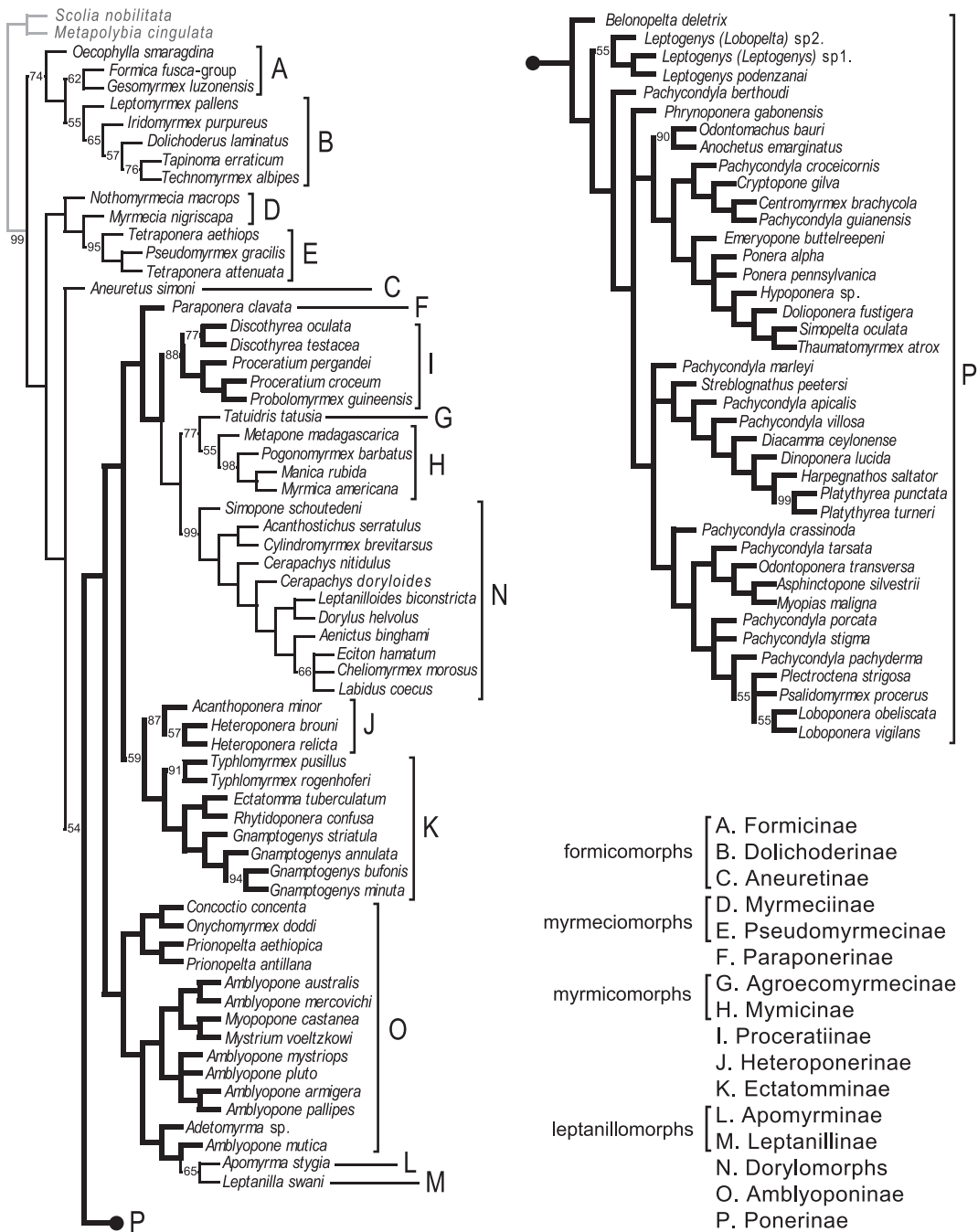


Fig. 37. Strict consensus of 3 optimal trees obtained under implied-weights analysis with $K = 10$ ($L = 793$, $CI = 0.23$, $RI = 0.72$). Thick lines correspond to poneromorph taxa. Symmetric resampling values above 50 are shown on branches.

TABLE 3
Weight Values (*F*) for Characters up to Four Steps Longer Based on the Concave Function of Homoplasy $F = KI/(K+ES)$ for $K = 1-10$, Where $K =$ Constant of Concavity; $ES =$ Number of Extra Steps (After Goloboff, 1997b).

<i>K</i>	<i>ES</i>				
	0	1	2	3	4
1	1.0000	0.5000	0.3333	0.2500	0.2000
2	1.0000	0.6667	0.5000	0.4000	0.3333
3	1.0000	0.7500	0.6000	0.5000	0.4286
4	1.0000	0.8000	0.6667	0.5714	0.5000
5	1.0000	0.8333	0.7143	0.6250	0.5556
6	1.0000	0.8571	0.7500	0.6667	0.6000
7	1.0000	0.8750	0.7778	0.7000	0.6364
8	1.0000	0.8889	0.8000	0.7273	0.6667
9	1.0000	0.9000	0.8182	0.7500	0.6923
10	1.0000	0.9091	0.8333	0.7692	0.7143

1993; Carpenter, 1994; Goloboff et al., 2008). For these reasons, $K = 10$ was chosen as the preferred value for subsequent discussion (see also below).

The alternative placements of leptanillo-morphs given the two weighting strategies, closely related to dorylomorphs under equal weighting or nested within Amblyoponinae under implied weighting, can be clearly understood at the character level. Six characters are most influential in discriminating between these alternatives: the longitudinal compression of the lateral portions of the clypeus (char. 4); the extension of median area of clypeus between the antennal sockets (char. 5); presence/absence of compound eyes (char. 47); ventral fusion of the lateral margins of the petiolar tergite (char. 107); reduction of petiolar poststernite (char. 108); and tergo-sternal fusion of abdominal segment IV (char. 122). Table 4 summarizes the fit of these characters on trees selected under equal and implied weighting. Taking only these characters into consideration, it can be seen that in terms of raw tree length the characters contribute two steps more to the total length of trees selected under equal weighting (48 steps) than to the total length of trees selected under implied weighting (46 steps). However, in terms of their fit there is an overall improvement on these characters in trees selected under implied weighting. Character 5, for example, is one step longer under

TABLE 4
Comparison of Consistency Index (ci), Retention Index (ri), and Length (l) for Seven Characters Optimized Into Trees Resulting from Equal Weights and Implied-weights Analyses. m = Minimum Number of Steps.

Char.	m	Equal weights				Implied weights ($K = 10$)		
		ci	ri	l		ci	ri	l
4	1	0.33	0.83	3	<	0.25	0.75	4
5	3	0.13	0.70	22	<	0.13	0.68	23
47	2	0.22	0.50	9	>	0.28	0.64	7
107	2	0.40	0.72	5	>	0.66	0.90	3
108	1	0.50	0.00	2	>	1.00	1.00	1
122	2	0.28	0.84	7	<	0.25	0.81	8
Total =				48		Total =		46

implied weighting, but was already highly homoplasious (incongruent) under equal weighting. Hence, there is no significant difference in the consistency index (CI) for this character between the equal- and implied-weighting trees. A similar case occurs with character 122. Character 108, on the other hand, is one step shorter under implied weighting, but it changes from requiring homoplasy (CI = 0.50) and not supporting any group (RI = 0.00) under equal weighting, to having a perfect fit and group support (CI = 1.00; RI = 1.00) under implied weighting. A similar case occurs with character 107.

In the case of the position of *Apomyrma*, the different ways in which the two weighting schemes resolve the conflict among these characters (specifically minimizing chars. 4, 5, and 122 versus chars. 107 and 108) mirrors the opinions expressed in the literature. Bolton (1990a, 1990b, 1990c) removed this genus from Amblyoponinae while reclassifying the subfamilies based on tergo-sternal fusion of abdominal segments (i.e., char. 122), and its close relationship with dorylomorphs was suspected in part due to the reduction of the clypeus and “exposed” antennal sockets (i.e., chars. 4 and 5, Baroni Urbani et al., 1992; Grimaldi et al., 1997). In spite of this, the similarities in the unusual arrangement of the petiole shared between *Apomyrma* and *Amblyopone mutica* (i.e., chars. 107 and 108) have been acknowledged repeatedly ever since the genus was first described as an amblyoponine (Brown et al., 1971; Ward, 1994; Bolton, 2003).

The observation that morphological data conform better to prior taxonomic expectation and to patterns recovered in simultaneous analysis of data from different sources (i.e., morphology, molecular, and behavioral) when weighted as a function of their implied homoplasy has been pointed out before. For example, in their study of the paper wasp genus *Apoica* Lepeletier, Pickett and Wenzel (2007) found that the behavior of morphological characters implying less homoplasy when analyzed alone improved in unconstrained simultaneous analysis (as measured by an increase in their consistency index). Such improvement occurred at the expense of morphological characters that were already highly incongruent. Giannini and Simmons (2005) reported similar outcomes on their reconstruction of megachiropteran bat relationships. They showed that trees resulting from analyses of the morphological partition under implied weighting resembles more the trees from simultaneous analysis of morphology + molecules (as measured by number of nodes in common), than trees derived from morphology analyses under equal weighting. Finally, Goloboff et al. (2008) carried out an extensive study of the effect of using equal weighting versus implied weighting in the analysis of morphological matrices. Their results show that analyzing morphology under implied weighting significantly improves the support for clades, as measured by jackknife frequencies, even under high values of K . Thus, they recommended the general use of implied-weighting techniques for the analysis of morphological data. For this reason, in this study the results of implied-weights analyses were chosen to discuss character evolution and to compare with the phylogenies recently derived from DNA-sequence data for the ants. Specifically, the consensus of trees obtained with $K = 10$ was chosen as the preferred summary hypothesis for the reasons discussed earlier.

It is difficult to perform an exact point-by-point comparison between the results obtained from the morphological data in the present study and the published phylogenies derived from DNA-sequence data (i.e., Brady et al., 2006; Moreau et al., 2006) because of the differences in taxon sampling among studies. In the present

work, the poneromorph subfamilies were sampled exhaustively while the rest of the subfamilies are represented by a few exemplars. In contrast, in studies by Brady et al. (2006) and Moreau et al. (2006), the large nonponeromorph subfamilies (i.e., Dolichoderinae, Formicinae, and Myrmicinae) are densely represented while poneromorphs are represented by the best-known genera only.

In general, both morphology and molecules recover all extant subfamilies as monophyletic with the exception of Formicinae and Amblyoponinae (see below), so most differences pertain to the relationships between the ant subfamilies (compare figs. 37 and 38). The three notable points of congruence are the monophyly of myrmeciomorphs, the sister-group relationship between Heteroponerinae and Ectatomminae, and the position of Apomyrminae and Leptanillinae as nested inside or closely related to Amblyoponinae (discussed extensively above). Although a close relationship between Myrmecinae and Pseudomyrmecinae (i.e., myrmeciomorphs) is a recent finding, the close relationship between the genera contained in Heteroponerinae and Ectatomminae was successfully established a little over a half a century ago in Brown's (1958) monograph on the then tribe Ectatommini. It was only recently that Bolton (2003) partitioned the group when splitting Ponerinae s.l. into multiple subfamilies. However, the morphological and molecular evidence suggest that Bolton's partitioning of this group may be unnecessary, and that these genera could be reclassified into a single subfamily Ectatomminae.

A notable point of incongruence between the results of morphology and DNA sequences pertains to the position of Formicinae. Current molecular data reconstruct this subfamily as sister to the large subfamily Myrmicinae (albeit with low support; see fig. 38); this relationship has never been hypothesized before. In contrast, the results from morphology (under both equal and implied weights) place Formicinae close to Dolichoderinae with a high support value. Besides the discrete, unique morphological characters supporting this relationship, ants in these subfamilies are difficult to tell apart given their overall similarity. In fact, until the

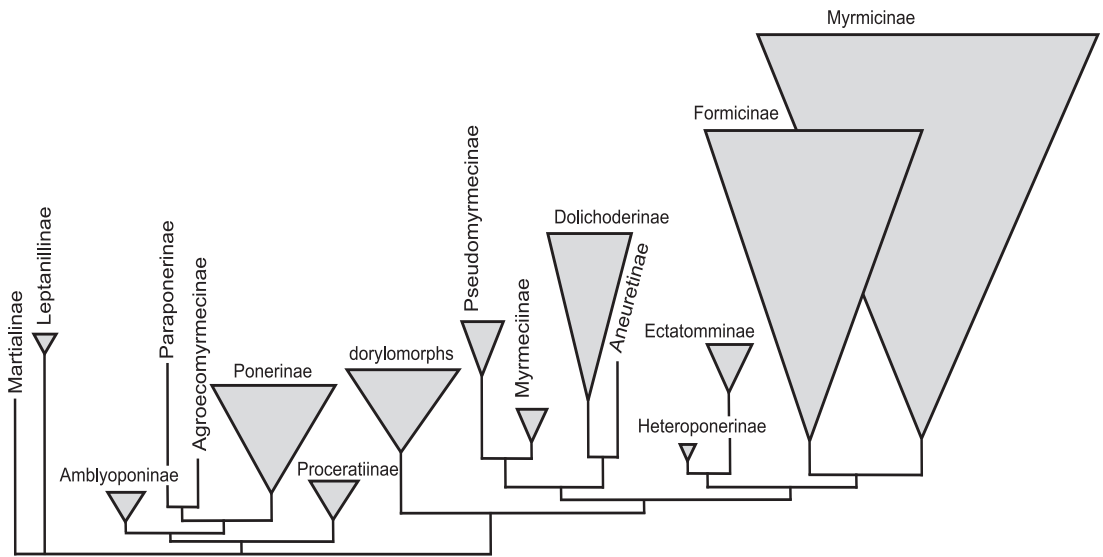


Fig. 38. Summary of phylogenetic relationships between ant subfamilies as reconstructed from several nuclear gene fragments. Redrawn after Brady et al. (2006), Moreau et al. (2006), and Rabeling et al. (2008).

present anatomical study, no character was known to separate the males into one or the other subfamily.

Another important point of incongruence is the phylogenetic position of dorylomorphs. DNA-sequence data place the army ants and their allies as the sister group of a clade containing all other nonponeromorph subfamilies but Heteroponerinae + Ectatomminae (fig. 38). Again, a result never hypothesized before. The morphological data, on the other hand, reflects a more traditional placement of dorylomorphs as nested somewhere within the poneromorph subfamilies (see figs. 1–4, 36, 37). Given the extreme behavioral specialization characterizing the army-ant subfamilies, resolving their exact position on the phylogeny will have a direct impact on our understanding of the complexity in social evolution in ants.

However, the most important difference from current molecular phylogenies pertains to rooting. Molecular data currently place the root of the ant tree somewhere within a “poneroid” group (sensu Brady et al., 2006, composed of Agroecomyrmecinae, Amblyoponinae, Paraponerinae, Ponerinae, and Proceratiinae) and subfamilies Leptanillinae and Martialinae (Brady et al., 2006; Moreau

et al., 2006; Rabeling et al., 2008; see fig. 38). The morphological data derived from this study place the subfamilies Dolichoderinae and Formicinae as a clade sister to the rest of the ants. This latter result reflects traditional views of ant phylogeny (figs. 1–4), especially those hypothesized by Bill Brown (see fig. 4). From a morphological perspective, members of these two subfamilies can be considered to display “generalized” traits overall for the family Formicidae when compared to non-formicid vespoids, even when the sting apparatus is greatly reduced or absent altogether. Workers in these groups have unspecialized mouthparts and antennal sockets, retain the greatest number of palp and antennal segments, do not show the extensive fusion of plates along the body characteristic of the other subfamilies, and have unmodified gastral sclerites. However, rather than arguing for the superiority of one type of data set over the other, it will be necessary to combine both types of data into an unconstrained, simultaneous analysis in order to resolve the apparent taxonomic incongruence (Nixon and Carpenter, 1996b), a type analysis that is beyond the scope of the current study, which deals only with the morphological aspect for the family.

FINAL REMARKS

There is a rich tradition in studies of comparative ant anatomy, but so far only a few works have attempted to integrate part of this information into quantitative phylogenetic analyses. These few studies dealt with only a limited sample of diversity across the Formicidae, and none has synthesized the morphological information in a way that facilitates its subsequent use and integration with other types of data. This study was done following an alternative model that incorporates digital imaging for character evaluation and documentation. The result is that each anatomical observation can be readily analyzed and understood in the context of phylogeny.

This work also shows that ant morphology, as a source of phylogenetic data, is by no means exhausted. All the characters discovered and discussed in this study were derived only from skeletal morphology of the adult worker. There is great phylogenetic potential in the study of yet unexplored systems like the musculature and glands. Moreover, the study of other life stages like larvae, different castes like queens and the highly dimorphic males, promise to yield many new phylogenetic characters and interesting evolutionary novelties. Our current system of ant classification is more diagnostic than phylogenetic, especially given the lack of integration between morphology and DNA data into simultaneous phylogenetic analyses. However, the progression toward achieving a phylogenetic classification can only increase the accuracy of diagnosis in our classification system, since phylogeny is the common pattern behind organismal diversity and therefore the best way to summarize biological data (Hennig, 1966; Farris, 1979a, 1979b).

ACKNOWLEDGMENTS

The present study would not have been possible without the dedication of all the collectors and curators that during centuries have contributed to and tended natural history museum collections for generations to come. For access to institutional collections I thank the curators James M. Carpenter (American Museum of Natural History, New York), Stefan Cover (Museum of Com-

parative Zoology, Cambridge, MA), and Barry Bolton (Natural History Museum, London). From single specimens to full collections, the following people kindly donated material that was key in completing the taxon sampling and allowed many of the necessary dissections: Barry Bolton, Christian Peeters, Donat Agosti, Mike J. McDonald, James M. Carpenter, Brian Fisher, Stefan Cover, Damon Little, Nico Franz, Kelly B. Miller, John Asher, Stefani Berghoff, and Akito Y. Kawahara.

My work on ants benefited greatly from discussions and suggestions by Donat Agosti, Barry Bolton, Stefan Cover, Christian Peeters, Philip Ward, and Brian Fisher. I thank James M. Carpenter, Quentin D. Wheeler, Kevin C. Nixon, Martin Ramirez, Patrícia Brito, Kurt Picket, Torsten Dikow, and Norberto Gianini for fruitful discussions on phylogenetic methods. Extensive comments by two anonymous reviewers greatly improved this manuscript.

Financial support came from a CONACyT (Mexico) scholarship for graduate studies abroad (no. 119626) and from an International Graduate Student Fellowship from the American Museum of Natural History (AMNH). The final preparation of this manuscript was done under a postdoctoral fellowship by the Portuguese Foundation for Science and Technology, FCT (SFRH/BPD/65529/2009). All the scanning electron microscopy work was done at the Microscopy and Image Facility Laboratory at the AMNH, and I thank Angela Klaus, Kevin Frischmann, and Jacob Louis Mey for their assistance. For literature support I thank Donat Agosti for compiling, digitizing and making available through antbase.org all the ant taxonomic literature from Linnaeus to the present.

REFERENCES

- Abouheif, E., and G.A. Wray. 2002. Evolution of the gene network underlying wing polyphenism in ants. *Science* 297: 249–252.
- Agosti, D. 1991. Revision of the Oriental ant genus *Cladomyrma*, with an outline of the higher classification of the Formicinae (Hymenoptera: Formicidae). *Systematic Entomology* 16 (3): 293–310.
- Agosti, D. 2003. Encyclopedia of life: should species description equal gene sequences? *Trends in Ecology and Evolution* 18: 273.

- Agosti, D. 2005. Productive ants run ahead. *Systematic Entomology* 30: 175–176.
- Agosti, D., and B. Bolton. 1990. New characters to differentiate the ant genera *Lasius* F. and *Formica* L. (Hymenoptera: Formicidae). *Entomologist's Gazette* 41: 149–156.
- Agosti, D., and N.F. Johnson. 2007. Antbase. World Wide Web electronic publication. antbase.org, (accessed 1.VI.2010).
- Arnol'di, K.V. 1930. Studien über die Systematik der Ameisen. IV. *Aulacopone*, eine neue Ponerinengattung (Formicidae) in Russland. *Zoologischer Anzeiger* 89: 139–144.
- Baratte, S., C. Peeters, and J.S. Deutsch. 2006. Testing homology with morphology, development and gene expression: sex-specific thoracic appendages of the ant *Diacamma*. *Evolution and Development* 8: 433–445.
- Baroni Urbani, C. 1989. Phylogeny and behavioural evolution in ants, with a discussion of the role of behaviour in evolutionary processes. *Ethology Ecology & Evolution* 1: 137–168.
- Baroni Urbani, C., B. Bolton, and P.S. Ward. 1992. The internal phylogeny of ants (Hymenoptera: Formicidae). *Systematic Entomology* 17: 301–329.
- Baroni Urbani, C., and M.L. de Andrade. 2003a. The ant genus *Proceratium* in the extant and fossil record (Hymenoptera: Formicidae). *Museo Regionale di Scienze Naturali Monografia* 36: 1–480.
- Baroni Urbani, C., and M.L. de Andrade. 2003b. The ant genus *Thaumatomyrmex* in Cuba (Hymenoptera: Formicidae) with description of two new species. *Mitteilungen der Schweizerischen Entomologischen Gesellschaft* 76: 263–277.
- Basibuyuk, H.H., and D.L.J. Quicke. 1995. Morphology of the antenna cleaner in the Hymenoptera with particular reference to non-aculeate families (Insecta). *Zoologica Scripta* 24: 157–177.
- Billen, J.P.J. 1986. Morphology and ultrastructure of the abdominal glands in dolichoderine ants (Hymenoptera, Formicidae). *Insectes Sociaux* 33: 278–295.
- Bisby, F.A., J. Shimura, M. Ruggiero, J. Edwards, and C. Haeuser. 2002. Taxonomy, at the click of a mouse. *Nature* 418: 367.
- Bolton, B. 1990a. Abdominal characters and status of the cerapachyine ants (Hymenoptera, Formicidae). *Journal of Natural History* 24: 53–68.
- Bolton, B. 1990b. Army ants reassessed: the phylogeny and classification of the doryline section (Hymenoptera: Formicidae). *Journal of Natural History* 24: 1339–1364.
- Bolton, B. 1990c. The higher classification of the ant subfamily Leptanillinae (Hymenoptera: Formicidae). *Systematic Entomology* 15: 267–282.
- Bolton, B. 1994. Identification guide to the ant genera of the world. Cambridge, MA: Harvard University Press, 222 pp.
- Bolton, B. 1995. A new general catalogue of the ants of the world. Cambridge, MA: Harvard University Press, 504 pp.
- Bolton, B. 2003. Synopsis & classification of Formicidae. *Memoirs of the American Entomological Institute* 71: 1–370.
- Bolton, B., and W.L. Brown, Jr. 2002. *Loboponera* gen. n. and a review of the Afrotropical *Plectroctena* genus group (Hymenoptera: Formicidae). *Bulletin of the Natural History Museum (Entomology)* 71: 1–18.
- Bolton, B., and B. Fisher. 2008. Afrotropical ants of the ponerine genera *Centromyrmex* Mayr, *Promyrmex* Santschi gen. rev. and *Feroponera* gen. n., with a revised key to genera of African Ponerinae (Hymenoptera: Formicidae). *Zootaxa* 1929: 1–37.
- Bolton, B., G. Alpert, P.S. Ward, and P. Naskrecki. 2007. Bolton's catalogue of ants of the world: 1758–2005. Cambridge, MA: Harvard University Press, CD-ROM.
- Brady, S.G. 2003. Evolution of the army ant syndrome: The origin and long-term evolutionary stasis of a complex of behavioral and reproductive adaptations. *Proceedings of the National Academy of Sciences of the United States and America* 100: 6575–6579.
- Brady, S.G., and P.S. Ward. 2005. Morphological phylogeny of army ants and other dorylomorphs (Hymenoptera: Formicidae). *Systematic Entomology* 30: 593–618.
- Brady, S.G., T.R. Schultz, B.L. Fisher, and P.S. Ward. 2006. Evaluating alternative hypotheses for the early evolution and diversification of ants. *Proceedings of the National Academy of Science of the United States and America* 103: 18172–18177.
- Brandão, C.R.F., J.L.M. Diniz, D. Agosti, and J.H. Delabie. 1999. Revision of the Neotropical ant subfamily Leptanilloidinae. *Systematic Entomology* 24: 17–36.
- Brandão, C.R.F., J.L.M. Diniz, and E.M. Tomotake. 1991. *Thaumatomyrmex* strips millipedes for prey: a novel predatory behaviour in ants, and the first case of sympatry in the genus (Hymenoptera: Formicidae). *Insectes Sociaux* 38: 335–344.
- Brothers, D.J. 1999. Phylogeny and evolution of wasps, ants and bees (Hymenoptera, Chrysidoidea, Vespoidea and Apoidea). *Zoologica Scripta* 28: 233–249.

- Brothers, D.J., and J.M. Carpenter. 1993. Phylogeny of Aculeata: Chrysidoidea and Vespoidea (Hymenoptera). *Journal of Hymenoptera Research* 2: 227–304.
- Brown, W.L., Jr. 1952. Contributions toward a reclassification of the Formicidae. I. Tribe Platythreini (Hymenoptera). *Breviora* 6: 1–6.
- Brown, W.L., Jr. 1954. Remarks on the internal phylogeny and subfamily classification of the family Formicidae. *Insectes Sociaux* 1: 21–31.
- Brown, W.L., Jr. 1958. Contributions toward a reclassification of the Formicidae. II. Tribe Ectatommini (Hymenoptera). *Bulletin of the Museum of Comparative Zoology at Harvard University* 118: 173–362.
- Brown, W.L., Jr. 1960. Contributions toward a reclassification of the Formicidae, III: Tribe Amblyoponini (Hymenoptera). *Bulletin of the Museum of Comparative Zoology at Harvard University* 122: 144–230.
- Brown, W.L., Jr. 1963. Characters and synonymies among the genera of ants. Part III. Some members of the tribe Ponerini (Ponerinae, Formicidae). *Breviora* 190: 1–10.
- Brown, W.L., Jr. 1965. Contributions to a reclassification of the Formicidae. IV. Tribe Typhlomyrmecini (Hymenoptera). *Psyche* 72: 65–78.
- Brown, W.L., Jr. 1968. An hypothesis concerning the function of the metapleural glands in ants. *American Naturalist* 102: 188–191.
- Brown, W.L., Jr. 1974. *Concoctio* genus nov. Pilot Registry of Zoology Card No. 29.
- Brown, W.L., Jr. 1975. Contributions toward a reclassification of the Formicidae. V. Ponerinae, tribes Platythreini, Cerapachyini, Cyldromyrmecini, Acanthostichini, and Aenictogitini. *Search Agriculture* 5: 1–116.
- Brown, W.L., Jr. 1976. Contributions toward a reclassification of the Formicidae. Part VI. Ponerinae, tribe Ponerini, subtribe Odontomachiti. Section A. Introduction, subtribal characters. Genus *Odontomachus*. *Studia Entomologica* 19: 67–171.
- Brown, W.L., Jr. 1978. Contributions toward a reclassification of the Formicidae. Part VI. Ponerinae, tribe Ponerini, subtribe Odontomachiti. Section B. Genus *Anochetus* and bibliography. *Studia Entomologica* 20: 549–638.
- Brown, W.L., Jr. 2000. Diversity of ants. *In* D. Agosti, J. Majer, E. Alonso, and T.R. Schultz (editors), *Ants: standard methods for measuring and monitoring biodiversity*, 45–79. Washington, D.C.: Smithsonian Institution Press.
- Brown, W.L., Jr, W.H. Gotwald, and J. Levieux. 1971. A new genus of ponerine ants from West Africa (Hymenoptera: Formicidae) with ecological notes. *Psyche* 77: 259–275.
- Carlin, N.F., and D.S. Gladstein. 1989. The “bouncer” defense of *Odontomachus ruginodis* and other odontomachine ants (hymenoptera: Formicidae). *Psyche* 96: 1–19.
- Carpenter, J.M. 1988. Choosing among multiple equally parsimonious cladograms. *Cladistics* 4: 291–296.
- Carpenter, J.M. 1992. Comparing methods, review: the comparative method in evolutionary biology. *Cladistics* 8: 191–195.
- Carpenter, J.M. 1994. Successive weighting, reliability and evidence. *Cladistics* 10: 215–220.
- Clarke, T. 2002. Formidable catalogue puts army of ants online. *Nature* 416: 115.
- Cobbett, A., M. Wilkinson, and M.A. Wills. 2007. Fossils impact as hard as living taxa in parsimony analyses of morphology. *Systematic Biology* 56: 753–766.
- Crozier, R.H. 2006. Charting uncertainty about ant origins. *Proceedings of the National Academy of Sciences (USA)* 103: 18029–18030.
- Daly, H.V. 1964. Skeleto-muscular morphogenesis of the thorax and wings of the honey bee *Apis mellifera* (Hymenoptera: Apidae). *University of California Publications in Entomology* 39: 1–77.
- de Andrade, M.L., and C. Baroni Urbani. 2003. The Baltic amber ant genus *Bradoponera* (Hymenoptera: Formicidae), with description of two new species and a reassessment of the Proceratiini genera. *Revue Suisse de Zoologie* 110: 913–938.
- de Laet, J. 2005. Parsimony and the problem of inapplicables in sequence data. *In* V.A. Albert (editor), *Parsimony, phylogeny, and genomics*, 81–118. New York: Oxford University Press.
- de Pinna, M.C.C. 1999. Species concepts and phylogenetics. *Reviews in Fish Biology and Fisheries* 9: 353–373.
- de Queiroz, A., and J. Gatesy. 2006. The supermatrix approach to systematics. *Trends in Ecology and Evolution* 22: 34–41.
- Donoghue, M.J., J.A. Doyle, J. Gauthier, A. Kluge, and T. Rowe. 1989. The importance of fossils in phylogeny reconstruction. *Annual Review of Ecology and Systematics* 20: 431–460.
- Donoghue, P.C.J., and M.J. Benton. 2007. Rocks and clocks: calibrating the tree of life using fossils and molecules. *Trends in Ecology and Evolution* 22: 424–431.
- Ehmer, B., and W. Gronenberg. 1997. Antennal muscles and fast antennal movements in ants. *Journal of Comparative Physiology, B* 167: 287–296.
- Eisner, T. 1957. A comparative morphological study of the proventriculus of ants (Hymenoptera: Formicidae). *Bulletin of the Museum of Comparative Zoology at Harvard University* 116: 439–490.

- Eisner, T., and E.O. Wilson. 1952. The morphology of the proventriculus of a formicine ant. *Psyche* 59: 47–60.
- Emery, C. 1870. Studi mirmecologici. *Bullettino della Società Entomologica Italiana* 2: 193–201.
- Emery, C. 1877. Saggio di un ordinamento naturale dei Mirmicidei, e considerazioni sulla filogenesi delle formiche. *Bullettino della Società Entomologica Italiana* 9: 67–83.
- Emery, C. 1900. Intorno al torace delle formiche e particolarmente dei neutri. *Bullettino della Società Entomologica Italiana* 32: 103–119.
- Emery, C. 1904. Le affinità del genere *Leptanilla* e i limiti delle Dorylinae. *Archivio Zoologico Italiano* 2: 107–116.
- Engel, M.S., and D. Grimaldi. 2005. Primitive new ants in Cretaceous amber from Myanmar, New Jersey and Canada (Hymenoptera: Formicidae). *American Museum Novitates* 3485: 1–23.
- Ettershank, G. 1966. A generic revision of the world Myrmicinae related to *Solenopsis* and *Pheidologeton* (Hymenoptera: Formicidae). *Australian Journal of Zoology* 14: 73–171.
- Farris, J.S. 1969. A successive approximations approach to character weighting. *Systematic Zoology* 18: 374–385.
- Farris, J.S. 1979a. The information content of the phylogenetic system. *Systematic Zoology* 28: 483–520.
- Farris, J.S. 1979b. On the naturalness of phylogenetic classification. *Systematic Zoology* 28: 200–214.
- Farris, J.S. 1983. The logical basis of phylogenetic analysis. In N.I. Platnick and V.A. Funk (editors), *Advances in cladistics*, 7–36. New York: Columbia University Press.
- Federle, W. 2002. Comments on “Relationships between pretarsus morphology and arboreal life in ponerine ants of the genus *Pachycondyla* (Formicidae: Ponerinae).” *Annals of the Entomological Society of America* 95: 141–142.
- Federle, W., E.L. Brainerd, T.A. McMahon, and B. Holldobler. 2001. Biomechanics of the movable pretarsal adhesive organ in ants and bees. *Proceedings of the California Academy of Sciences of the United States of America* 98: 6215–6220.
- Fisher, B.L. 2006. *Boloponera vicans* gen.n. and sp.n. and two new species of the *Plectroctena* genus group (Hymenoptera: Formicidae). *Myrmecologische Nachrichten* 8: 111–118.
- Francoeur, A., and R. Loiselle. 1988. Évolution du strigile chez les Formicides (Hyménoptères). *Naturaliste Canadien* 115: 333–353.
- Freeland, J., R.H. Crozier, and J. Marc. 1982. On the occurrence of arolia in ant feet. *Journal of the Australian Entomological Society* 21: 257–262.
- Gewin, V. 2002. Taxonomy: All living things, online. *Nature* 418: 362–363.
- Giannini, N.P., and N.B. Simmons. 2005. Conflict and congruence in a combined DNA–morphology analysis of megachiropteran bat relationships (Mammalia: Chiroptera: Pteropodidae). *Cladistics* 21: 411–437.
- Gibson, G.A.P. 1985. Some pro- and mesothoracic structures important for phylogenetic analysis of Hymenoptera, with a review of terms used for the structures. *Canadian Entomologist* 117: 1395–1443.
- Goloboff, P., J.S. Farris, and K. Nixon. 2003a. T.N.T.: tree analysis using new technology. Internet resource (<http://www.zmuk.dk/public/phylogeny>); program and documentation also available from the authors.
- Goloboff, P.A. 1993. Estimating character weights during tree search. *Cladistics* 9: 83–91.
- Goloboff, P.A. 1995. Parsimony and weighting: a reply to Turner and Zandee. *Cladistics* 11: 95–104.
- Goloboff, P.A. 1997a. NONA. Computer software and documentation distributed by the American Museum of Natural History, New York.
- Goloboff, P.A. 1997b. Pee-Wee. Computer software and documentation distributed by the American Museum of Natural History, New York.
- Goloboff, P.A., et al. (2003b). Improvements to resampling measures of group support. *Cladistics* 19: 324–332.
- Goloboff, P.A., J.M. Carpenter, J.S. Arias, and D.R. Miranda-Esquivel. 2008. Weighting against homoplasy improves phylogenetic analysis of morphological data sets. *Cladistics* 24: 1–16.
- Gotwald, W.H., Jr. 1969. Comparative morphological studies of the ants, with particular reference to the mouthparts (Hymenoptera: Formicidae). *Memoirs of the Cornell University Agricultural Experimental Station* 408: 1–150.
- Gotwald, W.H., Jr. 1970. Mouthpart morphology of the ant *Aneuretus simoni*. *Annals of the Entomological Society of America* 63: 950–952.
- Gotwald, W.H., Jr. 1973. Mouthpart morphology of the African ant *Oecophylla longinoda* Latreille (Hymenoptera: Formicidae). *Journal of the New York Entomological Society* 81: 72–78.
- Gotwald, W.H., Jr. 1998. Bill Brown, Myrmecologist, 1922–1997. *Sociobiology* 31: 147–150.
- Gotwald, W.H., Jr. and J. Levieux. 1972. Taxonomy and biology of a new West African ant belonging to the genus *Amblyopone* (Hymenoptera: Formicidae). *Annals of the Entomological Society of America* 65: 383–396.
- Grimaldi, D., D. Agosti, and J.M. Carpenter. 1997. New and rediscovered primitive ants (Hymenoptera: Formicidae) in Cretaceous am-

- ber from New Jersey, and their phylogenetic relationships. *American Museum Novitates* 3208: 1–43.
- Gronenberg, W. 1995. The fast mandible strike in the trap-jaw ant *Odontomachus*. I. Temporal properties and morphological characteristics. *Journal of Comparative Physiology, A* 176: 391–398.
- Gronenberg, W., and B. Ehmer. 1996. The mandible mechanism of the ant genus *Anochetus* (Hymenoptera, Formicidae) and the possible evolution of trap-jaws. *Zoology* 99: 153–162.
- Gronenberg, W., J. Tautz, and B. Hölldobler. 1993. Fast trap jaws and giant neurons in the ant *Odontomachus*. *Science* 262: 561–563.
- Hashimoto, Y. 1991. Phylogenetic study of the family Formicidae based on the sensillum structures on the antennae and labial palpi (Hymenoptera, Aculeata). *Japanese Journal of Entomology* 59: 125–140.
- Hashimoto, Y. 1996. Skeletomuscular modifications associated with the formation of an additional petiole on the anterior abdominal segments in aculeata Hymenoptera. *Japanese Journal of Entomology* 64: 340–356.
- Hennig, W. 1966. *Phylogenetic systematics*. Urbana: University of Illinois Press, 263 pp.
- Hermann, H.R., and M.S. Blum. 1968. The hymenopterous poison apparatus. VI. *Camponotus pennsylvanicus* (Hymenoptera: Formicidae). *Psyche* 75: 216–227.
- Hölldobler, B., and H. Engel. 1979. Tergal and sternal glands in ants. *Psyche* 85: 285–330.
- Hölldobler, B., and H. Engel-Siegel. 1984. On the metapleural gland of ants. *Psyche* 91: 201–224.
- Hölldobler, B., and J.M. Palmer. 1989. A new tarsal gland in ants and the possible role in chemical communication. *Naturwissenschaften* 76: 385–386.
- Hölldobler, B., and R.W. Taylor. 1983. A behavioral study of the primitive ant *Nothomyrmecia macrops* Clark. *Insectes Sociaux* 30: 384–401.
- Hölldobler, B., and J.F.A. Traniello. 1980. The pygidial gland and chemical recruitment communication in *Pachycondyla* (= *Termitopone*) *laevigata*. *Journal of Chemical Ecology* 6: 883–893.
- Hölldobler, B., and E.O. Wilson. 1990. *The ants*. Cambridge, MA: Harvard University Press, 732 pp.
- Hölldobler, B., M. Obermayer, and C. Peeters. 1996. Comparative study of the metatibial gland in ants (Hymenoptera, Formicidae). *Zoomorphology* 116: 157–167.
- Hölldobler, B., M. Obermayer, and E.O. Wilson. 1992. Communication in the primitive cryptobiotic ant *Prionopelta amabilis* (Hymenoptera: Formicidae). *Journal of Comparative Physiology, A* 170: 9–16.
- Hung, A.C.F., and W.L. Brown, Jr. 1966. Structure of gastric apex as a subfamily character of the Formicinae (Hymenoptera: Formicidae). *Journal of the New York Entomological Society* 74: 198–200.
- Janet, C. 1898. Études sur les fourmis, les guêpes et les abeilles. Note 17. Système glandulaire tégumentaire de la *Myrmica rubra*. Observations diverses sur les fourmis, 1–30. Paris: G. Carré et C. Naud Editeurs.
- Jenner, R.A. 2001. Bilaterian phylogeny and uncritical recycling of morphological data sets. *Systematic Biology* 50: 730–742.
- Jenner, R.A. 2004a. Accepting partnership by submission? morphological phylogenetics in a molecular millennium. *Systematic Biology* 53: 333–342.
- Jenner, R.A. 2004b. The scientific status of metazoan cladistics: why current research practice must change. *Zoologica Scripta* 33: 293–310.
- Jessen, K., U. Maschwitz, and M. Hahn. 1979. Neue abdominaldrüsen bei Ameisen. I. Ponerini (Formicidae: Ponerinae). *Zoomorphologie* 94: 49–66.
- Keller, R.A. 2000. Cladistics of the Ectatommini (Hymenoptera: Formicidae): A reappraisal. *Insect Systematics and Evolution* 31: 59–69.
- Kugler, C. 1978a. A comparative study of the myrmicine sting apparatus (Hymenoptera, Formicidae). *Studia Entomologica* 20: 413–548.
- Kugler, C. 1978b. Pygidial glands in the myrmicine ants (Hymenoptera, Formicidae). *Insectes Sociaux* 25: 267–274.
- Kugler, C. 1979a. Evolution of the sting apparatus in the myrmicine ants. *Evolution* 33: 117–130.
- Kugler, C. 1979b. Further studies of the myrmicine sting apparatus: *Eutetramorium*, *Oxyopomyrmex*, and *Terataner* (Hymenoptera, Formicidae). *Psyche* 85: 255–263.
- Kugler, C. 1980. The sting apparatus in the primitive ants *Nothomyrmecia* and *Myrmecia*. *Journal of the Australian Entomological Society* 19: 263–267.
- Kugler, C. 1986. Stings of ants of the tribe Pheidologetini (Myrmicinae). *Insecta Mundi* 1: 221–230.
- Kugler, C. 1991. Stings of ants of the tribe Ectatommini (Formicidae: Ponerinae). *Insecta Mundi* 5: 153–166.
- Kugler, C. 1992. Stings of ants of the Leptanillinae (Hymenoptera: Formicidae). *Psyche* 99: 103–115.
- Kusnezov, N. 1955a. Un nuevo caracter de importancia filogenética en las hormigas (Hymenoptera, Formicidae). *Dusenía* 6: 183–186.
- Kusnezov, N. 1955b. Zwei neue Ameisengattungen aus Tucuman (Argentinien). *Zoologischer Anzeiger* 154: 268–277.

- Lattke, J.E. 1992. Revision of the *minuta*-group of the genus *Gnamptogenys* (Hymenoptera, Formicidae). *Deutsche Entomologische Zeitschrift* (N.F.) 39: 123–129.
- Lattke, J.E. 1994. Phylogenetic relationships and classification of Ectatommine ants (Hymenoptera, Formicidae). *Entomologica Scandinavica* 25: 105–119.
- Lattke, J.E. 2003. The genus *Platythyrea* Roger, 1863 in Dominican amber (Hymenoptera: Formicidae: Ponerinae). *Entomotopica* 18: 107–111.
- Lattke, J.E. 2004. A taxonomic revision and phylogenetic analysis of the ant genus *Gnamptogenys* Roger in Southeast Asia and Australasia (Hymenoptera: Formicidae: Ponerinae). University of California Publications in Entomology 122: 1–266.
- Lepeletier de Saint-Fargeau, A.L.M. 1835. *Histoire naturelle des insectes*. Paris: Roret, 547 pp.
- Love, A.C. 2006. Evolutionary morphology and evo-devo: hierarchy and novelty. *Theory in Biosciences* 124: 317–333.
- Maddison, D.R. 1991. The discovery and importance of multiple Islands of most-parsimonious trees. *Systematic Zoology* 40: 315–328.
- Markl, H. 1973. The evolution of stridulatory communication in ants. *Proceedings of the VIIth Congress of the International Union for the Study of Social Insects*, London, 258–265. Southampton: University of Southampton.
- Mayr, E. 1981. Biological classification: toward a synthesis of opposing methodologies. *Science* 214: 510–516.
- Moreau, C.S., C.D. Bell, R. Vila, S.B. Archibald, and N.E. Pierce. 2006. Phylogeny of the ants: diversification in the age of angiosperms. *Science* 312: 101–104.
- Morgan, E.D., et al. (2003). Comparative survey of abdominal gland secretions of the ant subfamilie Ponerinae. *Journal of Chemical Ecology* 29: 95–114.
- Morphbank, (<http://www.morphbank.net>, 20 September 2007). Florida State University, School of Computational Science, Tallahassee, FL 32306-4026.
- Nixon, K.C. 1999. The parsimony ratchet, a new method for rapid parsimony analysis. *Cladistics* 15: 407–414.
- Nixon, K.C. 2002. WinClada. Published by the author. Internet resource (<http://www.cladistics.com>).
- Nixon, K.C., and J.M. Carpenter. 1996a. On consensus, collapsibility, and clade concordance. *Cladistics* 12: 305–321.
- Nixon, K.C., and J.M. Carpenter. 1996b. On simultaneous analysis. *Cladistics* 12: 221–241.
- Nixon, K.C., and Q.D. Wheeler. 1990. An amplification of the phylogenetic species concept. *Cladistics* 6: 211–223.
- O'Leary, M.A. and S.G. Kaufman (editors), MorphoBank 2.5: web application for morphological phylogenetics and taxonomy. Internet resource (<http://www.morphobank.org>).
- Orivel, J., and A. Dejean. 2002. Response to comments on "Relationships between pretarsus morphology and arboreal life in ponerine ants of the genus *Pachycondyla* (Formicidae: Ponerinae)." *Annals of the Entomological Society of America* 95: 142.
- Orivel, J., M.C. Malherbe, and A. Dejean. 2001. Relationships between pretarsus morphology and arboreal life in ponerine ants of the genus *Pachycondyla* (Formicidae: Ponerinae). *Annals of the Entomological Society of America* 94: 449–456.
- Ouellette, G.D., B.L. Fisher, and D.J. Girman. 2006. Molecular systematics of basal subfamilies of ants using 28S rRNA (Hymenoptera: Formicidae). *Molecular Phylogenetics and Evolution* 40: 359–369.
- Paul, J., and W. Gronenberg. 1999. Optimizing force and velocity: mandible muscle fibre attachments in ants. *Journal of Experimental Biology* 202: 797–808.
- Peeters, C. 1987. The diversity of reproductive systems in ponerine ants. In J. Eder and H. Rembold (editors), *Chemistry and biology of social insects*, 253–254. München: Verlag J. Peperny.
- Peeters, C., and M. Molet. 2010. Evolution of advanced social traits in phylogenetically basal ants: striking worker polymorphism and large queens in *Amblyopone australis*. *Insectes Sociaux* 57: 177–183.
- Perrault, G.H. 1999. L'Architecture thoracique associée à la jonction pronoto-mésothoracique des ouvrières de fourmis (Hymenoptera: Formicidae). Intérêt pour la phylogénie du groupe. *Annales de la Société entomologique de France* 35: 125–163.
- Perrault, G.H. 2000. Les Probolomyrmicinae, nouvelle sous-famille pour le genre *Probolomyrmex* (Hymenoptera, Formicidae). *Bulletin de la Société Entomologique de France* 105: 253–272.
- Perrault, G.H. 2004. Étude morphoanatomique et biométrique du métasoma antérieur des ouvrières. Contribution à la systématique et à la phylogénie des fourmis (Hymenoptera : Formicidae). *Annales de la Société Entomologique de France* 40: 291–371.
- Perrichot, V., S. Lacau, D. Néraudeau, and A. Nel. 2007a. Fossil evidence for the early ant evolution. *Naturwissenschaften* 95: 85–90.

- Perrichot, V., A. Nel, D. Néraudeau, S. Lacau, and T. Guyot. 2007b. New fossil ants in French Cretaceous amber (Hymenoptera: Formicidae). *Naturwissenschaften* 95: 91–97.
- Pickett, K.M., and J. Wenzel. 2007. Revision and cladistic analysis of the nocturnal social wasp genus, *Apoica* Lepeletie (Hymenoptera, Vespidae, Polistinae, Epiponini). *American Museum Novitates* 3562: 1–30.
- Prendini, L. 2001. Species or supraspecific taxa as terminals in cladistic analysis? Groundplans versus exemplars revisited. *Systematic Biology* 50: 290–300.
- Prentice, M.A. 1998. The comparative morphology and phylogeny of apoid wasps (Hymenoptera: Apoidea). Unpublished Ph.D. dissertation, University of California, Berkeley.
- Rabeling, C., J.M. Brown, and M. Verhaagh. 2008. Newly discovered sister lineage sheds light on early ant evolution. *Proceedings of the California Academy of Sciences of the United States of America* 105: 14913–14917.
- Ramírez, M.J., et al. (2007). Linking of digital images to phylogenetic data matrices using a morphological ontology. *Systematic Biology* 56: 283–294.
- Reid, J.A. 1941. The thorax of the wingless and short-winged Hymenoptera. *Transactions of the Royal Entomological Society of London* 91: 367–446.
- Rieppel, O. 2005. Modules, kinds, and homology. *Journal of Experimental Zoology B Molecular and Developmental Evolution* 304B: 18–27.
- Rieppel, O. 2006. The merits of similarity reconsidered. *Systematics and Biodiversity* 4: 137–147.
- Rieppel, O., and M. Kearney. 2002. Similarity. *Biological Journal of the Linnean Society* 75: 59–82.
- Robinson, G.E. 2002. Sociogenomics takes flight. *Science* 297: 204–205.
- Sameshima, S., T. Miura, and T. Matsumoto. 2004. Wing disc development during caste differentiation in the ant *Pheidole megacephala* (Hymenoptera: Formicidae). *Evolution and Development* 6: 336–341.
- Saux, C., B.L. Fisher, and G.S. Spicer. 2004. Dracula ant phylogeny as inferred by nuclear 28S rDNA sequences and implications for ant systematics (Hymenoptera: Formicidae: Amblyoponinae). *Molecular Phylogenetics and Evolution* 33: 457–468.
- Schönitzer, K., and G. Lawitzky. 1987. A phylogenetic study of the antenna cleaner in Formicidae, Mutillidae, and Tiphidae (Insecta, Hymenoptera). *Zoomorphology* 107: 273–285.
- Shattuck, S.O. 1992a. Generic revision of the ant subfamily Dolichoderinae (Hymenoptera: Formicidae). *Sociobiology* 21: 1–181.
- Shattuck, S.O. 1992b. Higher classification of the ant subfamilies Aneuretinae, Dolichoderinae and Formicinae (Hymenoptera: Formicidae). *Systematic Entomology* 17: 199–206.
- Shattuck, S.O. 1995. Generic-level relationships within the ant subfamily Dolichoderinae (Hymenoptera: Formicidae). *Systematic Entomology* 20: 217–228.
- Shattuck, S.O. 1999. Australian ants: their biology and identification. Collingwood, Australia: CSIRO Publishing, 226 pp.
- Snodgrass, R.E. 1935. Principles of insect morphology. Ithaca, NY: Cornell University Press, 667 pp.
- Snodgrass, R.E. 1956. Anatomy of the honey bee. Ithaca, NY: Cornell University Press, 334 pp.
- Taylor, R.W. 1965. A monographic revision of the rare tropicopolitan ant genus *Probolomyrmex* Mayr (Hymenoptera: Formicidae). *Transactions of the Royal Entomological Society of London* 117: 345–365.
- Taylor, R.W. 1978. *Nothomyrmecia macrops*: a living-fossil ant rediscovered. *Science* 201: 979–985.
- Taylor, R.W. 1979. Notes on the Russian endemic ant genus *Aulacopone* Arnoldi (Hymenoptera: Formicidae). *Psyche* 86: 353–361.
- Traniello, J.F.A., and B. Hölldobler. 1984. Chemical communication during tandem running in *Pachycondyla obscuricornis* (Hymenoptera: Formicidae). *Journal of Chemical Ecology* 10: 783–794.
- Traniello, J.F.A., and A.K. Jayasuriya. 1981. Chemical communication in the primitive ant *Aneuretus simoni*: the role of the sternal and pygidial glands. *Journal of Chemical Ecology* 7: 1023–1033.
- Vrana, P., and W. Wheeler. 1992. Individual organisms as terminal entities: laying the species problem to rest. *Cladistics* 8: 67–72.
- Ward, P.S. 1990. The ant subfamily Pseudomyrmecinae (Hymenoptera: Formicidae): generic revision and relationship to other formicids. *Systematic Entomology* 15: 449–489.
- Ward, P.S. 1994. *Adetomyrma*, an enigmatic new ant genus from Madagascar (Hymenoptera: Formicidae), and its implications for ant phylogeny. *Systematic Entomology* 19: 159–175.
- Ward, P.S. 2001. Taxonomy, phylogeny and biogeography of the ant genus *Tetraponera* (Hymenoptera: Formicidae) in the Oriental and Australian regions. *Invertebrate Taxonomy* 15: 589–665.
- Ward, P.S. 2006. Ants. *Current Biology* 16: 152–155.
- Ward, P.S., and S.G. Brady. 2003. Phylogeny and biogeography of the ant subfamily Myrmecinae (Hymenoptera: Formicidae). *Invertebrate Systematics* 17: 361–386.

- Ward, P.S., and D.A. Downie. 2005. The ant subfamily Pseudomyrmecinae (Hymenoptera: Formicidae): phylogeny and evolution of big-eyed arboreal ants. *Systematic Entomology* 30: 310–335.
- Ward, P.S., S.G. Brady, B.L. Fisher, and T.R. Schultz. 2005. Assembling the ant “Tree of Life” (Hymenoptera: Formicidae). *Myrmecologische Nachrichten* 7: 87–90.
- Wenzel, J.W. 1997. When is a phylogenetic test good enough? *In* P. Grandcolas (editor), *The origin of biodiversity in insects: phylogenetic test of evolutionary scenarios*, 31–45. Paris: Mémoires du Muséum National d’Histoire Naturelle 173.
- Werringloer, A. 1932. Die Sehorgane und Sehzentren der Dorylinen nebst Untersuchungen über die Facettenaugen der Formiciden. *Zeitschrift für Wissenschaftliche Zoologie* 141: 432–524.
- Wheeler, G.C., and J. Wheeler. 1951. The ant larvae of the subfamily Dolichoderinae. *Proceedings of the Entomological Society of Washington* 53: 169–210.
- Wheeler, G.C., and J. Wheeler. 1952a. The ant larvae of the subfamily Ponerinae – Part I. The American Midland Naturalist 48: 111–144.
- Wheeler, G.C., and J. Wheeler. 1952b. The ant larvae of the subfamily Ponerinae – Part II. The American Midland Naturalist 48: 604–672.
- Wheeler, G.C., and J. Wheeler. 1953. The ant larvae of the subfamily Formicinae. *Annals of the Entomological Society of America* 46: 126–171.
- Wheeler, G.C., and J. Wheeler. 1956. The ant larvae of the subfamily Pseudomyrmecinae (Hymenoptera: Formicidae). *Annals of the Entomological Society of America* 49: 374–398.
- Wheeler, G.C., and J. Wheeler. 1960. The ant larvae of the subfamily Myrmicinae. *Annals of the Entomological Society of America* 53: 98–110.
- Wheeler, Q.D. 1995. The “Old Systematics”: classification and phylogeny. *In* J. Pakaluk and S.A. Slipinski (editors), *Biology, phylogeny, and classification of coleoptera: papers celebrating the 80th birthday of Roy A. Crowson*, 31–62. Warszawa: Muzeum i Instytut Zoologii PAN.
- Wheeler, Q.D. 2004. Taxonomic triage and the poverty of phylogeny. *Philosophical Transactions of the Royal Society of London B* 359: 571–583.
- Wheeler, Q.D., and N.I. Platnick. 2000. The phylogenetic species concept (sensu Wheeler and Platnick). *In* Q.D. Wheeler and R. Meier (editors), *Species concepts and phylogenetic theory*, 55–69. New York: Columbia University Press.
- Wheeler, W.M. 1923. *Social life among the insects*. New York: Harcourt, Brace, vii + 375 pp.
- Wheeler, W.M. 1928. *The social insects: their origin and evolution*. New York: Harcourt, Brace, xviii + 378 pp.
- Wilson, E.O. 1958. Studies on the ant fauna of Melanesia. I. The tribe Leptogenyini. II. The tribes Amblyoponini and Platythyreini. *Bulletin of the Museum of Comparative Zoology at Harvard University* 118: 101–153.
- Wilson, E.O. 1971. *The insect societies*. Cambridge, Mass.: Harvard University Press, x + 548 pp.
- Wilson, E.O. 2000. A memorial tribute to William L. Brown (June 1, 1922–March 30, 1997). *Psyche* 103: 49–53.
- Wilson, E.O. 2003. *Pheidole in the New World: a dominant, hyperdiverse ant genus*. Cambridge, MA: Harvard University Press, 818 pp.
- Wilson, E.O., F.M. Carpenter, and W.L. Brown. 1967. The first Mesozoic ants, with the description of a new subfamily. *Psyche* 74: 1–19.
- Wilson, E.O., and B. Hölldobler. 2005. The rise of the ants: a phylogenetic and ecological explanation. *Proceedings of the National Academy of Science of the United States of America* 102: 7411–7414.
- Xu, Z. 2000. Two new genera of ant subfamilies Dorylinae and Ponerinae (Hymenoptera: Formicidae) from Yunnan, China. *Zoological Research* 21: 297–302.
- Yoder, M.J., I. Mikó, K.C. Seltsmann, M.A. Bertone, and A.R. Deans. 2010. A gross anatomy ontology for Hymenoptera. *PLoS One* 5 (12): e15991 (doi:10.1371/journal.pone.0015991).

APPENDIX 1

LIST OF SPECIES INCLUDED IN THIS STUDY

Information on locality, museum holdings and voucher codes correspond to the specimens use for SEM work for the digital atlas.

Taxon	Locality	Voucher	SEM Code#
FORMICIDAE			
Amblyoponinae			
<i>Adetomyrma</i> sp.	Madagascar	AMNH	RAK0003
<i>Amblyopone armigera</i>	Chile	AMNH	RAK0004
<i>Amblyopone australis</i>	Australia	AMNH	RAK0005
<i>Amblyopone mercovichii</i>	Australia	MCZ	RAK0006
<i>Amblyopone mutica</i>	Ivory Coast	MCZ	RAK0007
<i>Amblyopone mystriops</i>	Guatemala	MCZ	RAK0008
<i>Amblyopone pallipes</i>	USA	MCZ	RAK0009
<i>Amblyopone pluto</i>	Ivory Coast	MCZ	RAK0010
<i>Concoctio concenta</i>	Gabon	MCZ	RAK0011
<i>Myopopone castanea</i>	Indonesia	AMNH	RAK0012
<i>Mystrium voeltzkowi</i>	Madagascar	MCZ	RAK0013
<i>Onychomyrmex doddi</i>	Australia	AMNH	RAK0014
<i>Prionopelta aethiopica</i>	South Africa	MCZ	RAK0015
<i>Prionopelta antillana</i>	Peru	AMNH	RAK0016
Ectatomminae			
<i>Ectatomma tuberculatum</i>	Costa Rica	AMNH	RAK0017
<i>Gnamptogenys annulata</i>	Mexico	AMNH	RAK0018
<i>Gnamptogenys striatula</i>	Mexico	AMNH	RAK0019
<i>Gnamptogenys bufonis</i>	Costa Rica	MCZ	RAK0020
<i>Gnamptogenys minuta</i>	Costa Rica	MCZ	RAK0021
<i>Rhytidoponera confusa</i>	Australia	AMNH	RAK0022
<i>Typhlomyrmex pusillus</i>	Costa Rica	AMNH	RAK0023
<i>Typhlomyrmex rogenhoferi</i>	Costa Rica	AMNH	RAK0024
Heteroponerinae			
<i>Acanthoponera minor</i>	Colombia	AMNH	RAK0025
<i>Heteroponera brouni</i>	New Zealand	AMNH	RAK0026
<i>Heteroponera relicta</i>	Australia	AMNH	RAK0027
Paraponerinae			
<i>Paraponera clavata</i>	Venezuela	AMNH	RAK0028
Ponerinae			
<i>Anochetus emarginatus</i>	Venezuela	AMNH	RAK0029
<i>Odontomachus bauri</i>	Dominican Republic	AMNH	RAK0030
<i>Asphinctopone silvestrii</i>	Ivory Coast	MCZ	RAK0031
<i>Belonopelta deletrix</i>	Guatemala	MCZ	RAK0032
<i>Centromyrmex brachycola</i>	Venezuela	AMNH	RAK0033
<i>Cryptopone gilva</i>	Costa Rica	AMNH	RAK0034
<i>Diacamma ceylonense</i>	India	AMNH	RAK0035
<i>Dinoponera lucida</i>	Brazil	AMNH	RAK0036
<i>Dolioponera fustigera</i>	Gabon	MCZ	RAK0037
<i>Emeryopone buttelreepeni</i>	Malaysia	MCZ	RAK0038
<i>Harpegnathos saltator</i>	India	AMNH	RAK0039
<i>Hypoponera</i> sp1.	Mexico	AMNH	RAK0040
<i>Leptogenys (Leptogenys)</i> sp. 1	Mexico	AMNH	RAK0041
<i>Leptogenys (Lobopelta)</i> sp. 2	Nepal	AMNH	RAK0042
<i>Leptogenys (Leptogenys) podenzanai</i>	Australia	MCZ	RAK0043
<i>Loboponera obeliscata</i>	Gabon	AMNH	RAK0044
<i>Loboponera vigilans</i>	Cameroun	AMNH	RAK0045
<i>Myopias maligna</i>	Indonesia	MCZ	RAK0046
<i>Odontoponera transversa</i>	Nepal	AMNH	RAK0047

APPENDIX 1
(Continued)

Taxon	Locality	Voucher	SEM Code#
<i>Pachycondyla apicalis</i>	Venezuela	AMNH	RAK0048
<i>Pachycondyla berthoudi</i>	South Africa	MCZ	RAK0049
<i>Pachycondyla crassinoda</i>	Venezuela	AMNH	RAK0050
<i>Pachycondyla croceicornis</i>	Australia	AMNH	RAK0051
<i>Pachycondyla guianensis</i>	Costa Rica	MCZ	RAK0052
<i>Pachycondyla marleyi</i>	South Africa	MCZ	RAK0053
<i>Pachycondyla pachyderma</i>	Congo	AMNH	RAK0054
<i>Pachycondyla porcata</i>	Australia	AMNH	RAK0055
<i>Pachycondyla stigma</i>	Costa Rica	AMNH	RAK0056
<i>Pachycondyla tarsata</i>	Mozambique	AMNH	RAK0057
<i>Pachycondyla villosa</i>	Mexico	AMNH	RAK0058
<i>Phrynoponera gabonensis</i>	Kenya	AMNH	RAK0059
<i>Platythyrea punctata</i>	Dominican Republic	AMNH	RAK0060
<i>Platythyrea turneri</i>	Australia	MCZ	RAK0061
<i>Plectroctena strigosa</i>	Kenya	AMNH	RAK0062
<i>Ponera alpha</i>	Papua New Guinea	MCZ	RAK0063
<i>Ponera pennsylvanica</i>	USA	AMNH	RAK0064
<i>Psalidomyrmex procerus</i>	Cameroun	AMNH	RAK0065
<i>Simopelta oculata</i>	Costa Rica	MCZ	RAK0066
<i>Streblognathus peetersi</i>	South Africa	AMNH	RAK0067
<i>Thaumatomyrmex atrox</i>	Brazil	AMNH	RAK0068
Proceratiinae			
<i>Discothyrea oculata</i>	Cameroun	AMNH	RAK0069
<i>Discothyrea testacea</i>	USA	AMNH	RAK0070
<i>Proceratium croceum</i>	USA	AMNH	RAK0071
<i>Proceratium pergandei</i>	USA	AMNH	RAK0072
<i>Probolomyrmex guineensis</i>	Cameroun	AMNH	RAK0073
Aneuretinae			
<i>Aneuretus simoni</i>	Sri Lanka	MCZ	RAK0074
Dolichoderinae			
<i>Leptomyrmex pallens</i>	New Caledonia (Urea Is.)	AMNH	RAK0075
<i>Iridomyrmex purpureus</i>	Australia	AMNH	RAK0076
<i>Dolichoderus laminatus</i>	Venezuela	AMNH	RAK0077
<i>Tapinoma erraticum</i>	Portugal (Arrábida)	AMNH	RAK0078
<i>Technomyrmex albipes</i>	Japan	AMNH	RAK0079
Formicidae			
<i>Formica</i> sp. (fusca group)	USA	AMNH	RAK0080
<i>Gesomyrmex luzonensis</i>	Philippines	AMNH	RAK0081
<i>Oecophylla smaragdina</i>	Australia	AMNH	RAK0082
Apomyrminae			
<i>Apomyrma stygia</i>	Ivory Coast	MCZ	RAK0083
Leptanillinae			
<i>Leptanilla swani</i>	Australia	AMNH	RAK0084
Myrmeciinae			
<i>Myrmecia nigriscapa</i>	Australia	AMNH	RAK0085
<i>Nothomyrmecia macrops</i>	Australia	AMNH	RAK0086
Pseudomyrmecinae			
<i>Pseudomyrmex gracilis</i>	Costa Rica	AMNH	RAK0087
<i>Tetraoponera aethiops</i>	Congo (Avakubi)	AMNH	RAK0088
<i>Tetraoponera attenuata</i>	Malaysia	AMNH	RAK0089

APPENDIX 1
(Continued)

Taxon	Locality	Voucher	SEM Code#
Agroecomyrmecinae			
<i>Tatuidris tatusia</i>	Costa Rica	BMNH	RAK0001, RAK0002
Myrmicinae			
<i>Manica rubida</i>	Switzerland	AMNH	RAK0090
<i>Myrmica americana</i>	USA	AMNH	RAK0091
<i>Pogonomyrmex barbatus</i>	Mexico	AMNH	RAK0092
<i>Metapone madagascarica</i>	Madagascar	MCZ	RAK0093
Aenictinae			
<i>Aenictus binghami</i>	Myanmar	AMNH	RAK0094
Cerapachyinae			
<i>Acanthostichus serratulus</i>	Brazil	AMNH	RAK0095
<i>Cerapachys nitidulus</i>	Ghana	AMNH	RAK0096
<i>Cerapachys doryloides</i>	Maylasia	AMNH	RAK0097
<i>Cylindromyrmex brevitarsus</i>	Uruguay	AMNH	RAK0098
<i>Simopone schoutedeni</i>	Congo	AMNH	RAK0099
Dorylinae			
<i>Dorylus helvolus</i>	South Africa	AMNH	RAK0100
Ecitoninae			
<i>Cheliomyrmex morosus</i>	Mexico	AMNH	RAK0101
<i>Labidus coecus</i>	Mexico	AMNH	RAK0102
<i>Eciton hamatum</i>	Venezuela	AMNH	RAK0103
Leptanilloidinae			
<i>Leptanilloides biconstricta</i>	Brazil	AMNH	RAK0104
VESPIDAE			
<i>Metapolybia cingulata</i>	Trinidad	AMNH	RAK0120
SCOLIIDAE			
<i>Scolia nobilitata</i>	USA	AMNH	RAK0121

APPENDIX 2
DATA MATRIX

	1		2		3		4		5	
	1	5	0	5	0	5	0	5	0	5
<i>Adetomyrma</i> sp.	11003001020000	-00111100000000	1001200310000000	10000000						
<i>Amblyopone armigera</i>	11003001020000	-00111101000000	10012004200010	1010000000						
<i>Amblyopone australis</i>	11001001020001	-00101101000001	10012004200000	1010010000						
<i>Amblyopone mercovichii</i>	12001001020001	-0?11?1000000	1110012014200???	01001000						
<i>Amblyopone mystriops</i>	11001001020000	-0?11?10000000	10012002200???	0100?00						
<i>Amblyopone pallipes</i>	11001001020000	-00111101000000	10012002100101	1010010000						
<i>Amblyopone pluto</i>	11002001020000	-0?11?10000000	100120222000	101011010000						
<i>Amblyopone mutica</i>	10003001020000	-00111100000000	10012013?00???	01000000						
<i>Concoctio concenta</i>	11003001010000	-00101100000000	1001200420001001	1001001000						
<i>Myopopone castanea</i>	1200200-02000200	11101000000000	10012012100101	1011010000						
<i>Mystrium voeltzkowi</i>	11001001020001	-01110101000000	10012022100101	1010010000						
<i>Onychomyrmex doddii</i>	11003001010000	-00101100000001	10012004200010	1010010000						
<i>Prionopelta aethiopica</i>	11003001010000	-00101100000000	1001200420001001	1001001000						
<i>Prionopelta antillana</i>	11003001010000	-00101101000000	1001200420001001	1001001000						
<i>Ectatomma tuberculatum</i>	10001001010100	-10101120000000	1001101420001001	101101011						
<i>Gnamptogenys annulata</i>	10001001010100	-10101100000000	1001101320001001	101101021						
<i>Gnamptogenys striatula</i>	10001001010100	-10101100000000	1001101420001001	101101011						
<i>Gnamptogenys bufonis</i>	10001001010100	-10101100000000	10011015200-1001	10101021						
<i>Gnamptogenys minuta</i>	10001001010100	-10101100000000	1001101520001001	101101021						
<i>Rhytidoponera confusa</i>	10001001010100	-10101120000000	1001101420001001	101101011						
<i>Typhlomyrmex pusillus</i>	10001001010100	-00101110000000	1001101520001001	101101000						
<i>Typhlomyrmex rogenhoferi</i>	10001001010101	-00101110000000	1001101520001001	101101000						
<i>Acanthoponera minor</i>	10001001020000	-10101120000000	1001101000001001	101101000						
<i>Heteroponera brouni</i>	10001001020000	-10101120000000	1001101310001001	1001001000						
<i>Heteroponera relicta</i>	10001001020000	-10101120000000	1001101210001001	1001001000						
<i>Paraponera clavata</i>	10001001010000	-10001100000000	1001201110001001	101101011						
<i>Platythyrea punctata</i>	10001002120000	-00121100000000	1012000000?1001	1001001000						
<i>Platythyrea turneri</i>	10001002120000	-00121100000000	100120000000?1001	1001001000						
<i>Anochetus emarginatus</i>	10002002020000	-00101100000000	1011200200000000	1001001000						
<i>Odontomachus bauri</i>	10002002020000	-00101100000000	1011200210000000	1001001000						
<i>Asphinctopone silvestrii</i>	10003002120000	-00101100000000	11012002000???	01001000						
<i>Belonopelta deletrix</i>	10002001020000	-00101100000000	1001200310001001	1001001000						
<i>Centromyrmex brachycola</i>	10002002020000	-00101100000000	1101200210011001	1001001000						
<i>Cryptopone gilva</i>	10003002020000	-00101100000000	1001200420000000	11010000						
<i>Diacamma ceylonense</i>	10002002120000	-00101100000000	10012002000???	0110101000						
<i>Dinoponera lucida</i>	10002002120000	-00101100000000	1001200200010001	10101000						
<i>Dolioponera fustigera</i>	10003002020000	-00111100000000	10012004200???	1001001000						
<i>Emeryopone buttelreepeni</i>	10003002020000	-00101100000000	10012003100???	0110101000						
<i>Harpegnathos saltator</i>	10000002120000	-00101100000000	10012002000???	01101100						
<i>Hypoponera</i> sp.	10003002020000	-00101100000000	1001200530000000	11010000						
<i>Leptogenys (Leptogenys) sp. 1</i>	10002001020000	-00101100000000	1101210210000000	1001001000						
<i>Leptogenys (Lobopelta) sp. 2</i>	10002001020000	-00101100000000	1001210200000000	1001001000						
<i>Leptogenys podenzanai</i>	10002001020000	-00101100000000	1101210200010000	1001001000						
<i>Loboponera obeliscata</i>	10003003120000	-00121100000000	1101200420010001	101000						
<i>Loboponera vigilans</i>	10003003120000	-00121100000000	1101201420010001	1001001000						
<i>Myopias maligna</i>	10003002120000	-00101100000000	1101200200010001	101000						
<i>Odontoponera transversa</i>	10002002120000	-00101100000000	1101201200011001	101000						
<i>Pachycondyla apicalis</i>	10002002120000	-00101100000000	1001200200001001	1001001000						
<i>Pachycondyla berthoudi</i>	10002001020000	-00101100000000	1001200200011001	1001001000						
<i>Pachycondyla crassinoda</i>	10002002120000	-00101100000000	10012002000???	0110101000						
<i>Pachycondyla croceicornis</i>	10003002120000	-00101100000000	1001200310001001	1001001000						
<i>Pachycondyla guianensis</i>	10003002020000	-00101100000000	1001200210001001	10000000						
<i>Pachycondyla marleyi</i>	10002002120000	-00101100000000	1001200200001001	1001001000						

APPENDIX 2
(Continued)

	1		2		3		4		5	
	1	5	0	5	0	5	0	5	0	5
<i>Pachycondyla pachyderma</i>	10003003120000	-00121100000000	10012002000001001101000							
<i>Pachycondyla porcata</i>	10003002120000	-00121100000000	11012002000001001101000							
<i>Pachycondyla stigma</i>	10003002120000	-00121100000000	11012003100001001101000							
<i>Pachycondyla tarsata</i>	10002002120000	-00101100000000	1101200200011001001000							
<i>Pachycondyla villosa</i>	10002002120000	-00101100000000	1001200200011001101000							
<i>Phrynoponera gabonensis</i>	10002002020000	-00101100000000	10012002000001001001000							
<i>Plectroctena strigosa</i>	10003003120000	-00121100000000	11012013000001001101000							
<i>Ponera alpha</i>	10003002020000	-00101100000000	10012004200001001101000							
<i>Ponera pennsylvanica</i>	10003002020000	-00101100000000	10012004200001001101000							
<i>Psolidomyrmex procerus</i>	10002003120000	-00121100000000	11012013000001001101000							
<i>Simopelta oculata</i>	10003002120000	-00101100000000	10012104200000001102000							
<i>Streblognathus peetersi</i>	10002002120000	-00101100000000	10012002000001001001000							
<i>Thaumatomyrmex atrox</i>	10001002020000	-00101100000000	10012103100001001001000							
<i>Discothyrea oculata</i>	1000?010010000	-10001100000000	100120000001001001001021							
<i>Discothyrea testacea</i>	1000?010010000	-10001100000000	1001200??0101001001021							
<i>Proceratium croceum</i>	10011000010000	-10001100000000	1001200421001001000022							
<i>Proceratium pergandei</i>	10002000010000	-10001100000000	1001200211001001001022							
<i>Probolomyrmex guineensis</i>	1000?010010000	-10001100000000	1001200221001001000022							
<i>Aneuretus simoni</i>	10001001010000	-00001100000000	10010003100001001001000							
<i>Leptomyrmex pallens</i>	10000000000000	-00001100000000	1000-00000001000001000							
<i>Iridomyrmex purpureus</i>	10001000000000	-00001100000000	1000-00000001000001000							
<i>Dolichoderus laminatus</i>	10001000000000	-00001100000000	1000-00000001000001000							
<i>Tapinoma erraticum</i>	10001000000000	-00001100000000	1000-00000001000001000							
<i>Technomyrmex albipes</i>	10001000000000	-00001100000000	1000-00000001000001000							
<i>Formica fusca</i>	10000000000000	-00001100000000	1100-00000001000001100							
<i>Gesomyrmex luzonensis</i>	10001000000000	-00001100000000	1000-00000001000001100							
<i>Oecophylla smaragdina</i>	10000100000000	-00001100000000	10010001000001001101100							
<i>Apomyrma stygia</i>	10012000020000	-0?101100000001	10012004200000001000000							
<i>Leptanilla swani</i>	1001-0000000000	-00001100000000	10012004300000001000000							
<i>Myrmecia nigriscapa</i>	10001001010000	-100011001000010012000000001000001100								
<i>Nothomyrmecia macrops</i>	10001001010000	-00001100000000	100100000000010000001000							
<i>Tatuidris tatusia</i>	10001001010010	-10000100000000	10012005200001001101021							
<i>Manica rubida</i>	10001001010000	-10000100000000	10011000000001001011021							
<i>Myrmica americana</i>	10001001010000	-10000100000000	10011000000001001011021							
<i>Pogonomyrmex barbatus</i>	10001001010000	-10000100000000	10011002100001001011021							
<i>Metapone madagascariensis</i>	1000000-010001	-00000100000000	10012014100001001101021							
<i>Pseudomyrmex gracilis</i>	10000001011100	-0000110000000000	100100000001001101100							
<i>Tetraponera aethiops</i>	10000001011101	-0000110000000000	100100000001001101100							
<i>Tetraponera attenuata</i>	10000001011100	-0000110000000000	100100000001001101000							
<i>Acanthostichus serratulus</i>	1001200-020002001101100010001001202410010001001021									
<i>Cerapachys nitidulus</i>	1001200-02000210110110000000010011024200001001001021									
<i>Cerapachys doryloides</i>	1001200-020002101101100000000100110242000010000021									
<i>Cylindromyrmex brevitarsus</i>	1000200-0200020011011000000001001102410010001001021									
<i>Simopone schoutedeni</i>	1001100-0200020011011000000001001102010011001001111									
<i>Leptanillodes biconstricta</i>	1011300-02000210110110000000010013024200???01000000									
<i>Dorylus helvolus</i>	1001200-02000210110110000010010013024200000011000011									
<i>Aenictus binghami</i>	1001200-0200021011011000000001001300420010001000022									
<i>Cheliomyrmex morosus</i>	1001200-020002101101100010001001302410010001000021									
<i>Labidus coecus</i>	1001200-020002101101100010001001302410010001000022									
<i>Eciton hamatum</i>	1001200-020002101101100010001001302410010001002022									
<i>Metapolybia cingulata</i>	00000100000000	-00001100000000002	-00000000000001100							
<i>Scolia nobilitata</i>	00000000000000	-00001000000000002	-00000000000001100							

	5	6	6	7	7	8	8	9	9	1
	5	0	5	0	5	0	5	0	5	0
<i>Adetomyrma</i> sp.	010000111120011000000000000001100110001200000000000									
<i>Amblyopone armigera</i>	01001010112001101000010000011100110002221000001000									
<i>Amblyopone australis</i>	01000010112001101000120100011100100002200000001000									
<i>Amblyopone mercovichii</i>	01000010112001101000120100011100?00002200000001000									
<i>Amblyopone mystriops</i>	0?01010112001101000000000011100110001221000001000									
<i>Amblyopone pallipes</i>	01100010112001101000120100011100110001221000001000									
<i>Amblyopone pluto</i>	02101020112001101000000000011100110001221000001000									
<i>Amblyopone mutica</i>	02100021112001101000010000011110110001221000001000									
<i>Concoctio concentra</i>	11110011112001101000?200000111001100000-0001001000									
<i>Myopopone castanea</i>	01000010112001101000110200001000111101201100001000									
<i>Mystrium voeltzkowi</i>	02001011112001101000021200001100100001200000001000									
<i>Onychomyrmex doddi</i>	010000111120011010100001000112001100000-0001001000									
<i>Prionopelta aethiopica</i>	01100011112001101000100000011100110000200001001001									
<i>Prionopelta antillana</i>	01100011112001101000120100011100110000200001001001									
<i>Ectatomma tuberculatum</i>	000000101110011010001201010111010000001000000001001									
<i>Gnamptogenys annulata</i>	02001020111001101000010000011101000010200000001001									
<i>Gnamptogenys striatula</i>	02000020111001101000010000011101000010200000001001									
<i>Gnamptogenys bufonis</i>	02101021111001101000020000011101000010100000002100									
<i>Gnamptogenys minuta</i>	02101021111001101000020000011201000000100000002100									
<i>Rhytidoponera confusa</i>	000010101110011010001200000011101000000200000001001									
<i>Typhlomyrmex pusillus</i>	01100011111001101000010000011101000002000000001001									
<i>Typhlomyrmex rogenhoferi</i>	011000111110011010000100000111010000001000000001001									
<i>Acanthoponera minor</i>	01001010110101111010000101011001000000200000001001									
<i>Heteroponera brouni</i>	01101010110101101010110101011100000000200000001001									
<i>Heteroponera relictata</i>	02101011110101101010120101011100000000200000001001									
<i>Paraponera clavata</i>	02100010110001001000020101111001110000201100011001									
<i>Platythyrea punctata</i>	02100020110001101000010101011001110002210000001001									
<i>Platythyrea turneri</i>	0210002011000110100001010101001110002210000001001									
<i>Anochetus emarginatus</i>	000000101100011110001211100112000000001210000001001									
<i>Odontomachus bauri</i>	000000101100011010001211100112000000001210000001001									
<i>Asphinctopone silvestrii</i>	00001010110001101000021100011200000000200000001001									
<i>Belonopelta deletrix</i>	01000010110001101000120100011200110001210000001001									
<i>Centromyrmex brachycola</i>	01000020110011001000010100011000001100210000001001									
<i>Cryptopone gilva</i>	01000010110011011000121100011100001000100210000001001									
<i>Diacamma ceylonense</i>	02000010110001001000121000011000110001200000001001									
<i>Dinoponera lucida</i>	02100020110001001000121100011101110001200000001001									
<i>Dolioponera fustigera</i>	02100021110001101000011000011200000000200000001001									
<i>Emeryopone buttelreeperi</i>	020000201100011010001210000112000000002100000001001									
<i>Harpegnathos saltator</i>	02100020110001001010221000011001110001200000001001									
<i>Hypoponera</i> sp	0100001111001101000021000011200000000200000001001									
<i>Leptogenys (Leptogenys) sp. 1</i>	010000101100011010000000000011102000001210000001001									
<i>Leptogenys (Lobopelta) sp. 2</i>	000000101100011010000000000011102000001200000001001									
<i>Leptogenys podenzanai</i>	000000101100011010000001100011102000001210000001001									
<i>Loboponera obeliscata</i>	02101020111001101000022000011200000000200000001001									
<i>Loboponera vigilans</i>	02101020110001101000022000011200000001020000001001									
<i>Myopias maligna</i>	0100101011001101000122100011100000001200000001001									
<i>Odontoponera transversa</i>	000000101100011010001201000111000000001210000001001									
<i>Pachycondyla apicalis</i>	00001010110001001000121100011000110001210000001001									
<i>Pachycondyla berthoudi</i>	000000101100010010001211000111030000001210000001001									
<i>Pachycondyla crassinoda</i>	020000201100010010001211000111000000001210000001001									
<i>Pachycondyla croceicornis</i>	00000010110011101000021100011203000001200000001001									
<i>Pachycondyla guianensis</i>	0110002011001101101000111100011100001001210000001001									

(Continued)

	5	6	6	7	7	8	8	9	9	1
	5	0	5	0	5	0	5	0	5	0
<i>Pachycondyla marleyi</i>	00001010110001001000121100011101000001210000001001									
<i>Pachycondyla pachyderma</i>	02001020110001001000121100011103000001210000001001									
<i>Pachycondyla porcata</i>	02000020110001001000221100011100000001210000001001									
<i>Pachycondyla stigma</i>	01000010110001101000121100011100002001210000001001									
<i>Pachycondyla tarsata</i>	02000020110001001000121100011001000001210000001001									
<i>Pachycondyla villosa</i>	01000010110001001000121100011000110001210000001000									
<i>Phrynoponera gabonensis</i>	02000020110001001000121100011100000002210000001000									
<i>Plectroctena strigosa</i>	02001020110001101000022100011100000000200000001001									
<i>Ponera alpha</i>	01000010110001101000021000011200000000200000001001									
<i>Ponera pennsylvanica</i>	01000010110001101000021000011200000000200000001001									
<i>Psalidomyrmex procerus</i>	01000020110001101000022100011100000000200000001001									
<i>Simopelta oculata</i>	02100021110201101000020000001100110000200000001001									
<i>Streblognathus peetersi</i>	01000010110001001000121100011000000002200000001001									
<i>Thaumatomyrmex atrox</i>	02100021110001101000000000011203110000210000001001									
<i>Discothyrea oculata</i>	02100121110001101010000000011200110000200000001101									
<i>Discothyrea testacea</i>	0210012111000110101000000011200110000200000001101									
<i>Proceratium croceum</i>	0210012111000110101000000011200110000200000002101									
<i>Proceratium pergandei</i>	02101121110001101010000000011200110000200000001101									
<i>Probolomyrmex guineensis</i>	0210012111000110101002000011200110000200000001001									
<i>Aneuretus simoni</i>	00000000010001111001100000011100110000100000010001									
<i>Leptomyrmex pallens</i>	00100000010001100010200000011000110000200000000001									
<i>Iridomyrmex purpureus</i>	00100000010001100010100000011000110000200000100001									
<i>Dolichoderus laminatus</i>	00100010010001100010100000011000110000200000100001									
<i>Tapinoma erraticum</i>	00100010010001100010100000011000110000200000100001									
<i>Technomyrmex albipes</i>	00100010010001100010100000011000110000200000100001									
<i>Formica fusca</i>	00000000010001100010110000011000110000200000000001									
<i>Gesomyrmex luzonensis</i>	0010000001000110001010000001100011000000000000001									
<i>Oecophylla smaragdina</i>	001000000-00101010000000011000110000000000010001									
<i>Apomyrma stygia</i>	021000211120011010101100000010100110001220000001001									
<i>Leptanilla swani</i>	021000211101011000100000000??100110001200000000001									
<i>Myrmecia nigriscapa</i>	00000000010000001000120100011001110002201100011001									
<i>Nothomyrmecia macrops</i>	00000000110000001000210100011001110001201100010001									
<i>Tatuidris tatusia</i>	02100021111001101010000000011100100000200000000101									
<i>Manica rubida</i>	00001011111001101010010000011000110000200000010001									
<i>Myrmica americana</i>	02100011111001111010010000011000110000200000010000									
<i>Pogonomyrmex barbatus</i>	02100021111001111010110000011100110000200000010001									
<i>Metapone madagascariensis</i>	02100021111001101010100000001100110000200000000001									
<i>Pseudomyrmex gracilis</i>	00000000010100101010020101011001110001200000010001									
<i>Tetraponera aethiops</i>	00000000010100001010020101011001110001201100010001									
<i>Tetraponera attenuata</i>	0000000001010101010000101011001110001200100010001									
<i>Acanthostichus serratus</i>	0210002011020110101000000001000111000200000001000									
<i>Cerapachys nitidulus</i>	0210112111020110101000000001100110000200000002001									
<i>Cerapachys doryloides</i>	0210012111020110101000000002100110000200000001001									
<i>Cylindromyrmex brevitarsus</i>	0210002011020110101000000001100110002200000001000									
<i>Simopone schoutedeni</i>	0210102111020110101000000001101110000200010001001									
<i>Leptanillodes biconstricta</i>	0210002121020110111000000002100110000200000001001									
<i>Dorylus helvolus</i>	02100021210201100010100000001000110000200000001001									
<i>Aenictus binghami</i>	02100121110201101010010000001100110000100000000001									
<i>Cheliomyrmex morosus</i>	01100111110201100010110000002101110000200000002001									
<i>Labidus coecus</i>	02100121110201101010110000002101110000200000001001									
<i>Eciton hamatum</i>	02100121110200001010100000002001100000200000001001									
<i>Metapolybia cingulata</i>	0--000-0-0--00001010200000001000110002200000010001									
<i>Scolia nobilitata</i>	0--000-0-0--000010102002000000001100001000000000001									

	1	1	1	1	1	1	1
	0	1	1	2	2	3	3
	5	0	5	0	5	0	5
<i>Adetomyrma</i> sp.	0001001000000100000000000000000000?0000						
<i>Amblyopone armigera</i>	000300100000010000011120000000000000?0000						
<i>Amblyopone australis</i>	0003000000000100000111200000000000010000						
<i>Amblyopone mercovichii</i>	000300000000010000011120000000000000?0000						
<i>Amblyopone mystriops</i>	000300100000010000011120000000000000?0000						
<i>Amblyopone pallipes</i>	0003001000000100000111200000000000010000						
<i>Amblyopone pluto</i>	000300100000010000011120000000000000?0000						
<i>Amblyopone mutica</i>	000300210000010000011120000000000000?0000						
<i>Concoctio concenta</i>	1003000000000100?001112000000000000?0000						
<i>Myopopone castanea</i>	000100100000010000011120000000000000?0000						
<i>Mystrium voeltzkowi</i>	0001001000000100000111200000000000010000						
<i>Onychomyrmex doddi</i>	100301000000010000011120000000000000?0000						
<i>Prionopelta aethiopica</i>	100300000000010000011120000000000000?0000						
<i>Prionopelta antillana</i>	100300000000010000011120000000000000?0000						
<i>Ectatomma tuberculatum</i>	1003010000000110100111201010000001010000						
<i>Gnamptogenys annulata</i>	10030100000001101001112000100000010?0000						
<i>Gnamptogenys striatula</i>	10030100000001101001112000100000010?0000						
<i>Gnamptogenys bufonis</i>	10030100000001101001112000200000010?0000						
<i>Gnamptogenys minuta</i>	10030100000001101001112000200000010?0000						
<i>Rhytidoponera confusa</i>	1003000000000110100111201110000000010000						
<i>Typhlomyrmex pusillus</i>	10030100000001101001112000000000010?0000						
<i>Typhlomyrmex rogenhoferi</i>	10030100000001101001112000000000010?0000						
<i>Acanthoponera minor</i>	000300000000011010011120000000000000?0000						
<i>Heteroponera brouni</i>	10030000000001101001112000100000000?0000						
<i>Heteroponera relicta</i>	10030000000001101001112000100000000?0000						
<i>Paraponera clavata</i>	1003010001001100000111201000000000010000						
<i>Platythyrea punctata</i>	0003000001101100000111201000000000010000						
<i>Platythyrea turneri</i>	0003000001101100000111201000000000010000						
<i>Anochetus emarginatus</i>	00030000011001200001112010000000000?0000						
<i>Odontomachus bauri</i>	0003000001100120000110201000000000010000						
<i>Asphinctopone silvestrii</i>	0003000001100120000110200000000000?0000						
<i>Belonopelta deletrix</i>	10030000011001200001112010000000000?0000						
<i>Centromyrmex brachycola</i>	0003000001100110000111200000000000?0000						
<i>Cryptopone gilva</i>	1003000001100110000111200000000000?0000						
<i>Diacamma ceylonense</i>	1003000001100120000111200000000000010000						
<i>Dinoponera lucida</i>	0003000001100120000111201000000200010000						
<i>Dolioponera fustigera</i>	000300000110011000011120?0000000000?0000						
<i>Emeryopone buttelreepeni</i>	10030000011001200001112000100000000?0000						
<i>Harpegnathos saltator</i>	1003000001100110000111201000000000010000						
<i>Hypoponera</i> sp.	1003000001100120000111201000000000?0000						
<i>Leptogenys (Leptogenys)</i> sp. 1	0003000001100120000111201000000000010000						
<i>Leptogenys (Lobopelta)</i> sp. 2	0003000001100120000111201000000000010000						
<i>Leptogenys podenzanai</i>	0003000001100120000111201000000000010000						
<i>Loboponera obeliscata</i>	00020000011001200001112000200000000?0000						
<i>Loboponera vigilans</i>	0002000001100120000111200020000000?0000						
<i>Myopias maligna</i>	0003000001100120000111201000000000?0000						
<i>Odontoponera transversa</i>	0003000001100120000111201000000000010100						
<i>Pachycondyla apicalis</i>	0003000001100120000111201000000000010000						
<i>Pachycondyla berthoudi</i>	00030000011001200001112010000000100?0000						
<i>Pachycondyla crassinoda</i>	000300000110012000011120000000000101?0000						
<i>Pachycondyla croceicornis</i>	1003000001100120000111201000000000?0000						
<i>Pachycondyla guianensis</i>	000300000110012000011120000000000?0000						

APPENDIX 2
(Continued)

	1	1	1	1	1	1	1
	0	1	1	2	2	3	3
	5	0	5	0	5	0	5
<i>Pachycondyla marleyi</i>	0003000011001200001112000000000000?0000						
<i>Pachycondyla pachyderma</i>	0003000011001200001112010000000000?0000						
<i>Pachycondyla porcata</i>	0003000011001200001112000000000000?0000						
<i>Pachycondyla stigma</i>	0003000011001200001112000000000000?0000						
<i>Pachycondyla tarsata</i>	0003000011001-0000111200000000000010000						
<i>Pachycondyla villosa</i>	0003000011001200001112010000000000?0000						
<i>Phrynoponera gabonensis</i>	00030000110120000111200000000000?0000						
<i>Plectroctena strigosa</i>	000200001100120000111200010000000010000						
<i>Ponera alpha</i>	100300001100120000111201000000000010000						
<i>Ponera pennsylvanica</i>	100300001100120000111201000000000010000						
<i>Psalidomyrmex procerus</i>	0002000011001200001112000100000000?0000						
<i>Simopelta oculata</i>	1003000011001200001102000000000000?0000						
<i>Streblognathus peetersi</i>	0003000011001200001112010000000000?0000						
<i>Thaumatomyrmex atrox</i>	1003000011001200001102010000000000?0000						
<i>Discothyrea oculata</i>	1003000000001100001112000200000000?0000						
<i>Discothyrea testacea</i>	1003000000001100101112000200000000?0000						
<i>Proceratium croceum</i>	1003000000001100001112000200000000?0000						
<i>Proceratium pergandei</i>	100300000000110000111200020000000010000						
<i>Probolomyrmex guineensis</i>	1003100000001100001112000100000000?0000						
<i>Aneuretus simoni</i>	10030100?00011000010000000000000010000						
<i>Leptomyrmex pallens</i>	110301001100111000100000000010000010010						
<i>Iridomyrmex purpureus</i>	110301001100121000100000000010000010010						
<i>Dolichoderus laminatus</i>	110301001100121000100000000010000010010						
<i>Tapinoma erraticum</i>	110301001100221000100000000010000010010						
<i>Technomyrmex albipes</i>	110301001100221000100000000000000010010						
<i>Formica fusca</i>	110301001100021000100000000000000001011						
<i>Gesomyrmex luzonensis</i>	110301001100021000100000000000000001011						
<i>Oecophylla smaragdina</i>	110301000000111000100000000000000001011						
<i>Apomyrma stygia</i>	0013002100000100001000000000000000?0000						
<i>Leptanilla swani</i>	10100?2??001110000111100000000000?0000						
<i>Myrmecia nigriscapa</i>	000300001101110100001100000000000010000						
<i>Nothomyrmecia macrops</i>	100300001100110000000000100000000010000						
<i>Tatuidris tatusia</i>	1003010000011100100012010200000000?0000						
<i>Manica rubida</i>	100301000001110111001001000000000000000						
<i>Myrmica americana</i>	100301000001110111001001000000000010000						
<i>Pogonomyrmex barbatus</i>	100301000001110111001001000000000010000						
<i>Metapone madagascariensis</i>	1003010000011100110010010000000000?0000						
<i>Pseudomyrmex gracilis</i>	100300001101110000001001000000000010000						
<i>Tetraponera aethiops</i>	100300001101110000001001000000000010000						
<i>Tetraponera attenuata</i>	100300001101110000001001000000000010000						
<i>Acanthostichus serratus</i>	1003000010001000101111000010002100?0000						
<i>Cerapachys nitidulus</i>	1003000010001000101111000010002100?0000						
<i>Cerapachys doryloides</i>	1003000000001100101111000010012100?0000						
<i>Cylindromyrmex brevitarsus</i>	1003000000001000101111010010002100?0000						
<i>Simopone schoutedeni</i>	1003000000001100101111000010002100?0000						
<i>Leptanillodes biconstricta</i>	10000100000111001011110100010010000?0000						
<i>Dorylus helvolus</i>	1000000010001100101111010001000110010000						
<i>Aenictus binghami</i>	1003000000001100101111000010010000?0000						
<i>Cheliomyrmex morosus</i>	10030000100011001011110000011010100?0000						
<i>Labidus coecus</i>	1003000010011100101111000001101210010000						
<i>Eciton hamatum</i>	1003000010011100101111000001101001010000						
<i>Metapolybia cingulata</i>	1000000000001100110000000000000000000000						
<i>Scolia nobilitata</i>	0000000000001000000000000000000000000000						